KTH Industrial Engineering
and Management

Combining Solar Energy and UPS Systems

Tobias Bengtsson

Håkan Hult

Master of Science Thesis

KTH School of Industrial Engineering and Management
Energy Technology EGI-2014-067MSC
Division of Applied Thermodynamics and Refrigeration
SE-100 44 STOCKHOLM

Master of Science Thesis EGI 2014:067

KTH Industrial Engineering and Management

Combining Solar Energy and UPS Systems

Tobias Bengtsson

Håkan Hult

Approved	Examiner	Supervisor
Date	Per Lundqvist	Björn Palm
	Commissioner	Contact person

Abstract

Solar Power and Uninterruptible Power Supply (UPS) are two technologies that are growing rapidly. The demand for solar energy is mainly driven by the trend towards cheaper solar cells, making it economically profitable for a larger range of applications. However, solar power has yet to reach grid parity in many geographical areas, which makes ways to reduce the cost of solar power systems important.

This thesis investigates the possibility and potential economic synergies of combining solar power with UPS systems, which have been previously researched only from a purely technical point of view. This thesis instead evaluates the hypothesis that a combined solar and UPS system might save additional costs compared to regular grid-tied systems, even in a stable power grid. The primary reason is that online UPS systems rectifies and inverts all electricity, which means that solar energy can be delivered to the DC part of the UPS system instead of an AC grid, avoiding the installation of additional inverters in the solar power system.

The study is divided into three parts. The first part is a computer simulation using MATLAB, which has an explorative method and aims to simulate a combined system before experimenting physically with it. The second part consists of experiments on a physical prototype system based on basic UPS and solar power components. The third part is an economical assessment of investment costs and energy balances, comparing two separate systems (UPS and solar power separate) to one combined (UPS & solar power). The results from the prototype system show that adding solar power to an UPS system does not interfere with the UPS functionality in any major way, however for optimal performance some additional integration may be necessary. On the contrary, the additional power terminal that the solar panels constitute, can increase system performance during certain operational conditions. The result of the economic analysis shows that a combined system has potential for both a lower investment cost due to cheaper components and increased energy savings through lower conversion losses.

The conclusion from the study is that a combined solar energy and UPS system is technically feasible. Furthermore, a combined system has clear economic advantages over two separate systems. This means that a combined system might be economically profitable even in situations where a separate system is not.

SAMMANFATTNING

Solenergi och avbrottsfri kraftförsörjning (UPS) är två tekniker som växer snabbt. Efterfrågan på solenergi ökar huvudsakligen på grund av den snabba utvecklingen mot billigare solceller, vilket lett till att solenergi blivit lönsamt i en större mängd applikationer. I många områden är solenergi dock fortfarande inte kostnadsmässigt konkurrenskraftigt jämfört med traditionella energikällor, vilket gör en fortsatt sänkning av kostnaderna för solenergi till en viktig fråga för solenergiindustrin.

Detta examensarbete har som syfte att undersöka om det är tekniskt möjligt att kombinera solenergi med UPS-system samt potentialen för ekonomiska synergier med denna kombination. Tidigare forskning inom området har endast undersökt denna kombination från en rent teknisk synvinkel. Detta examensarbete driver istället hypotesen att ett kombinerat solenergi- och UPS-system kan leda till större kostnadsbesparingar jämfört med ett traditionellt nätanslutet solenergisystem, även i ett stabilt elnät som i Sverige. En on-line UPS skyddar en känslig last genom att kontinuerligt likrikta och sedan åter växelrikta inkommande ström för att därmed både isolera lasten från nätet samt höja strömkvalitén. I UPS-systemet finns därmed en likströmsdel dit solpanelerna direkt kan kopplas istället för att skicka den genererade solenergin ut på elnätet. Därmed undviks inköp och installation av sol-växelriktare i solenergisystemet.

Studien är uppdelad i tre delar. Första delen är en datorsimulering i MATLAB och syftar till att explorativt undersöka det kombinerade systemet för en optimerad design innan fysiska experiment utförs. Den andra delen av studien utgörs av experiment på ett fysiskt prototypsystem baserat på ett principiellt UPS- och solenergisystem. Den tredje delen av studien är en ekonomisk analys av både investeringskostnader och energibalanser som jämför ett kombinerat system (UPS & sol) med två separata system (UPS & sol separat). Resultaten från prototypsystemet visar att påkopplandet av solceller i en principiell UPS har mycket låg påverkan på UPS-systemets funktionalitet, samt att solcellerna som en extra energikälla under vissa driftförhållanden kan ha en positiv påverkan på UPS-systemet. För optimal prestanda kan dock en viss integration av systemen krävas. Resultatet från den ekonomiska analysen visar att ett kombinerat system har potential att sänka investeringskostnaden genom billigare komponenter. Ett kombinerat system kan även leda till en högre energibesparing jämfört med ett nätanslutet solenergisystem eftersom konverteringsförlusterna i UPS-systemet sjunker i det kombinerade systemet.

Slutsatsen av studierna är att ett kombinerat solenergi- och UPS-system är tekniskt möjligt. Dessutom finns betydande ekonomiska synergier med ett kombinerat system. Detta innebär att ett kombinerat system kan vara lönsamt även i fall där ett separat solelsystem inte är det.

FOREWORD

This Master's thesis has been conducted as the final project in the Industrial Engineering and Management Master's program with a specialization in Energy Systems. The project has been carried out in cooperation with a manufacturer of batteries and a company specializing in thin film solar technology. The physical experiments have been conducted at the Department of Energy Technology at the Royal Institute of Technology (KTH).

This thesis would not have been possible without the knowledge and support of others. We would like to offer our sincere thanks and gratitude to the following persons:

Our sponsor Marcus Wigren at Nilar International AB – for supporting us with everything from the initial idea to the final version of this thesis report.

Peter Hill, Benny Sjöberg and Karl-Åke Lundin at the Laboratory of Applied Thermodynamics and Refrigeration – for lending us the technical expertise, measurement equipment and tools necessary for the construction of the experimental system.

Our supervisor Björn Palm – for academic support and feedback.

Anders Malmquist at the department of Heat and Power Technology – for technical expertise and for helping us to structure our initial idea into a project.

Light Energy – for expertise regarding solar energy.

Our professor Per Lundqvist – for overall support and for teachings during four years of study in the field of energy systems.

And finally we wish to thank our families, friends and everyone else who has supported us during this semester.

Håkan Hult & Tobias Bengtsson

Contents

List of Figures

List of Tables

List of Abbreviations

Abbreviation	Meaning
AC	Alternating Current
a-Si	Amorphous Silicon
BOS	Balace of System
CdTe	Cadmium-Telluride
CIGS	Copper-Indium-Gallium-Selenide
c-Si	Crystalline Silicon
DAU	Data Acqusition Unit
DC	Direct Current
DG	Distributed Generation
ES	Energy Storage
GHG	Greenhouse Gases
G-VSC	Grid-connected Voltage Source Converter
IC	Incremental Conductance
IPCC	Intergovernmental Panel on Climate Change (UN)
LCC	Life Cycle Cost(ing)
LCOE	Levelized Cost of Electricity
mono-Si	Monocrystalline Silicon Solar Cell
MOSFET	Metal–Oxide–Semiconductor Field-Effect Transistor
MPP	Maximum Power Point
MPPT	Maximum Power Point Tracking
NiMH	Nickel Metal Hydrid
NOx	Nitrogen Oxides
P&O	Perturb and Observe
poly-Si	Polycrystalline Silicon
PV	Photovoltaic/Photovoltaics
PWM	Pulse-Width Modulation
RMS	Root Mean Square
SOC	State Of Charge
SOx	Sodium Oxides
STC	Standard Testing Conditions
THD	Total Harmonic Distortion
UPS	Uninterruptible Power Supply
USD	U.S Dollars

1 Introduction

In this section the background, purpose, implications and scope of this thesis is presented. This section also includes an outline of the thesis report.

1.1 Background

The fifth assessment by the Intergovernmental Panel on Climate Change (IPCC) shows overwhelming scientific proof that emissions of greenhouse gases from human activities affect the climate and is the primary cause of global warming (IPCC, 2013). The energy sector plays an important role in reducing global emissions since energy generation from fossil fuels is a major source of greenhouse gas emissions (U.S Environmental Protection Agency, 2013). The global energy demand is also predicted to rise sharply in the coming decades (U.S. Energy Information Administration, 2013). Electricity generation through solar photovoltaic (PV) systems is widely accepted as a low-emission, non-depletable energy source with the potential to solve the sustainability issues in the energy sector (Fthenakis, 2009). Solar power is generally divided into being either utility-scale, commercial-scale or small-scale (Reichelstein and Yorston, 2013). In scenarios concerning future energy systems, solar power is usually seen as an important source of electricity (Komiyama and Kraines, 2008) with visions of solar power being the main source of electricity generation in year 2100 (Nakicenovic, 2000). The main barrier to large-scale solar generation is the historically higher costs compared with conventional energy sources (Kumar Chinnaiyan et al., 2013).

In order to harness the energy of the sun, solar cells (where the photovoltaic conversion takes place) needs supporting balance-of-system (BOS) components for controlling, transforming and transmitting the generated electricity (Kalogirou, 2014). While the production cost of solar modules has historically decreased exponentially compared to production levels, the costs of other components in solar power systems have experienced a much slower rate of reduction (Reichelstein and Yorston, 2013). This has led to the BOS components constituting an increasing share of overall system costs; presently they are more than half of total investment costs (Reichelstein and Yorston, 2013).

Since the development of computer systems and the internet the number of sensitive computerized systems that require an absolute reliable power supply has increased sharply (Nasiri, 2011). Systems for uninterruptible power supply (UPS) protect highly sensitive equipment in hospitals, airports and data centers while guaranteeing a continuous supply of clean power even in the case of blackouts in the conventional power grid (Price, 1989). In on-line UPS systems this is achieved through continuous treatment of the electricity to remove sags and spikes by first rectifying and then inverting the incoming electricity during normal operation. In the case of a blackout the UPS system enters islanding mode, powering the load from a battery bank designed to last until either mains power supply is restored or back-up generators have started (Nasiri, 2011). The number of UPS systems in use is predicted to continue to rise as critical computer systems become increasingly common (Ward, 2001).

UPS systems and small scale solar power systems share many technical components related to power electronics (Kumar Chinnaiyan et al., 2013, Price, 1989) and could thus potentially be combined.

1.2 Problem statement & Implications

Making solar-based energy cost-competitive with traditional, fossil-based sources is a major challenge within the energy industry (Sims et al., 2007, Kalogirou, 2014). Scientists have realized that there is no panacea—a variety of solutions will be needed for different sizes of solar power systems in locations with different cultural, juridical and environmental conditions.

If UPS and solar power systems could be successfully combined (resulting in lower overall system costs), many users of UPS systems might consider investing in their own solar energy generation. This would benefit the users, the overall energy system and the environment.

From the perspective of a UPS manufacturer, a combination of solar energy and UPS systems could lead to both lower costs and expansion to new market segments by new product offerings. For users of the proposed system the benefit would be lower lifetime cost of the installed system compared to a conventional stand-alone solar power system. Increased usage of solar energy also decreases the emission intensity of the energy sector, contributing to a more sustainable energy system.

1.3 Purpose

The purpose of this study is to evaluate the technical feasibility and economic benefits of combining UPS systems with solar PV systems. The aim is to connect the two systems in order to continuously use solar energy to power part of the load. The technical study aims to construct a prototype system in order to evaluate the impact of the added solar power on key UPS parameters. In the economic study, the aim is to evaluate the cost reductions of the combined system compared to two separate systems as well as potential gains in total system efficiency and thus total energy generation.

1.4 Delimitations

In this section the general scope of the study is presented. More specific delimitations and limitations are presented directly in the related sections of this thesis.

For the entire study the major delimitations defining the scope of the study are:

- The location of the combined UPS and solar energy system in the study is limited geographically to Sweden, which leads to the usage of country-specific climate data and power grid data.
- The study focus on data centers as the application of the full-scale system.
- The economic assessment compares the relative investment cost of a combined system to that of two separate systems, without focusing on the lifetime costs and revenues of the systems. Thus, only components exclusively used in one of the alternatives are compared. Regarding energy generation only the results for the first year of operation is presented, together with a basic payback calculation using a fixed electricity price. This simplification eliminates the need of complex forecasting of for example electricity prices, which are not the focus of this thesis.

1.5 Outline

Relevant literature related to solar energy, UPS systems, power electronics and microgrids is presented in the literature review. Previous research in the combination of solar power and UPS systems is also discussed in this section.

In the method section, the three studies conducted (computer simulation, experiments on a prototype system and economic analysis) is presented in detail. The delimitations and limitations of each study are also discussed.

In the results section, the outcomes of each study are presented individually and the results are analyzed and explained. The results from the prototype system are mainly focused on the technical feasibility while the economic analysis compares the combined system to the stand-alone grid-tied solar power system in terms of energy generation and component cost. Each study is concluded with an analysis of the impact of the results.

In the discussion section the results of the combined studies are discussed together with a thorough analysis of the impact of the delimitations and limitations of the study. The section is concluded with an outlook of the future for integrated solar energy and microgrids.

The final section of this thesis presents the conclusion of the combined studies and answers the questions posed in the purpose of the thesis along with suggestions for future research.

Literature Review

In this section, relevant literature regarding solar energy systems, UPS, power electronics, microgrids and the economics of solar PV will be reviewed. This information constitutes the base of this study. Previous research in the combination of solar energy and UPS is also presented and the study is placed in the context of previous research.

2 Literature: Solar Power

Solar PV is a broad field with many different technologies and applications. In this section the sustainability, economy, development and technology of common types of solar PV are discussed.

2.1 General information

The most common type of solar electricity generation is through the utilization of the photovoltaic effect. Solar PV applications range from pocket calculators to utility scale solar power plants with several megawatts of installed power.

The first solar PV cells were produced in the 1950s by Bell Labs, but the low efficiency and high production cost rendered it too expensive for almost any application except in space (Chen, 2011). During the last decades however, the interest for electricity generation from solar PV has increased sharply, taking the technology from the lab to commercial applications used worldwide (Tyagi et al., 2013).

Since the year 2000, global solar PV production has increased exponentially with annual growth numbers ranging from 40% to 250% (Jäger-Waldau et al., 2011, Reichelstein and Yorston, 2013). The region with the largest increase in production capacity has been East Asia (Figure 1), with China now dominating global production of solar PV (Jäger-Waldau et al., 2011).

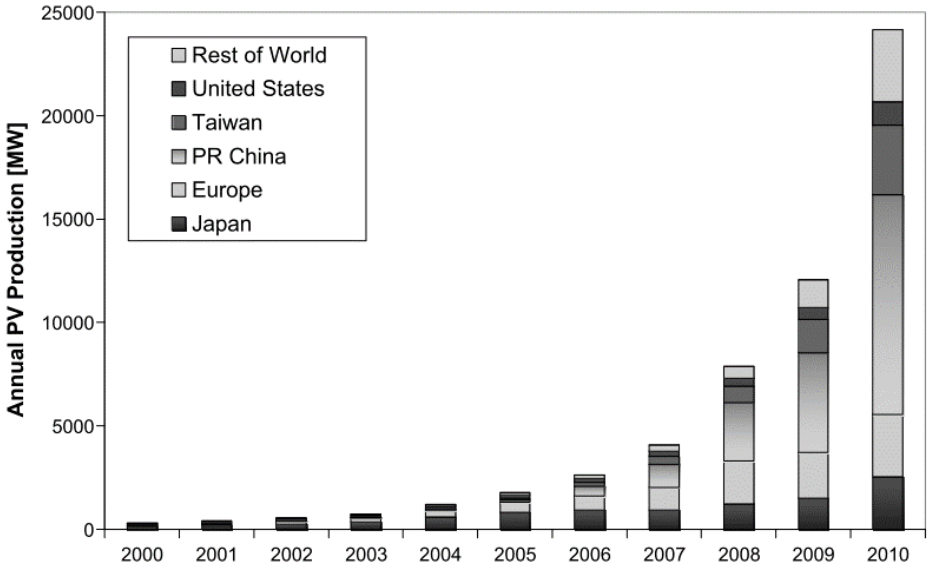

Figure 1: Global annual PV production (Jäger-Waldau et al., 2011)

A major contributor to the exponential growth in PV installations is the increased attention by governments and public institutions towards sustainability and renewable energy production, especially through the introduction of subsidies and tax reductions for renewable energy sources (Tyagi et al., 2013).

There is no strict definition of sustainability, but two central concepts related to sustainability is the emission of greenhouse gases (GHG) and fuel usage (United Nations, 1987, Welford, 2000). Since the energy sector contributes approximately 25% of global GHG emissions today (U.S Environmental Protection Agency, 2013), increased production from low-emission sources is key to a sustainable world. Energy sources are commonly divided into renewable and non-renewable energy sources based on the fuel used, where the fuel used by renewables are considered to be non-exhaustible (U.S. Energy Information Administration, 2013).

In light of the previous discussion regarding sustainability, electricity generation from solar PV can be considered favorable compared to many other energy sources. Solar PV is considered a low-emission energy source with virtually no emission during operations (Kalogirou, 2014) requiring no fuel except the incoming light from the sun (Fthenakis, 2009).

When comparing the lifetime GHG emissions from different energy sources including mining, manufacturing and post-operation disposal, solar PV technologies have significantly lower emissions compared to non-renewable sources (Tyagi et al., 2013). In the case of thin film solar panels in standard US conditions Fthenakis (2009) concludes that GHG-emissions per kWh of produced energy is only 2–4% of an average fossil-based power plant, with similar reductions in NOx and SOx gases. This is supported by Dubey et al. (2013) who evaluates the socio-economic as well as the environmental impact of silicon-based solar PV and concludes that solar PV has the potential to significantly reduce GHG-emissions, fossil fuel usage and overall material consumption in the energy sector. However, a drawback of solar energy is the use of heavy metals and other environmentally harmful substances in the production of solar panels (Fthenakis, 2009).

2.2 The technology of different types of solar cells

All PV electricity generation can be summarized in 4 basic steps (Fonash, 2010):

1. The energy from incoming photons in sunlight is absorbed by the absorber material in the solar cell, causing a transition in the material from a ground state to an excited state.
2. The excited state causes the generation of a negatively charged and a positively charged carrier.
3. The free positive and negative carriers are separated by either an electric or effective field. This causes the negative carriers to travel towards the front contact of the solar cell and the positive carriers to travel towards the opposite (back) contact.
4. Arriving at the front contact, the negative carriers release electrons into an external circuit between the front and back contact of the solar cell where the electric current powers a load before returning to the back contact. Here the electrons recombine with the positive charge carriers, returning to the original ground state.

While these basic steps are common for all solar PV systems, the materials, chemical reactions, type of charge carriers, separation mechanism and overall design differs significantly between different types of solar cells (Badawy, 2013, Kalogirou, 2014).

Solar PV is classified into first, second and third generation solar cells, based on the different technologies used to generate electricity. The materials used in the semiconductor can also be used to classify solar cells, with silicon-based PV being the dominating technology.

The solar cells classified as belonging to the first generation is of the same general type as the original ones developed by Bell Labs 55 years ago, and are based on crystalline silicon (c-Si). These solar cells are utilizing a thick silicon wafer as semiconductor and can generally be divided into either mono-crystalline or poly-crystalline cells, with the macro structures of the silicon crystals being the difference between the two cell types (Fonash, 2010).

The mono-crystalline cell consists of a single silicon crystal grain, with a fixed atom structure covering the entire wafer, resulting in higher conversion efficiency due to the lower amounts of impurities in the crystal (Wenham, 2007). A typical efficiency for mono-crystalline silicon (mono-Si) solar modules in mass production is around 18% (Glunz et al., 2012). The best efficiency reached in laboratories using single cells and not complete modules is 24.7% (Razykov et al., 2011).

The high performance of mono-Si cells however comes at the price of higher manufacturing costs, which is the reason why polycrystalline silicon (poly-Si) is another common semiconductor material (Kalogirou, 2014). Poly-Si has a crystal lattice consisting of smaller crystal grains that are joined together. In the boundaries between the crystal grains there is an area without a higher level atom structure. These impurities in the crystals results in areas where the free carriers driving the photovoltaic current can recombine, lowering the overall efficiency of the cell (Fonash, 2010). The size of the crystal grains has a major impact on the efficiency of the cell, but smaller grain sizes allows for simpler manufacturing processes and thus lower overall costs (Tyagi et al., 2013).The grain sizes in different types of poly-Si ranges from 1 μm to 10 cm (Wenham, 2007). The smaller sizes compared to mono-Si results in typical efficiencies around 16.5% (Glunz et al., 2012).

The dominating technology used in field applications is still c-Si, both for utility scale and small scale systems. The market shares of different types of solar panels are shown in Figure 2, with c-Si panels constituting almost 90% of the market. The internal distribution of market share of c-Si solar cells is according to ActEnergy (2014) approximately 60% poly-Si and 40% mono-Si. During the last couple of years however, c-Si has started to be challenged by other types of solar cells referred to as second generation solar cells.

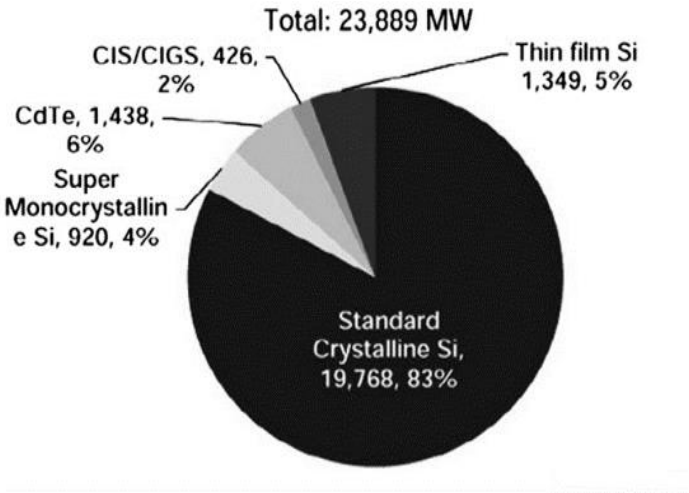

Figure 2: 2010 Market shares for different types of solar cells (Tyagi et al., 2013)

The second generation of solar cells is generally referred to as thin film solar cells and the main types are Copper-Indium-Gallium-Selenide (CIGS), Cadmium-Telluride (CdTe) and amorphous silicon (a-Si). The aim of thin film solar cells is to reduce manufacturing costs by using a much thinner layer of the semiconductor material compared to traditional silicon wafers (Figure 3), resulting in both lower material costs and simpler manufacturing processes (Badawy, 2013).

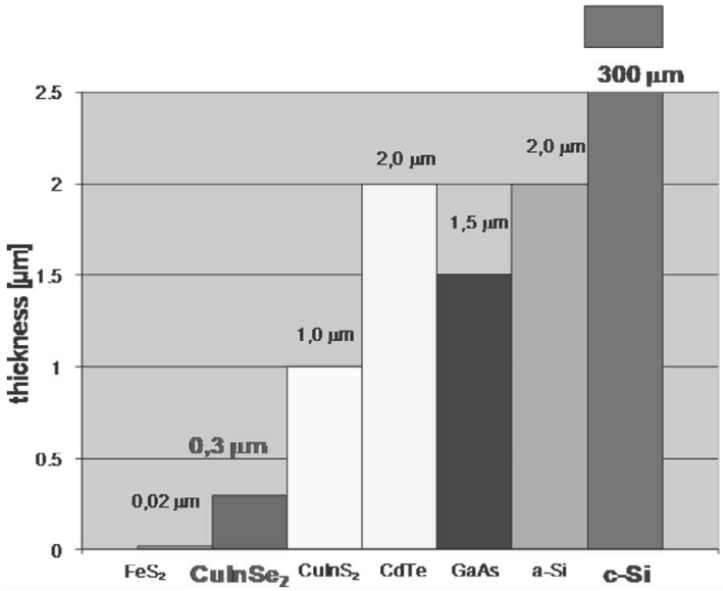

Figure 3: Typical semiconductor thickness of different types of solar cells (Badawy, 2013)

The most common type of thin film technology in mass production is a-Si, but both CIGS and CdTe have been gaining market shares in the last few years (Tyagi et al., 2013). The crystals used in the semiconductor in a-Si solar cells have very small grains, so that almost no macrostructure exist (Fonash, 2010). This makes the manufacturing cheaper, but also lowers the module efficiency.

The availability of materials for CIGS and CdTe solar cells is largely determined by the mining of copper and zinc, since the materials used are by-products of copper and zinc mining. As the demand for CIGS and CdTe solar cells rise, more of these by-products are being recovered during copper and zinc mining. This has had the result that the potential shortage that previously capped the production of these types of solar cells now has disappeared. The increased production has led to both lower prices and higher efficiencies due to increased research and development. (Fthenakis, 2009)

As of 2013 thin film solar cells in mass production have a typical efficiency of around 11.5–13.5%, with the best lab-produced cells achieving above 18.8% efficiency (Fraunhofer Institute, 2012, Rau and Schock, 2013).

Third generation solar cells are yet to reach commercial applications, but the main focus is to use nanotechnology for increased efficiency or to utilize organic compounds to solve the problem of scarcity of key materials (Badawy, 2013). Since any widespread application for these types of solar cells are still many years in the future (Wenham, 2007), they have been omitted from this thesis.

2.3 Applications – influencing factors

Solar cells used outside the controlled environments of laboratories invariably experience changes in efficiencies compared to the standard testing conditions (STC). There are numerous factors affecting the efficiency of solar cells; the ones with the largest influence of lifetime energy generation will be discussed here.

While most factors influencing the solar module energy production are extremely site-specific (shading, wind shelter, dust particles etc.) (Feist et al., 2011) there are also several region-specific factors. The most important of these are solar irradiance, temperature and changes in the spectral distribution of the sunlight. Another factor which influences the performance of the solar cells is degradation over the lifetime of the cells, which is heavily influenced by the choice of semiconductor material (Feist et al., 2010).

During their lifetime, solar panels will be subjected to a loss of efficiency due to degradation of both the crystalline structure in the semiconductor and the glass cover (Grunow et al., 2004). Generally the glass cover degrades by less than 1% per year regardless of cell type (Grunow et al., 2004), while the degradation of the semiconductor is larger in less pure poly-Si cells (Kalogirou, 2014). Generally the warranty for c-Si specifies a maximum annual degradation of 1%, but with actual degradation rates closer to 0.3–0.7% (Branker et al., 2011).

A critical factor for the energy generation in solar panels is the voltage–current characteristics of the chosen module. The power (P) generated by the solar panel is the product of the current (I) and voltage (V). The maximum amount of current is produced during short-circuit, in which case the anode and cathode of the module is in direct contact with each other. Due to the direct contact of the two electrical terminals there can be no difference in electric potential and the voltage is thus zero. Similarly the maximum possible voltage occurs in a situation when the circuit is open, which by definition means that no current can flow between the two poles. In order to maximize power the product of current and voltage must be maximized, which leads to an ideal situation where the current is only an infinitesimal step below the short-circuit current while the voltage is equally close to the open circuit voltage for an ideal cell, which has a totally flat I–V curve up to the open-circuit voltage where it drops instantaneously to zero. (Fonash, 2010)

Since no real solar panel is ideal, the maximum current decreases as the voltage increases and vice versa, and there is thus a trade-off between voltage and current. Four typical I–V curves with corresponding power curves for Stion STN solar cells are shown in Figure 4. It is clear from the figure that there is an optimal level of voltage and current where the panel produces its maximum amount of power; this is called the maximum power point (MPP) (Chen, 2011).

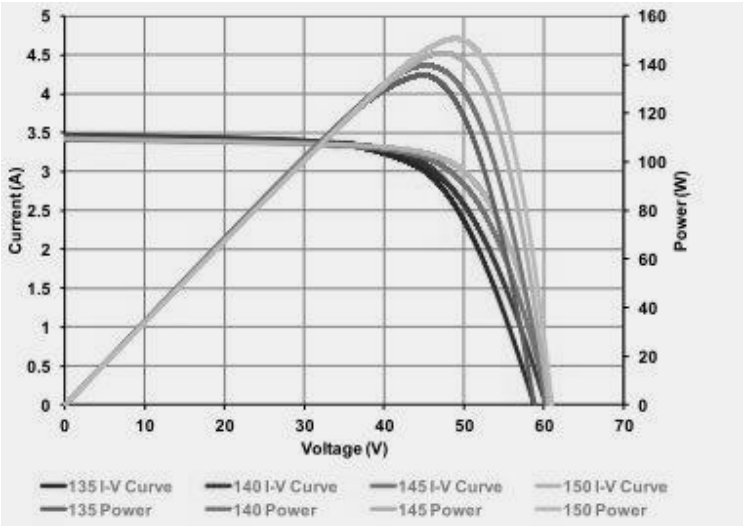

Figure 4: I–V curves with corresponding power curves for Stion STN solar cells (Stion Corporation, 2012)

The nominal power of a solar panel is the power produced at the MPP during STC (Wenham, 2007), but during field operation the cells almost never operate at STC. For any given solar panel the I–V curve and corresponding P curve changes, mainly due to variations in temperature and solar irradiance (Feist et al., 2011). There is thus a different I–V curve for every level of irradiance and temperature.

The most profound changes in power are due to changes in incoming energy from the sun (Chen, 2011). At STC the incoming energy is exactly 1,000 W/m² (Eikelboom and Jansen, 2000). If a solar panel has an efficiency of 20% and is 1 m² large it has a power of 200 W at STC. If the irradiance level dropped to 150 W/m² (a typical cloudy spring day) the panel would need an efficiency of more than 100% to have the same power output, which naturally is impossible. Instead the efficiency of the cells

is approximately constant for irradiance levels close to STC but drops as the irradiance levels decrease (Razykov et al., 2011). The average and peak irradiance depends on the geographical location of the solar panel; in northern Europe the irradiance levels of STC are almost never reached (Wenham, 2007). Since the geographical area in focus of this thesis is Sweden the low-light performance of solar panels is a key factor.

For irradiance levels below STC either voltage or current decreases if the other is held constant, resulting in a decrease of power output from the solar panel. Experiments by Feist et al. (2010) has shown that the open circuit voltage generated by several different types of commercially available solar panels are basically unaffected by irradiance levels. At an irradiance level of 150 W/m² all the panels in the experiment still operated at voltage levels close to the ones at STC. It is thus mainly the photovoltaic short-circuit current that decreases at lower irradiance levels. Below light levels of 850 W/m² the efficiencies of solar panels start to decrease (Kalogirou, 2014), but the efficiency at lower light levels depends heavily on the type of panel used.

Thin film solar cells (CIGS, CdTe and a-Si) are generally promoted as performing well in low light conditions (Razykov et al., 2011). The superior performance of thin film cells is supported by experiments by Feist et al. (2010), with results showing that the efficiency of the tested c-Si cell dropped to less than 10% of nominal efficiency at 100 W/m². At 100 W/m² the best CIGS cell still performed at above 60% of nominal efficiency with several other CIGS cells performing well above the c-Si cell. The results is in line with similar experiments by Reich et al. (2005), which showed that CIGS and a-Si outperformed crystalline silicon cells at irradiance levels between 100 and 850 W/m². The excellent performance of a-Si in low light conditions is also showed experimentally by Yunaz et al. (2009).

Another factor related to changes in irradiance levels is the distribution of energy levels in the incoming photons—the solar spectrum. During STC a standardized solar spectrum (AM 1.5) is used, but during field operations this spectrum is not constant. During direct sunlight the solar spectrum is close to that of STC, but with overcast sky the light becomes diffuse due to reflections in the clouds resulting in a different spectrum (Kalogirou, 2014). Crystalline silicon solar cells are generally designed to have an electron band gap (and thus being able to absorb photons) in the photon rich part of the solar spectrum at direct sunlight. During diffuse light conditions the efficiency of the cells decrease significantly due to changes in the solar spectrum (Wenham, 2007). Thin film cells, particularly CIGS cells because of the many different materials in the semiconductor (Fonash, 2010), are designed to absorb a wide spectrum of incoming photons. The efficiencies of these types of cells are similar during direct and diffuse light conditions. The generated power of these cells is however still higher during direct sunlight, as the irradiance is higher.

The temperature of the solar cell affects the internal resistance in the cell, and thereby changes the current and voltage in accordance with Ohm's law. Generally the current increases with increased temperature, while the opposite is true for the voltage (Tyagi et al., 2013). However, the maximum power decreases with increased temperature (hence the term thermal degradation) and large temperature increases in the cells are to be avoided. Thermal degradation typically occurs when the solar panel is subjected to high ambient temperatures and high levels of direct irradiance, making effective ventilation of the panels beneficial for operation in warm areas.

Solar cells with a low electron band gap generally experience higher rates of thermal degradation, i.e. higher rates of decreased efficiency as the solar modules gets warmer (Feist et al., 2010). The degradation of the MPP is typically in the order of 0.4–0.6%/°C for crystalline silicon and 0.1–0.6% for thin film solar cells during normal operating conditions (Feist et al., 2010). Generally, thin film cells has lower thermal degradation than c-Si, with CIGS panels having the highest thermal degradation of the

thin film cells due to its characteristic low electron band gap (Wenham, 2007). An interesting observation made by Feist et al. (2011) is that the thermal degradation decreases in low light conditions for CIGS solar cells. This gives CIGS solar cells additional advantages in low light conditions, even though the overall effect on panel efficiency is low.

2.4 System components

While the previous discussion has been centered on the solar modules themselves, in order to generate any useful energy the solar modules needs to be complemented with additional system components.

The components needed in order to transmit and process the generated electricity are referred to as balance of system-components (BOS). This includes everything from fuses and wiring to the components converting current and voltage to suitable levels (Reichelstein and Yorston, 2013).

The most important BOS component is the power converter, which can convert the power to either alternating current (AC) or to direct current (DC) of another voltage level. The photovoltaic current generated by the solar panel is DC, but since most electrical systems use AC the solar energy systems for most applications need inverters to convert the power into AC (Rashid, 2011). Over 99% of all solar power systems use inverters (Fraunhofer Institute, 2012), which are required for grid-connected systems in order to transmit the generated power to the regular power grid.

For off-grid applications, or for applications where no feeding into the power grid is required, DC microgrids are an option to AC systems. For a DC system, a DC–DC converter is needed in order to convert the varying voltage from the solar panels into another voltage which is controllable by the user (Rashid, 2011). This type of application is commonly used to charge a battery bank in order to store energy from solar panels for use when there is no sunlight available, which is especially important for off-grid applications. The DC–DC converter in a solar power system is thus commonly referred to as a solar charge controller (Jawaid et al., 2012).

As explained above, the current and voltage generated by the solar panel (and the corresponding MPP) changes when the panel temperature or the irradiance changes. During field operation there are constantly small changes in temperature and irradiance due to dynamic weather conditions, thus the MPP also constantly changes. In order to adapt the voltage and current to maximize power during the constant changes of the I–V curve the solar energy system needs a maximum power point tracking (MPPT) algorithm (Yadav et al.).

This MPPT control system can either be integrated in the converter or work as a stand-alone component. There are several types of algorithms for MPPT, but the general working principle is that the MPPT continuously makes small changes in voltage and then checks if the output power increased or decreased. Based on that information the tracker knows if the voltage is below or above the MPP-voltage, and adapts accordingly (Yadav et al.). Without a MPPT the solar panel will almost never generate maximum power, and thus the lifetime energy generation can be greatly increased with an efficient MPPT (Fraunhofer Institute, 2012).

Since the angle between the incoming sunlight and the solar panel also affects the generated power an optional component with the potential to increase energy production is a solar tracking system (Kalogirou, 2014). A solar tracking system tilts the panels in order to align the solar panels perpendicularly to the incoming sunlight in order to maximize the incoming energy to the panel. The tracking system can be of different grades of complexity. For example either 1, 2 or 3 axis tracking can be used, where 3-axis tracking is both the most efficient and expensive alternative. Sun tracking is most important for crystalline silicon cells as the efficiency of these types of panels decrease rapidly for a larg-

er angle of incidence (Kalogirou, 2014). Thin film solar cells are generally less sensitive to the irradiance angles and thus solar trackers has lower benefits (Chen, 2011).

2.5 Economy of Solar Power Systems

The profitability of solar energy has been debated heavily during the last decade. Proponents state that solar energy in certain favorable locations already has reached grid parity, meaning that the cost of energy from solar power systems can match that of traditional fossil power sources (Fthenakis, 2009). One such example is California where the combination of a climate with high solar irradiance and carbon-based energy taxes has made the solar power reach grid parity (Branker et al., 2011).

Critics of solar power instead state that the increased interest in solar based energy is caused by public subsidies of solar energy, and that the existence of such subsidies shapes the entire solar market. According to the critics, without governmental subsidies the cost of solar energy compared to traditional energy sources would be too high to ever make solar energy reach grid parity (Reichelstein and Yorston, 2013). While the profitability of solar energy is debated, the costs related to solar power is much easier to determine.

Since the start of commercial manufacturing of solar panels the prices of cells have dropped dramatically. Looking at the market price per watt-peak power (Wp) Reichelstein and Yorston (2013) have noted that the price has fallen to 80% on average every time the total production rates have doubled, which they term the 80–50 rule. Annual production rates has increased rapidly for the past decade (Razykov et al., 2011) with total production increased almost by two orders of magnitude since the year 2000 (Tyagi et al., 2013). During the same time the prices for solar panels have fallen rapidly. The historical development of the market price per watt-peak for solar modules is shown in Figure 5, showing that the 80–50 relationship seems to be valid. Reichelstein and Yorston (2013) predict that this price–production relationship will hold in the future.

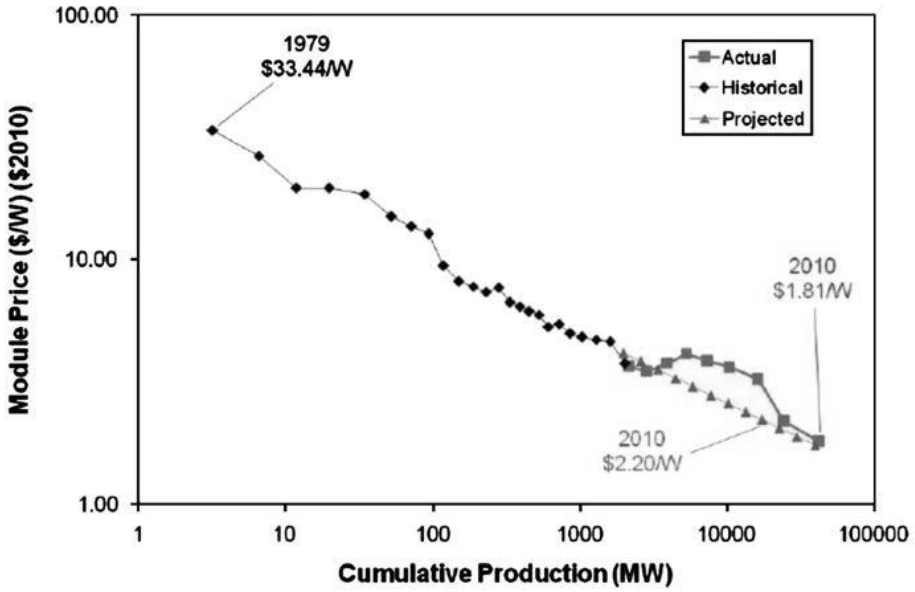

Figure 5: Historical price curve for solar panels (Reichelstein and Yorston, 2013).

The target for the solar industry is currently to be able to produce solar energy systems with a total price below 1 USD/Wp. The manufacturing costs are continuously decreasing, both through more efficient processes and through new designs of solar panels. The efficiency of the panels produced are naturally also of key importance, and the widespread goal is to have modules with an efficiency above 10% below 1 USD/Wp (Tyagi et al., 2013).

The cost for BOS components has also decreased as production capacity increased (Kalogirou, 2014), but the price drop has not been as rapid as for the solar panels. Instead of the exponential decline in costs valid for solar panels, BOS components have a linear price decline on average (Reichelstein and Yorston, 2013). The share of solar panel costs to total system costs depends on the size, location and type of system, and is generally not constant. As of 2011, BOS constitutes more than 50% of the total system cost for most commercial size systems (Reichelstein and Yorston, 2013).

Because of the slower decline in prices for supporting system components compared to solar panels, solar panels constitute a decreasing share of overall system costs. During the last few years this has increased attention to the need of developing more cost-efficient system components. The inverter itself typically constitutes 15% of the total system cost for a grid-tied system and also has an impact on the total system losses (Rashid, 2011). Hence the profitability of solar energy systems could be greatly enhanced by improvements and cost reductions in the supporting system components.

3 Literature: Uninterruptible Power Supply (UPS)

A UPS system is used to protect sensitive electric loads in a wide variety of applications. The UPS is situated upstream from the load it is designed to protect, and is tailored to fit the requirements of the individual load that it is used to power (Nasiri, 2011). Generally an UPS system consists of power electronic components to rectify and invert electricity, an energy storage medium (typically a battery), filters to suppress distortions in the power output and static switches that detects power failures and switches the system into islanding mode which powers the load from the inbuilt energy storage (i.e. battery) (Roth et al., 2002).

Since the introduction of internet the amount of critical computerized equipment in operation has increased sharply. Because of the sensitivity of such loads the demand for absolute reliable power supply and high power quality has increased the usage of UPS systems in the same pace (Ward, 2001). For many companies relying on computerized systems, the costs for system downtime due to power failures are much higher than the cost of the UPS system, making UPS a core technology when building computerized systems (Roth et al., 2002). Ward (2001) estimated in 2001 that about 30% of the electricity used by companies are used to power sensitive loads which would benefit from the increased protection of UPS, and that this number would double by 2010. Even though these numbers are old, the development towards more computerized systems is still continuing and consequently also the increase in demand for UPS systems.

The UPS system and its principal functionality is not a new invention. In fact, the functionality of UPS has remained the same for several decades (a principle text still referred to by many is Price (1989)), but the increased demand has improved the efficiency and sharply decreased costs of UPS systems. Certain advanced designs of UPS have also been developed for large-scale applications consuming much power (i.e. large data centers) to increase conversion efficiencies in order to save electricity (Nasiri, 2011).

3.1 Functionality and applications

The UPS system can serve several functions related to power quality and power reliability. The main functionality of UPS systems is to provide back-up electric power for a specified time (the autonomy time) if the main power supply is cut off or in any other way is unable to deliver satisfying power for a specific application (Falk, 1990). The typical time range can be anything between a few seconds up to several hours depending on application (Chow, 2012). For large-scale applications such as computer halls, UPS systems typically only serve as an intermediate power source before reserve generators can be started (Nasiri, 2011) In less critical systems, for example household applications, a UPS commonly constitutes the sole reserve power system (Moreno-Munoz et al., 2011).

For more advanced types of UPS systems the sensitive load protected by the UPS is also isolated from the power grid, and thus protected from sags and surges in the grid. In these applications the power quality of the electricity provided from the UPS to the load is much higher than the power grid. At the same time the UPS also protects other devices from the harmonics caused by the sensitive equipment powered by the UPS (Moreno-Munoz et al., 2011). When the UPS is converting the incoming power from the grid during normal operation it is also possible for the UPS to adjust the voltage and frequency to user-defined levels. This can be used when the load uses another voltage or frequency compared to the power grid (Nasiri, 2011).

Typical large-scale systems that need to be protected by UPS systems are data centers, airport lighting, medical systems and industrial processing plants (Chow, 2012). These applications typically use more

advanced UPS systems that not only serve as back-up power but also use the power quality protection that certain UPS systems provide. Applications of smaller scale are typically distributed telecommunication stations, automatic weather monitoring stations and personal computers where the back-up power in case of power grid failures is the main functionality provided by the UPS (Nasiri, 2011).

3.2 Types of UPS

Since UPS systems are used in a wide variety of applications, ranging from safe shutdown of individual computers to back-up systems for entire server halls with a total power of several MW, the types, sizes and functionalities of UPS systems differ significantly.

One general categorization used is to classify the UPS based on the energy storage system used. With this classification method the UPS systems are either stationary—utilizing a battery for energy storage—or rotary, relying on flywheels to store energy as mechanical energy (Nasiri, 2011). The majority of UPS systems are stationary, and flywheel technology is mainly used in applications with high power where back-up power is only needed for a few seconds. By the use of batteries the back-up time for the UPS is determined by the dimensioning of the battery bank, which can be adjusted to the demands of the load. Hybrids of the two technologies are also possible, but due to the increased costs they are only used in large scale systems powering critical loads (Nasiri, 2011). Only stationary UPS systems are of interest for this thesis.

Stationary UPS systems are divided into four main categories based on their functionality and basic working principle. Sorted by increasing complexity the categories are: off-line, line-interactive, on-line and true (delta conversion) UPS.

An off-line UPS is mainly used in smaller applications, for example in back-up systems for individual computers or other similar household applications. The off-line UPS only serves as a second source of power in case of loss of the normal power supply (Ward, 2001). The working principle of an off-line UPS is shown in Figure 6.

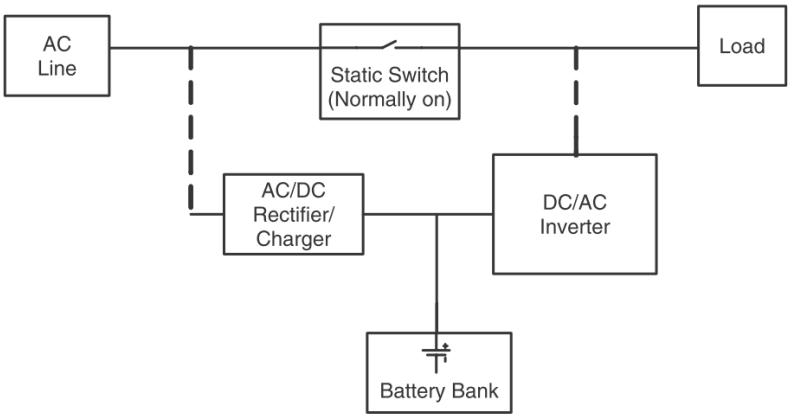

Figure 6: Off-line UPS (Nasiri, 2011)

The figure shows that the load is powered directly from the normal power grid during normal operation, and the UPS is disconnected from the load. During normal operation a small (trickle) current is used to charge the battery and then keep it fully charged. Since an off-line UPS does not isolate the load from the power grid the load is not protected from sags and surges in the grid (Moreno-Munoz et al., 2011).

In case of a power failure, or when the quality of the incoming power is decreased below a pre-set threshold, the switch switches off the power grid and instead connects the battery to the load. Since the switch has to detect a power failure and then make a switching before the battery back-up can be

used to power the load there is a delay between the two power sources. This delay is in the order of a quarter of a cycle and less sensitive equipment like personal computers are unaffected by this transition time. An off-line UPS cannot be used to power highly sensitive loads however, as the transition time could damage such equipment (Nasiri, 2011).

For applications where the power quality of the normal power grid could be a problem, on-line UPS systems are typically used. In an on-line UPS system the load is completely isolated from the power grid and all electricity flow through the UPS. The UPS uses double conversion where the incoming electricity during normal operation is rectified into DC and a minor current is used to charge the battery. The remaining power is converted back to AC through an inverter and used to power the critical load (Figure 7) (Roth et al., 2002).

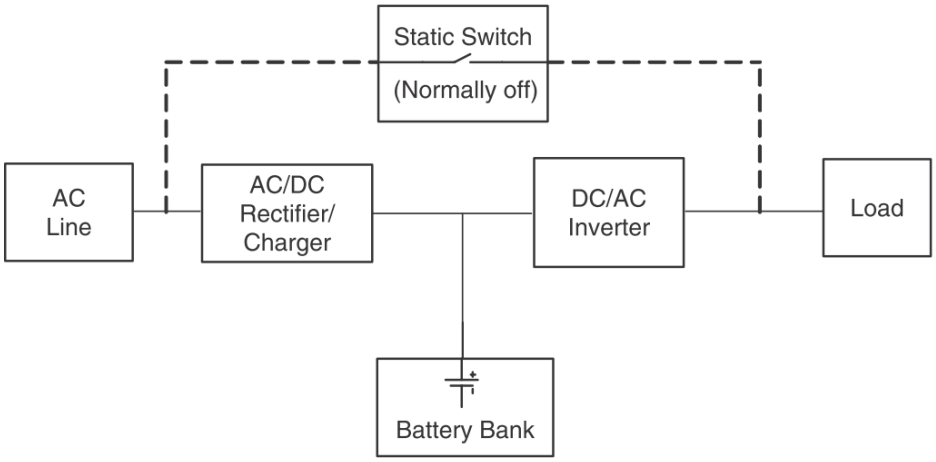

Figure 7: Online UPS (Nasiri, 2011)

This design has the advantages that the load is protected from all types of power contamination present in the power grid, that the voltage and frequency of the AC can be adjusted in the UPS and that in the case of power failure there is no transition time before the battery start to power the load (Chow, 2012). The multi-functionality provided by on-line UPS is the reason why this type of UPS is most common for digital offices and data centers (Moreno-Munoz et al., 2011).

However the double conversion also results in a lower efficiency due to conversion losses in the power electronic components. Since the power is continuously fed through both a rectifier and an inverter the power losses makes the operation of an on-line UPS more expensive than an off-line UPS (Nasiri, 2011). Efficient components is thus of critical importance in an on-line UPS.

Apart from the two main types of stationary UPS—off-line and on-line—there are also two other models which have been developed to solve specific problems related to on-line and off-line UPS.

The line-interactive UPS is shown in Figure 8 and can function as both an off-line and on-line UPS. The bi-directional AC–DC converter can both rectify power to charge the battery and invert the power from the battery in order to power the load. During normal operations the line-interactive UPS can go into on-line mode in order to either adjust the voltage (but not frequency) or improve the power factor of the load. If this is not required the UPS works as an off-line UPS with the electricity from the power grid going directly into the load. In the case of a power failure the static switch disconnects the grid and the system enters islanding mode with the battery powering the load. (Nasiri, 2011)

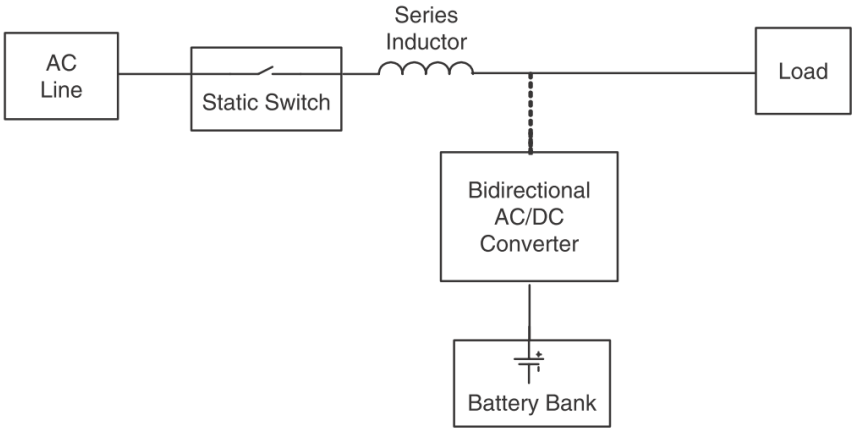

Figure 8: Line-interactive UPS (Nasiri, 2011)

The advantage of the line-interactive UPS is that it can provide some power factor correction and voltage adjustment without the increased complexity and losses of double conversion in on-line UPS (Nasiri, 2011). However the load is not isolated from the power grid and is thus still subjected to some power contaminations from the power grid (Moreno-Munoz et al., 2011). The line-interactive UPS can thus be seen as an intermediate between off-line and on-line UPS.

Large data centers use large amounts of energy, and in such applications the high losses connected to the double conversion of the on-line UPS can result in high costs. For such applications an advanced version of UPS called true (or delta conversion) UPS can be utilized (Moreno-Munoz et al., 2011).

The principle outline of a true UPS (consists of two bi-directional converters – one in series and one in parallel with the main power line. Both of the converters can be used to charge the battery but only the parallel converter can be used to supply the load in islanding mode (Nasiri, 2011).

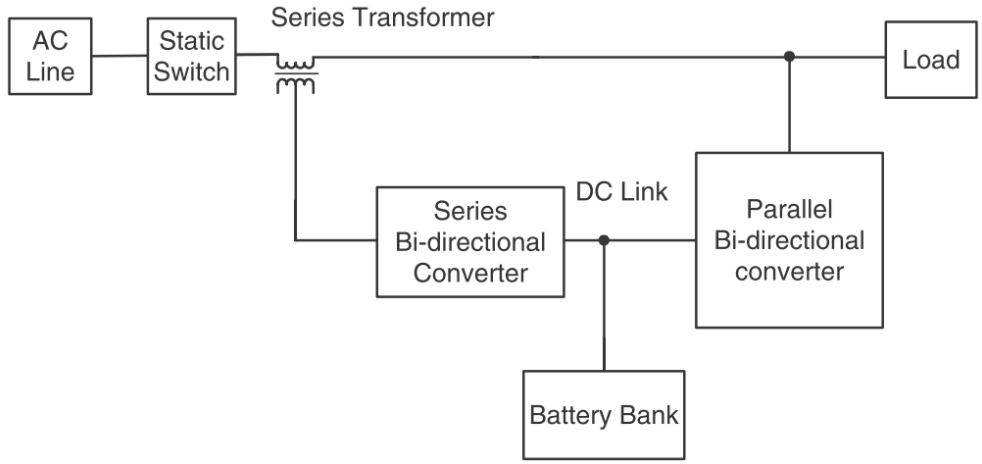

Figure 9: True UPS (Nasiri, 2011)

During normal operation the parallel converter is used to absorb power irregularities related to harmonic distortion and current distortions. At the same time the series converter mitigates surges and sags in the voltage, while charging the battery (Nasiri, 2011). The main advantage of this system is that most of the power goes directly from the grid into the load, with the battery and converters only providing power to even out all irregularities. By avoiding the double conversion of all power – as in the on-line UPS – the efficiency is increased from approximately 90% to 95% (Roth et al., 2002). This type of UPS has still not reached maturity and thus still have a relative low market share (Moreno-Munoz et al., 2011).

Since the scope of this thesis is to evaluate the combination of solar power and UPS in larger applications (such as data centers and industry) off-line and line-interactive UPS are not applicable. Because most industry-scale UPS systems are on-line, this study will be limited to on-line UPS. The system design with a DC-link in between the two converters in the on-line UPS design is also the only UPS system where all power is converted to DC and back to AC, which increases the potential for large combined systems.

4 Literature: Power Electronics

The field of power electronics is concerned with electronic circuits designed to control the flow of electrical energy in a system. Power electronic devices use semiconductor switches (thyristors, MOSFETs, IGBTs etc.) to accomplish this. Particularly, resistors are not used since the objective of a power electronic circuit is to control the flow of energy while not consuming energy itself. (Rashid, 2011)

4.1 Inverters

The objective of an inverter (also called DC–AC converter) is to convert direct current to alternating current, and in some cases to also adjust the voltage level. Inverters are common in both solar power systems and required in on-line UPS systems with batteries as energy storage (Fuchs and Masoum, 2011, Strzelecki and Benysek, 2008). Inverters can be classified into three different categories regarding the output—pure sine wave, modified sine wave and square wave (Kumar Chinnaiyan et al., 2013). Ideally, a pure sine wave inverter produces an output voltage that is a perfect sine wave regardless of load. A modified sine wave inverter on the other hand is designed to produce a waveform that is similar but not identical to a sine wave. Square wave inverters produce a square wave output and are the simplest in design. Modified sine wave and square wave inverters are typically cheaper than pure sine wave inverters, but in many applications (such as UPS) pure sine wave inverters are preferable. Both modified and square wave inverters introduce harmonics that can be harmful to sensitive equipment (Kumar Chinnaiyan et al., 2013).

Of special interest to this thesis are grid-tied photovoltaic inverters. Grid-tied inverters must be able to sense the output (grid) waveform and be able to adjust its own operation based on it in order to deliver maximum active power. Grid-tied inverters are very common in solar PV installations. Grid-tied inverters are typically pure sine wave in order to not pollute the grid with unwanted harmonics (Eltawil and Zhao, 2010). An important parameter in a grid-tied system is the conversion efficiency of the inverter. Driesse et al. (2008) propose a linear model with six (Equation 1) or nine coefficients to model the power losses in a grid-tied PV inverter. The main determinants of efficiency for a certain inverter are the input/output power and input voltage, and that fact is reflected in the model. Typically an inverter has its peak efficiency at around 30% of rated power. Below the peak efficiency the drop in efficiency as the power goes to zero decreases rapidly while the efficiency above the peak decreases slowly up to 100% power. An example graph is shown in Figure 10, from SMA's Sunny Tripower TL17000 17 kW inverter.

$$p_{loss} = \left(b_{0,0} + b_{0,1}(V_{in} - 1)\right) + \left(b_{1,0} + b_{1,1}(V_{in} - 1)\right) p_{in} + \left(b_{2,0} + b_{2,1}(V_{in} - 1)\right) {p_{in}}^2 \quad (1)$$

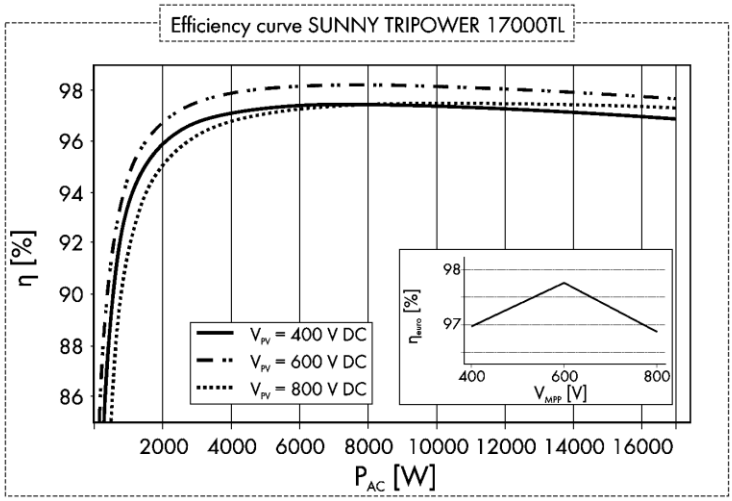

Figure 10: The efficiency curve for a SMA Sunny Tripower TL17000 inverter (SMA Solar Technology AG, 2013)

The inversion in any non-ideal inverter results in the addition of non-linear components such as harmonic distortions to the output. Harmonic distortions are ripples with frequencies of integer multiplicities of the fundamental frequency of the wave (Chattopadhyay et al., 2011). For example an inverter with a 230V, 50Hz AC output is likely to also have non-linear components with frequencies of 100Hz and 200Hz present in the outgoing waveform.

In order to enhance the power quality, harmonic distortion should be minimized or ideally be eliminated from the output wave. A measure of harmonic distortion frequently used for inverters is total harmonic distortion (THD) which is represented by a percentage indicating how much of the total voltage or current that is of other frequencies than the fundamental frequency—thus it is essentially a measure of impurities of the waveform (Rashid, 2011). Pure sine wave inverters typically have a lower THD than modified sine wave inverters as indicated earlier, making them more suitable for UPS purposes since high power quality is a critical functionality of the UPS system. Grid-tied inverters usually have a THD of below 3%—making it a cleaner source than the utility grid in many cases (Eltawil and Zhao, 2010).

4.2 DC–DC converters

A DC–DC converter converts direct current from one voltage/current level to another. There are three types of DC–DC converters considering voltage characteristics: the buck converter can only convert the voltage down, the boost converter can only convert the voltage to a higher level while the buck-boost converter is a combination of the two and can thus convert an input voltage to both a higher or lower output voltage. (Shepherd and Zhang, 2004)

4.2.1 Buck Converters

The principal diagram of a non-isolating buck converter is presented in Figure 11. When the switch S is on, the current flows directly from the source to the load through the inductor L. When the switch is off that is not possible, but the inductor strives to maintain the current which will continue through the load as the inductor discharges and return through the diode D until the inductor is discharged. The two capacitors are used to smooth the input and output voltages respectively. If the inductor is always conducting current the buck converter is said to be operating in continuous conduction mode. (Shepherd and Zhang, 2004)

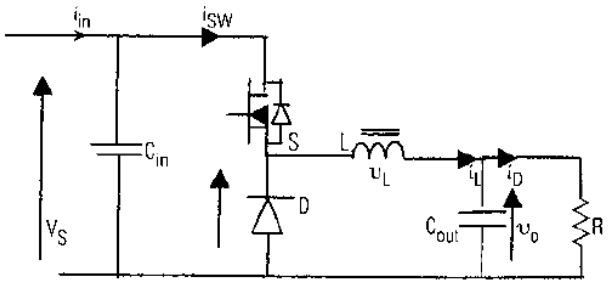

Figure 11: Principle electrical diagram of a buck converter (Shepherd and Zhang, 2004)

4.2.2 Boost converters

Non-isolating DC–DC boost converters (Figure 12) are similar in design to buck converters. When the switch S is on, the only component between the source terminals (except for the input capacitor) is the inductor L and the switch, which have a constant voltage drop. This means that current will start to build up in the inductor, and since there are no resistance in series in the ideal case, the current will continue to rise until the switch S is turned off. When the switch is turned off, the inductor will strive to maintain the current through it but now the current instead goes to the load through the output filter. (Shepherd and Zhang, 2004)

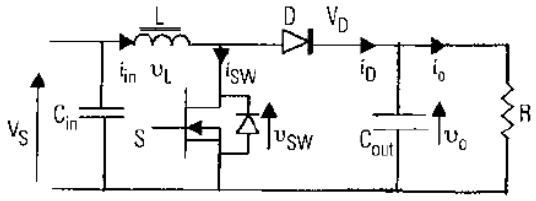

Figure 12: Principle electrical diagram of a boost converter (Shepherd and Zhang, 2004)

4.2.3 Buck-Boost converters

DC–DC converters that are capable of converting an input voltage to both a lower and higher output voltage are called buck-boost converters. A typical non-isolated buck-boost converter is shown in Figure 13. When the switch S is on, current is drawn from the source through the inductor L. When the switch is turned off, the inductor maintains the current but it must now go through the load and the diode D. Since the output voltage is negative with respect to the ground, this converter is called an inverting buck-boost converter. One way of constructing a non-inverting buck-boost converter is to provide galvanic isolation through a transformer.

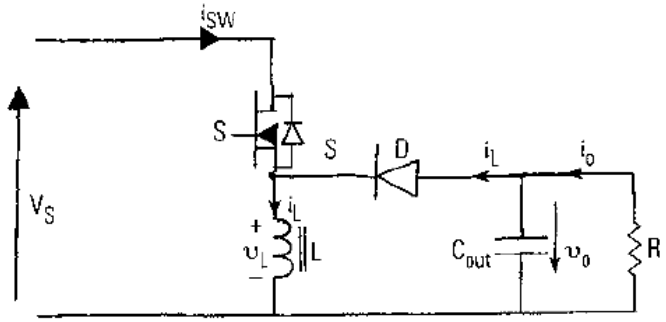

Figure 13: Principle electrical diagram of a buck-boost converter (Shepherd and Zhang, 2004)

An especially important topology in non-inverting buck-boost converters is the flyback converter as illustrated in Figure 14. The transformer provides galvanic isolation as well as a mean of constructing a

non-inverting buck-boost converter. Moreover, the number of windings can be adjusted so that the transformer can participate in the voltage conversion. (Rashid, 2011)

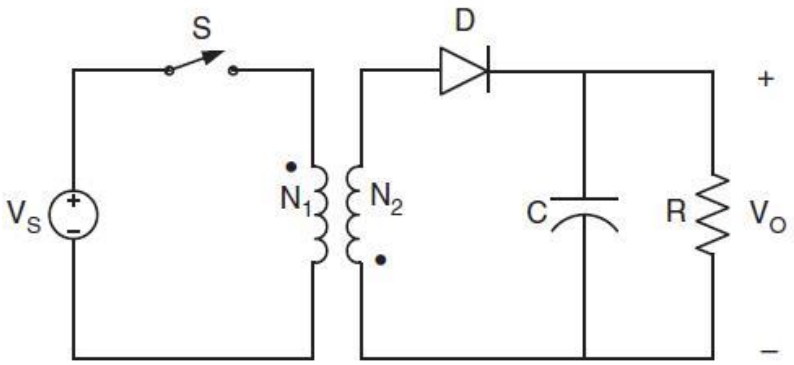

Figure 14: Principal electrical diagram of flyback converter (Rashid, 2011)

4.3 AC–DC converters

To convert power from alternating current to direct current, an AC–DC converter, also called rectifier, can be used. The simplest form of rectification for a single-phase circuit is achieved by one diode in series with the load, as shown in Figure 15. However the waveform produced is far from an ideal DC voltage which is why this arrangement is seldom used in practice. The circuit simply removes the negative part of the AC current which means that there will be no current flowing in the circuit 50% of the time, considering a pure resistive load. (Shepherd and Zhang, 2004)

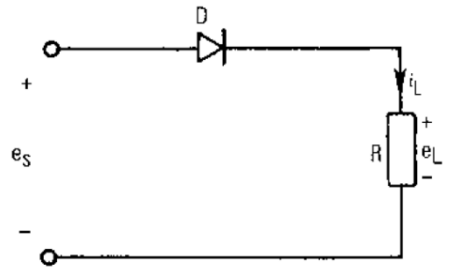

Figure 15: Electrical diagram of a half-wave rectifier (Shepherd and Zhang, 2004)

An improvement of the single-diode rectifier is the full-wave rectifier seen in Figure 16, consisting of four diodes instead of one. The load is shown as a resistance R in the diagram. A full-wave diode rectifier is designed to convert both the positive and negative parts of the AC current into positive current. The resulting waveform (Figure 17) is still far from ideal DC current, but it is possible to smooth the current with the use of filters. Particularly, a high inductance in series with the load will try to preserve the current through the load which results in a waveform that is closer to ideal DC. (Shepherd and Zhang, 2004)

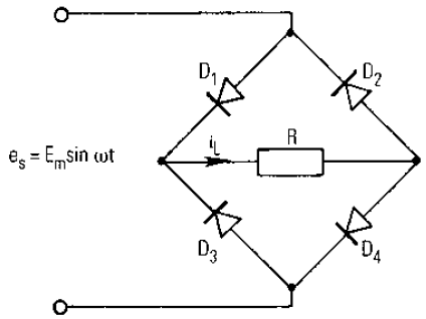

Figure 16: Electrical diagram of a full-wave bridge rectifier (Shepherd and Zhang, 2004)

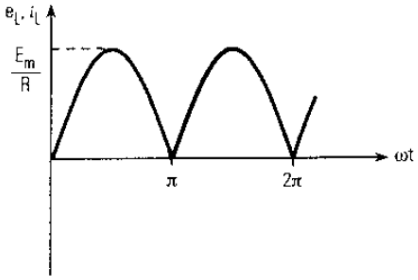

Figure 17: Voltage and current waveform over the load (R) in the full-wave bridge rectifier shown in Figure 16 (Shepherd and Zhang, 2004)

In order to establish control over the RMS output voltage in a full-wave rectifier, a controllable switching device can be connected in series with the load. Alternatively, some or all of the diodes in the bridge can be replaced by controlled switching devices, such as thyristors. The first option is the cheapest, but if all diodes are replaced by thyristors the device can work as both a rectifier and an inverter (Shepherd and Zhang, 2004). To control the device, it is necessary to control the firing angle of the thyristors, which can be seen as *a* in Figure 18. Although increasing values of *a* will reduce the RMS value of the resulting current, it will unfortunately increase the ripple factor of the output which can be defined as the ratio of the root mean square value of the AC component divided by the value of the DC component (Electronics Project, 2014). (Shepherd and Zhang, 2004)

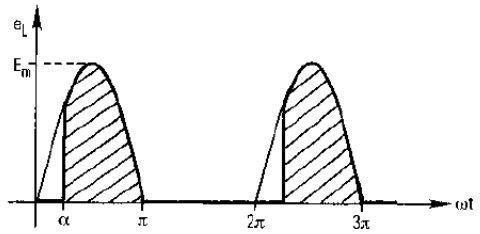

Figure 18: Waveform of a controlled half-wave rectifier, where α is the firing angle of the thyristors (Shepherd and Zhang, 2004)

To reduce the ripple factor and make the output closer to ideal DC, filters can be used. There are two major typologies commonly employed in rectifier applications: inductor-input and capacitor-input filters. The typology is determined by which component is present directly after the rectifying bridge, and a capacitor-input filter can thus have both capacitors and inductors such as the so-called n-filter showed in Figure 19. What makes this filter a capacitor-input filter is the fact that the capacitor C1 is placed upstream of the inductor L.

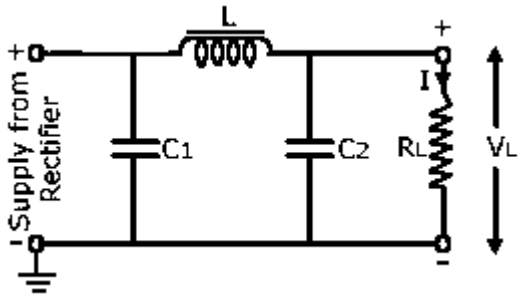

Figure 19: One type of capacitor-input filter: the n-filter (CircuitsToday, 2014)

Inductor-input filters are preferred in high power circuits, while capacitor-input filters are typically cheaper but entail problems with excessive turn-on and surge currents. In inductor-input filters, the inductance needs to be sufficiently large to maintain current to the load. The borderline between continuous and discontinuous operation is called critical inductance and is dependent on the load; a higher load decreases the load impedance and thus increases the ratio between the inductor impedance and load impedance, creating a smoother waveform. (Rashid, 2011)

Capacitor-input filters strive to maintain the rectifier output voltage rather than the current. This leads to voltage and current waveforms as seen in Figure 20. From this figure the major drawback of capacitor filters can be seen, namely that the supply current is very distorted and large compared to inductor filters. Another problem with capacitor filtering is that the inrush current can be very large. When powering up the circuit, the capacitor acts as a short circuit in practice if the initial capacitor voltage is zero. Therefore a resistor placed on the AC side is typically applied to limit the inrush current, unfortunately leading to losses in the circuit. (Rashid, 2011)

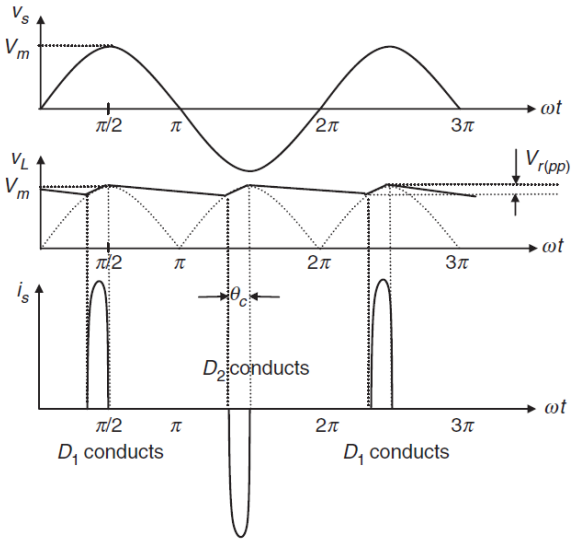

Figure 20: Effects on voltage and source current of a rectifier capacitor filter (Rashid, 2011)

The efficiency of an AC–DC converter is on average lower than that of DC–DC and DC–AC converters. For example Nguyen and Yoon (2014) uses a practical efficiency of 91% for AC–DC converters while DC–DC are assumed to be 94% efficient and DC–AC converters 97% efficient.

4.4 Power Electronics in Solar Power Systems

Applying power electronics to solar power system means that the design of conversion components is subject to the characteristics of PV systems. Regular inverters and DC–DC converters are not seldom designed to work with a relatively constant input voltage, thus the input range is not very diverse. Converting power from solar panels however often means that the input voltage must be allowed to take on a range of values that a normal power converter cannot handle (Eltawil and Zhao, 2010).

Even more importantly, the converter must be able to monitor and adjust the input voltage in order to deliver maximum power at the maximum power point (MPP) of the solar panels. This technique is known as maximum power point tracking (MPPT) (Rashid, 2011).

There are many different algorithms for implementing MPPT, the two most common being perturb and observe (P&O) and incremental conductance (IC) described by for example (Ishaque et al., 2014). A thorough description of MPPT algorithms is outside of the scope for this thesis; readers are referred to the rich amount of literature on the subject.

5 Literature: Microgrids

An UPS system, especially when combined with electricity generation sources, can be closely resembled to the concept of microgrids in the academic literature. A microgrid is part of a larger power distribution system and is designed to work either autonomously parallel to the grid or in transition between grid-connected mode and autonomous mode. The autonomous mode can also be termed islanding mode (Lidula and Rajapakse, 2011).

A microgrid consists of three parts: generation, storage and load. Some researchers also separate generation from grid connected voltage source converters (G-VSC) which are used in DC microgrids to extract power from a connected AC grid (typically the utility grid) (Dong and Lie, 2012). Energy generation sources in microgrids typically falls into the category of distributed generation (DG), which means that their output power is low compared to utility-sized power plants. Especially renewable energy sources such as wind and solar PV has been identified as suitable for microgrids for various reasons. This is the reason why the academic interest in DG and microgrids has increased recently (Sullivan et al., 2014). Energy storage (ES) is used to maintain the power balance in the microgrid which reduces the effects of transients, provide ride-through capabilities in case of variation in generation and helps to provide power during transitions between islanding and grid-connected mode. In theory almost any energy-storage device can be used but the most suitable for microgrids are batteries, fly-wheels and super capacitors (Lidula and Rajapakse, 2011).

Microgrids can be categorized according to which configuration of AC and DC it uses. There are four major configurations in the literature: DC, AC, AC–DC hybrid and 3–NET microgrids. The latter combines a high-quality DC network for sensitive loads, a low-quality DC network for non-critical loads and an AC network. (Nguyen and Yoon, 2014)

Among the central questions concerning the implementation of a microgrid is how to control the system for achieving optimal performance. A typical microgrid utilizes two or more sources of electrical power at the same time, and the balancing between these sources have to be chosen considering technical and economical parameters. One common set-up is one or more renewable energy sources as an energy source of first priority (maximizing power), while using the power grid or energy storage as second priority energy sources (Dong and Lie, 2012). The reason is that the variable cost of producing renewable energy is generally lower than the cost of utility power. Thus power from renewable sources should be maximized, and energy storage and mains should step in when the energy produced from the renewable sources is not enough to supply the load (Su and Wang, 2012).

There are two major types of control when it comes to a microgrid: centralized or autonomous. A central control system collects data from several different components and points in the microgrid and also has the ability to control several components at the same time. Autonomous control builds on the fact that components can communicate indirectly by sensing the common DC voltage of the components, and assumes that the components have the ability to control themselves to achieve the desired system configuration. Alternatively for AC microgrids, autonomous frequency control is a viable option if there is enough rotating energy in motor loads and generators. (Dong and Lie, 2012)

When controlling a microgrid autonomously, generation terminals and the G-VSC have to be either a power terminal or a slack terminal. A power terminal always maximizes output power while a slack terminal strives to deliver enough power to maintain balance in the system. A slack terminal often does this by sensing the output voltage and adjusting its output to maintain a specific voltage. For example Dong and Lie (2012) use the G-VSC and the energy storage as slack terminals while using the generation from renewables as power terminals.

6 Literature: Economic factors

The economics of solar energy has been widely debated and researched during the past decades, but no single answer has been agreed on. Thus this section does not focus on the numbers presented by previous researchers (since these constantly change and are strongly influenced by the specific installations) but rather on the factors and tools used when calculating the economic value of solar energy. Tools used for more general investment calculations are also discussed.

6.1 Life cycle costing (LCC)

Life cycle costing (LCC) is a method used when making investment calculations in general, and includes all costs related to an investment alternative over the entire lifetime of the investment while also taking the time value of money into account (Kalogirou, 2014).

The method is an alternative that counters the simple investment decisions which commonly puts too much emphasis on the investment costs related to the purchasing of equipment at the start of the investment. LCC usually includes operating costs, maintenance costs, environmental costs and the different lifetime of investment alternatives (Harvard University Office for Sustainability, 2013). A very similar concept is cost of ownership which includes all costs related to owning a system or a machine, which is a tool gaining in popularity in company investments.

Related to small-scale solar PV, LCC analysis is typically used to compare the higher initial costs of solar PV with the much higher operating costs of for example diesel generators (Jawaid et al., 2012). As more costs which before have been seen as externalities—mainly related to GHG emissions and pollution—is internalized as taxes and fees, the LCC calculations generally favor renewable energy and particularly solar PV over traditional fossil energy sources (Sherwani et al., 2010, Varun et al., 2009).

Other benefits of solar PV in LCC calculations are the low maintenance costs which are essentially zero, and the long lifetime. The value at the end of the lifetime is also included in LCC, which for solar PV means that the low recycling and scrapping costs (Fthenakis, 2009) further benefits this energy source in comparison with others.

6.2 Levelized cost of electricity (LCOE)

A general method for comparing the overall costs of different energy sources is to calculate the levelized cost of electricity (LCOE) for the energy sources. LCOE is mainly used as a benchmark which enables widely different installations and energy sources to be compared related to its costs (Branker et al., 2011). LCOE is a method which aims to include all costs over the lifetime of the installation and present the energy price which makes the installation precisely reach the break-even point over its lifetime, with regard taken to paying an acceptable return to investors (Reichelstein and Yorston, 2013). Thus the lower the LCOE, the lower energy price is necessary to make the installation profitable.

Basically, calculation of LCOE is a calculation of discounted cash flows over the lifetime of the installation, taking the time value of money, expected lifetime of the installation and all types of costs and profits into the calculation. Major factors influencing LCOE for renewables are discount rates, taxes, legislation and subsidies. Reichelstein and Yorston (2013) argue that the resulting LCOE for solar PV is heavily influenced by assumptions made regarding subsidies, taxes and solar irradiance. In their analysis they conclude that the available sun hours per year—which is translated into generated electricity—has the highest influence on the resulting LCOE, thus making the specific environment of an installation the most important factor. This means that a general LCOE for solar PV is very hard to calculate and regional approximations of LCOE is probably a more feasible alternative in order to benchmark dif-

ferent energy sources. Even though LCOE is quite unambiguously defined, the methods for calculating the discounted cash flows is not completely agreed upon, making the resulting LCOE differ significantly between different assessments (Reichelstein and Yorston, 2013).

Additionally, the debate regarding when solar energy will reach grid parity (i.e. be cost-competitive with traditional fossil energy sources) is a question of public energy policy. If the subsidies for solar energy would be removed in Germany the LCOE of solar PV would increase by 70%, making solar energy not reach grid parity until after 2030 (Reichelstein and Yorston, 2013). Branker et al. (2011) argue that the LCOE of solar energy is often calculated higher (less attractive) compared to other alternatives due to very conservative assumptions on technical parameters such as lifetime of the panels, degradation and performance of the system. Due to the rapid development of solar PV technologies investment calculations are often based on outdated data and thus the LCOE does not reflect the newer systems on the market. Equally important is the discount rate which for all investment calculations should reflect the risk of the investment. The risks are often overestimated for solar PV due to its rapid development, once again increasing the LCOE (Branker et al., 2011).

From the previous discussion, the conclusion can be drawn that the assumptions used when calculating life cycle costs and the corresponding LCOE has a significant impact on the final result. Thus calculating the benefits of solar energy requires a careful analysis of the development of both electricity prices and legislation.

7 Literature: Previous research in the combination of UPS and solar PV

The aim of this study is to explore the possibilities to combine UPS and solar PV systems. This is an area where little previous research has been carried out, but there have been a few previous publications regarding this combination. None of the previous publications does however have the same aim— economical synergies with reliable power grids— and thus is rather used to test the results of specific parts of our study against.

Nonaka and Harada (1997) present a prototype for a utility interactive solar power system which is combined with a battery used as energy storage. This paper is quite old (published in 1997) and have a heavy focus on the electrical behavior of the components used. The circuit which the authors have built consists of a solar PV panel used to charge a battery with the DC current from the solar panels. In order to power a load the DC current of the battery and PV panels is inverted in a bi-directional inverter. The load can also be served directly by the mains utility supply, and this supply can also be used to charge the battery with the inverter acting as a rectifier. In the case of a power failure the battery can serve the load, and thus the system performs one of the critical tasks of an UPS system— providing back up energy.

Considering that the design of the system does not provide any possibility to isolate the load from the main power grid and thus cannot improve power quality makes it unfit for the type of loads normally served by on-line UPS, which is the focus in this thesis. Similarly the conversion methods and power flow design indicate significant conversion losses, making the system uneconomical. The paper is however a good reference regarding the electrical behavior of power electronic systems, and is very detailed regarding conversion methods and components used.

A more recent publication by Cavallaro et al. (2009) also discusses possible combinations of UPS and solar power systems. The authors do not build a prototype but instead uses computer simulations in MATLAB and Simulink to model a set of solar modules charging a battery bank which is used in an UPS system. The paper discusses the time required to charge a battery bank using only solar power in different weather conditions in Italy, and also methods for intelligent battery charging and load management (Figure 21).

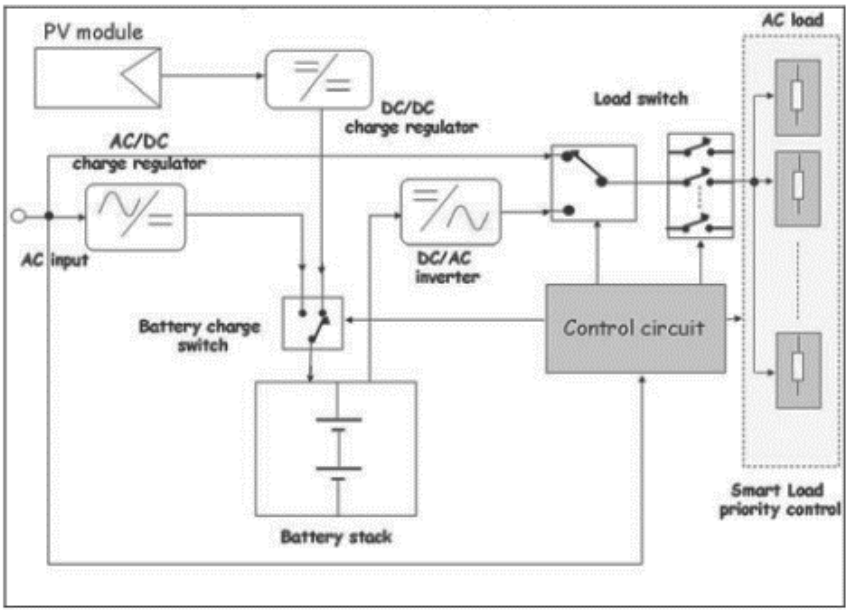

Figure 21: The system presented by Cavallaro et al. (2009)

The system presented in the paper (Figure 21) is in general similar to the system in focus in this thesis, but with some differences. In the work by Cavallaro et al. (2009) the solar modules are only connected to the battery, thus the power from the solar system cannot power the load without going through the battery. Since the battery in a UPS system needs to be kept at full charge this means that the solar panels are only used to restore the battery pack to full charge after a power failure (which in many European countries is rare). As long as the battery is fully charged the solar panels is not used. This is a major difference from this study since the system in this thesis is designed to always prioritize the usage of energy from the solar modules in order to minimize the cost of electricity from the power grid. Since load management is separated from the UPS, the system proposed in this thesis relies on autonomous control and thus there is no need for a central control system.

Another similar system is presented by Jawaid et al. (2012). The research focuses on small scale UPS systems for household applications in Pakistan in order to provide a more reliable power supply than the normal power grid, which in Pakistan can have daily power outages for 3–4 hours according to the author. The system proposed in the study can be seen as an alternative to having a diesel/petroleum generator as the energy source during power outages.

The system proposed by Jawaid et al. (2012) consists of solar panels connected to a DC–DC converter acting as the charge controller of the batteries. The charge controller can also supply power to the load via an inverter, without the power passing through the batteries. There is a switch after the inverter which either uses power from the grid or the solar UPS in order to power the load. As with the system proposed by Nonaka and Harada (1997) this means that the UPS only serves as a back-up power source, and have no impact on power quality or electrical isolation to protect the load. It is thus not suitable for sensitive equipment but rather as an alternative for household applications.

The publications discussed above all differ from the aim of this thesis in two major ways. Firstly, the previous research has a technical focus, mainly on ways to charge the batteries in the UPS in order to provide back-up energy in the case of power outages. In this thesis the expected duration of power outage in the power grid is in the order of minutes per year. Instead the main role of the UPS is to provide higher power quality, with the back-up energy storage only being used a fraction of the time. The solar energy will continuously power part of the load.

Secondly the aim of this study is to find economic benefits when combining UPS and solar power due to both the possibility for higher total system efficiency and the sharing of power handling components. The study assumes that the usages of UPS is necessary in order to protect a sensitive load and aims to explore if the additional installation of solar energy would decrease the costs compared to using two separate systems.

Method

In this section the methods in the studies conducted are presented. Since the study is divided into three parts, three different methods are used. All three are presented in this part along with the assumptions, limitations and delimitations for each study.

8 Method: A summary

This thesis is divided into three consecutive studies: a computer simulation of the designed technical system, experiments on a small scale physical prototype system including solar panels, and finally an economic analysis of a full scale system used for computer hall applications.

Computer simulation
The aim with the computer simulation is two-fold. Firstly, it provides a design tool where it is possible to change and adjust the system conveniently to try different configurations and designs without the need to rebuild a physical system. System parameters can be adjusted in the model in order to quickly find the optimal levels, which will save time during the study of the physical system. In the simulation each component can also be tested individually, during any condition we specify. This will provide increased knowledge about the system, such as the configuration of components.

Secondly, the computer model provides a safe environment to try the most extreme conditions that the UPS system could be subjected to, without the risk of damage to physical components. Such situations include the shut-down of the entire system due to deep discharge of the battery, and the start of the system after a major failure. It also includes fault conditions which are not supposed to happen. The time scale can also be adjusted to suit the specific purpose of an experiment.

The system is simulated in the MATLAB extension Simulink Power Systems, and all components in the designed system are modelled except the inverter which is seen as purely resistive.

Prototype system
After finalizing the simulated computer model of the system a small-scale physical system was constructed, consisting of the principal components of an on-line double conversion UPS with solar panels and a solar charge controller. The load is designed to require a typical power of 300 W, with a peak load well under 1,000 W. The aim of the physical system is to make experiments in order to see if the addition of solar panels and the related solar charge controller (DC–DC converter) has any negative or positive effect on the electrical behavior of the system.

Experiments corresponding to the operational modes studied in the computer simulation were conducted first without and then with the solar panels and solar charge controller connected to the system. Measurements of voltages, power consumption and current were made in order to analyze both the continuous levels and transients. With the addition of the solar panels several other experiments were added related to the operation of the solar panels to ensure that the designed operational modes of the solar panels are working properly. The physical experiments aim to evaluate the technical feasibility of combining solar energy and UPS systems.

Economic Analysis
While the physical prototype system has a power output of less than 1000 W, a full-scale double conversion UPS is typically in the scale of 50 kW to 1000 kW. Since the aim of this study is to evaluate economical synergies when combining UPS and solar energy, an economic model was constructed in order to compare full-scale systems.

The aim of this part of the study is to compare the up-front investment costs of the components which are exclusively related to either the connected system or a stand-alone solar power system. This means that only the parts of the system which is dependent on the decision of a combined or a stand-alone system is included in the model, since all other components are independent of the choice of combining the systems.

The economic study also explores total system efficiency, which will generally not be the same in a combined system as with two separate systems. The total system efficiency is represented by calculating the differences in energy bought from the electricity grid, which requires the incoming energy from the sun to be modelled. Thus, a model of the solar panels was made using meteorological data for a standard year in Stockholm. The efficiency of solar inverters and solar charge controllers were estimated based on data from popular components available in the market.

9 Method: Computer simulation

The first study conducted was a computer simulation of the system. The purpose of the simulation is to provide a safe, flexible and reliable design environment where the system can easily be adjusted and tested without the need for changes in a physical system. The primary results of the simulation are the information of how to build the physical system in practice and increased knowledge of the system and how to operate it. Identification of potential issues with the system is also an important part of the computer simulation.

Additionally some experiments which were judged to be safer in the simulation than in practice were conducted in the model only.

9.1 Delimitations and Limitations

The MATLAB simulation was constructed with one primary purpose: to get an indication how the real system could work and what problems may arise. The MATLAB system was thus constructed before the physical system was designed which leads to limitations in the simulation's correspondence with the prototype system.

Regarding the simulation, consideration must be taken that the components are very basic in their design. Only the basic functionality of for example the rectifier and the DC–DC converter has been implemented, because there was no knowledge of the specific typology of the actual components. Some of the components' characteristics have been chosen arbitrarily because it would be out of the scope for this thesis to optimize every part of the system. Much was achieved by trial and error as well as heuristics based on practicality and what can be considered realistic. This limitation leads to a simulated system that behaves differently in certain regards compared to a physical system.

One of the largest discrepancies between the simulated and the physical prototype system is the inverter input impedance. Whereas it is modelled as purely resistive in the simulation, it has a large capacitive element in the prototype system. The reason for this is that the simulation was conducted before a specific inverter was chosen, and the topology of the inverter was thus not known. A purely resistive inverter was chosen in the simulation because of simplicity and speed of simulation. This difference has the effect of significantly higher oscillations in the current entering the inverter in the prototype system compared to the simulated system.

A delimitation of the simulation is the implementation of MPPT. It is simply assumed that the DC–DC converter has an algorithm for determining the MPP. To operate the MPPT in the DC–DC converter in the simulation, a pre-calculated value of the MPP voltage is simply inputted to the control system of the DC–DC converter.

9.2 The MATLAB model

The model is built in the MATLAB extension Simulink Power Systems which is a tool developed for designing and simulating electrical systems. It has four major components: an AC–DC converter, a battery, a DC–DC converter and a load which is meant to symbolize an inverter. The major components will be discussed in separate sections. The components are connected in parallel as seen in Figure 22. The system voltage is set to 56.8 V, which means that the AC–DC converter and the DC–DC converter will strive to keep this voltage while the battery has a nominal voltage of 48 V.

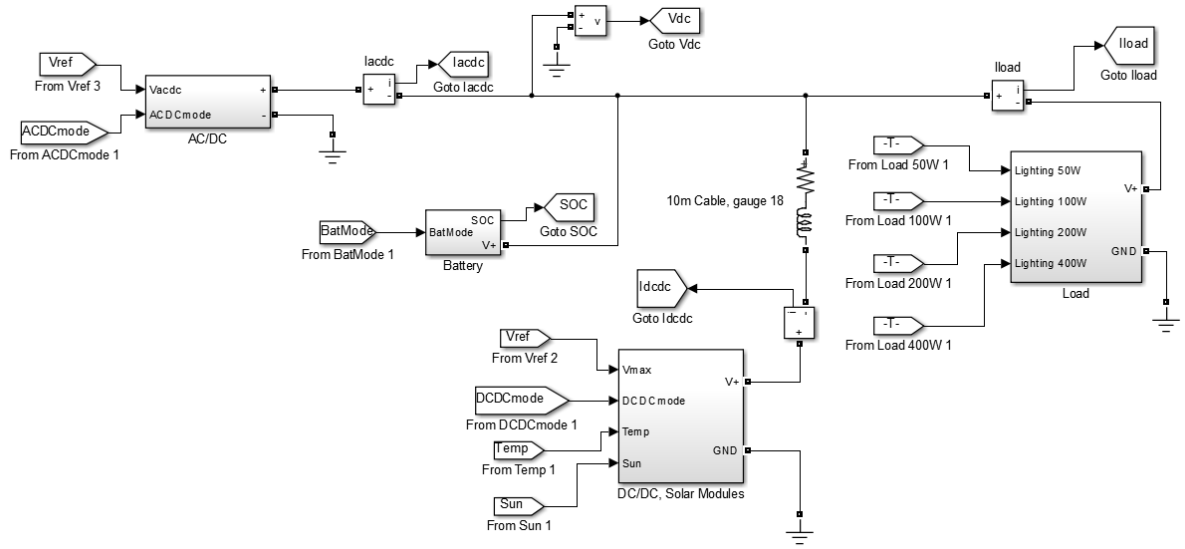

Figure 22: The entire Simulink system

9.2.1 Rectifier

The Simulink representation of the simulated rectifier can be seen in Figure 23.The rectifier converts a simulated mains voltage into 56.8 V DC using a full-wave rectifying bridge and an n-filter.

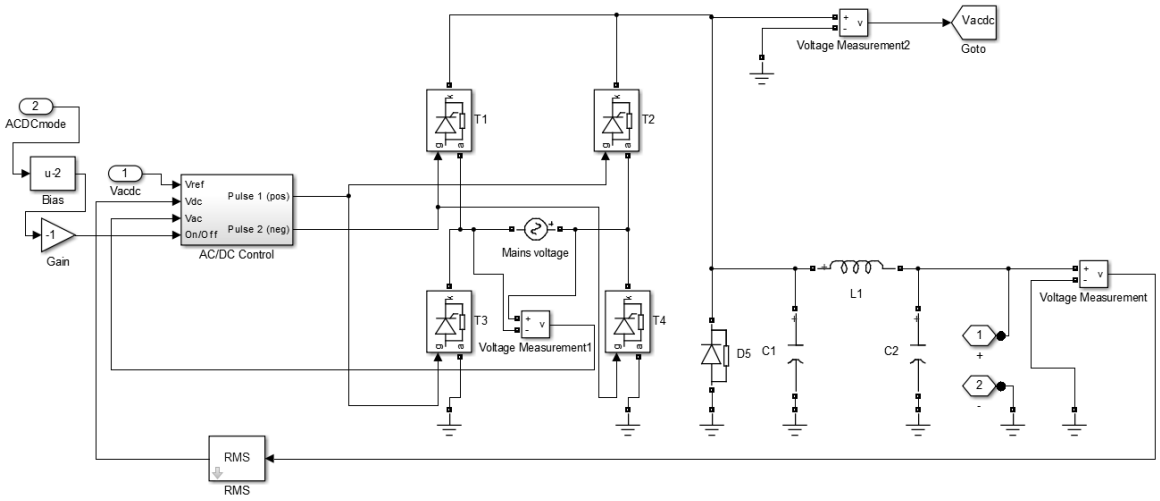

Figure 23: Simulink model of a rectifier

The rectifier is modelled as a full-wave rectifier with all four diodes replaced by thyristors in order to establish control over the output voltage. An output filter is used, and is modelled as an n-filter with the capacitors C1 and C2 at 10 mF and the inductor L1 at 5 mH. A diode D5 is added to allow the inductor L1 to discharge through the load. The output voltage is measured and fed into the control system (Figure 24) which controls the firing angle of the thyristors. The thyristors have a forward voltage drop of 0.8 V, an on-resistance of 0.001 Ω, a snubber resistance of 500 Ω and a snubber capacitance of 250 nF.

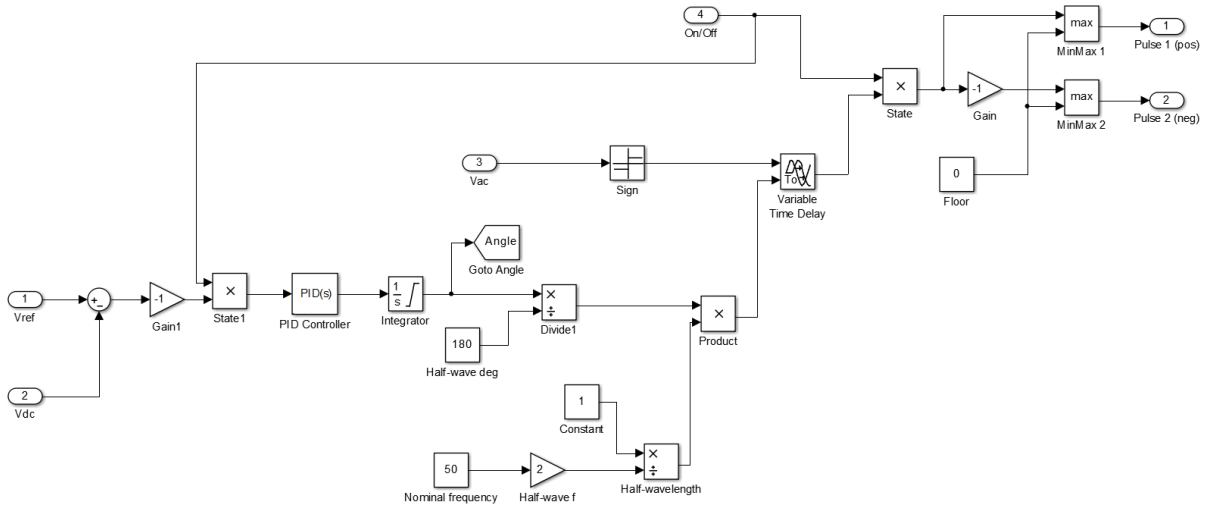

Figure 24: Simulink model of rectifier control system

The control system works as follows. A desired output voltage Vref is compared with the actual output voltage Vdc. If the reference voltage is above the actual voltage, the firing angle needs to be decreased in order to raise the output voltage, which explains the gain of −1 in the model. However, if the AC–DC converter is in the "off" state, the feedback signal is removed by multiplying with zero. This ensures that the control system of the AC–DC converter does not react to changes in output terminal voltage when it is turned off.

The feedback signal is fed into a PID controller which in turn acts upon an integrator which holds the value (in degrees) of the firing angle. The integrator is not allowed to go above 180 degrees or below 0 degrees. The PID controller was tuned using the Ziegler-Nichols method (Co, 2004). The firing angle currently used is divided by 180 degrees, which gives a value between 0 and 1; this represents the fraction of time in which the thyristors are conducting. This value is then divided with the frequency of the input multiplied by two to represent the number of seconds that thyristors should be turned off before conducting (there are two half-waves in each full wave of the input voltage). This signal controls a variable time delay of a different signal, namely the AC voltage fed through a "sign"-block. What this actually does is converting the AC signal into a square wave with amplitude 1, which is positive when the AC voltage is positive and negative when the AC voltage is negative. However, by delaying this signal the thyristor turn-on can be delayed by the right amount of time to fire at the specified firing angle as shown in Figure 25. The first plot in this figure shows the AC mains voltage and the corresponding sign function. The second plot shows how the sign function is delayed by the variable time delay. Finally the third plot shows the resulting bridge output, controlled by the delayed sign function.

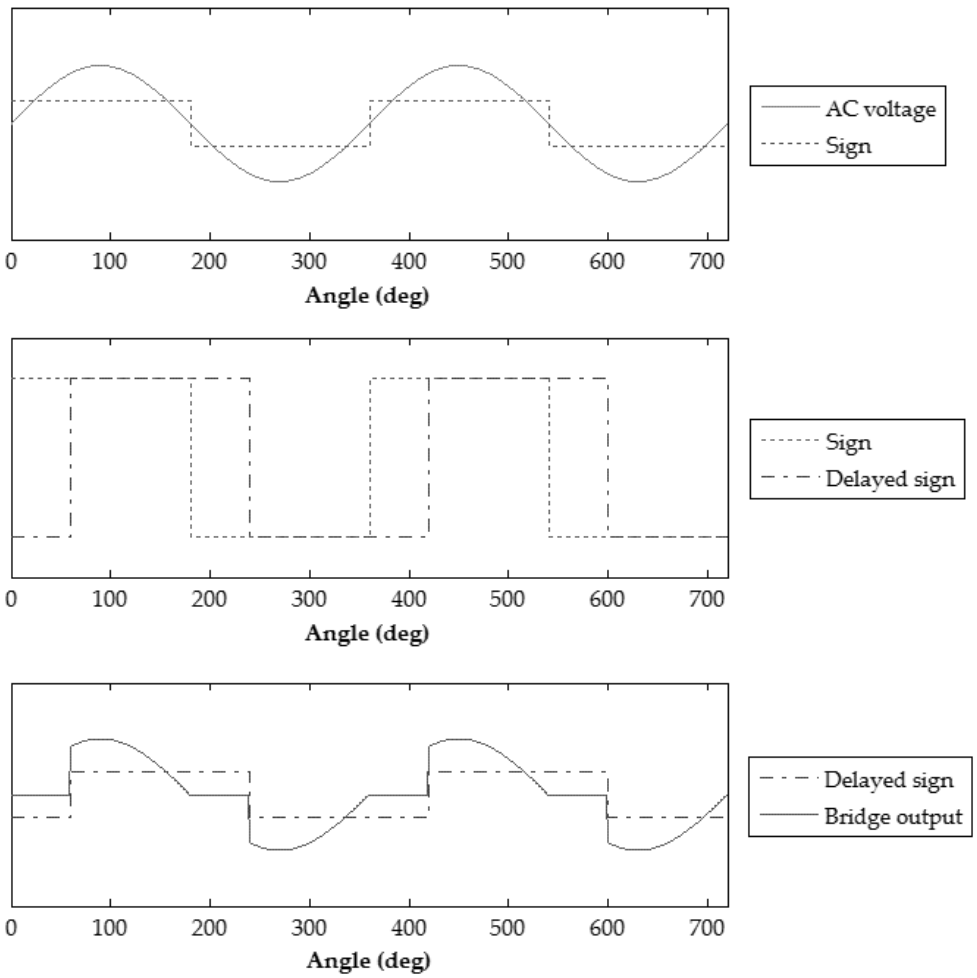

Figure 25: AC–DC converter control system operation

The actual pulses to the thyristors are logically calculated by the rightmost part of the system in Figure 24. There are two output pulses, one for the two conducting thyristors when the AC voltage is positive and one for the two conducting thyristors when the AC voltage is negative. The delayed sign function is taken as input to both pulses, but the negative pulse is gained by −1 to produce an output of positive 1 when the (delayed) AC voltage is negative. Both pulses are floored with zero, so that the outputs are either 0 or 1 instead of −1 or 1. The pulses are also multiplied by the state of the AC–DC converter; when it is off (zero), there will be no pulse and hence no turn-on of the thyristors.

9.2.2 Battery

The battery model is heavily dependent on MATLAB's own battery model. The typology chosen for the battery is a NiMH typology, primarily because a NiMH battery was chosen for the prototype system. Exactly how the MATLAB battery component works is out of scope for this presentation, but can be found in the MATLAB 2013a documentation. The most important characteristics are the discharge characteristics of the battery at different SOC's. Therefore, the MATLAB produced plots of the battery characteristics along with the battery parameters are presented in Figure 26.

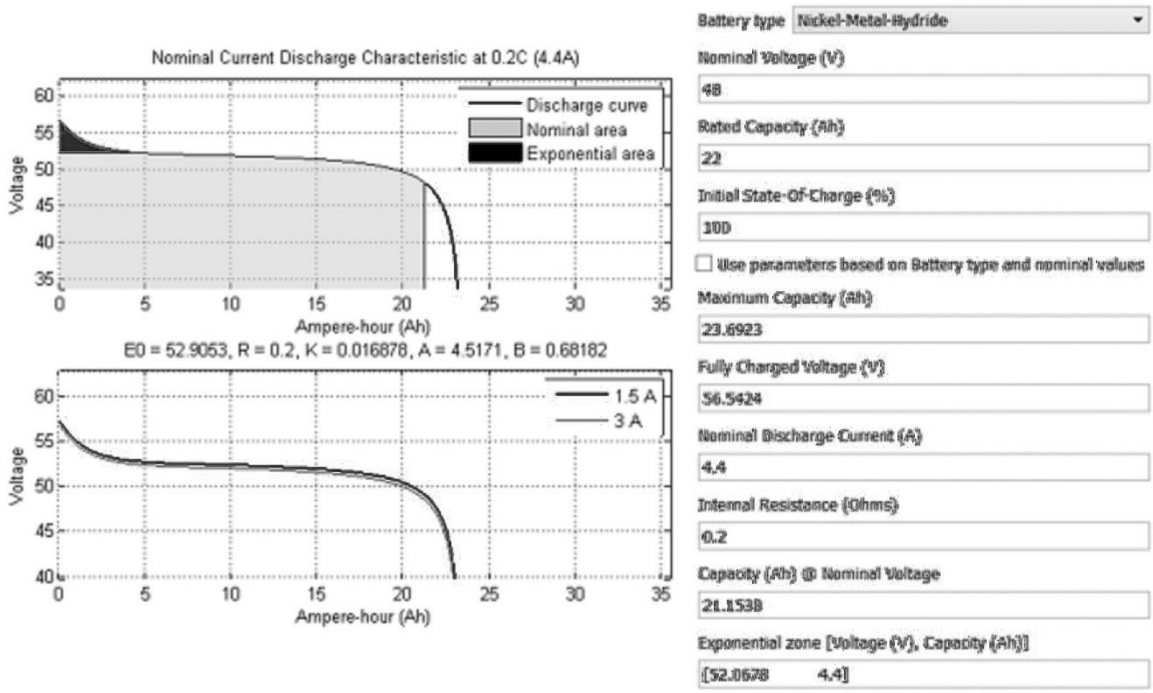

Figure 26: Simulated battery discharge characteristics and values of parameters

The battery characteristics can be compared with the characteristics of the battery used in the prototype system, seen in Figure 27. The latter is based on a battery with a nominal voltage of 12 V, but otherwise the curves are quite similar. Four such 12 V modules are used in the physical prototype system.

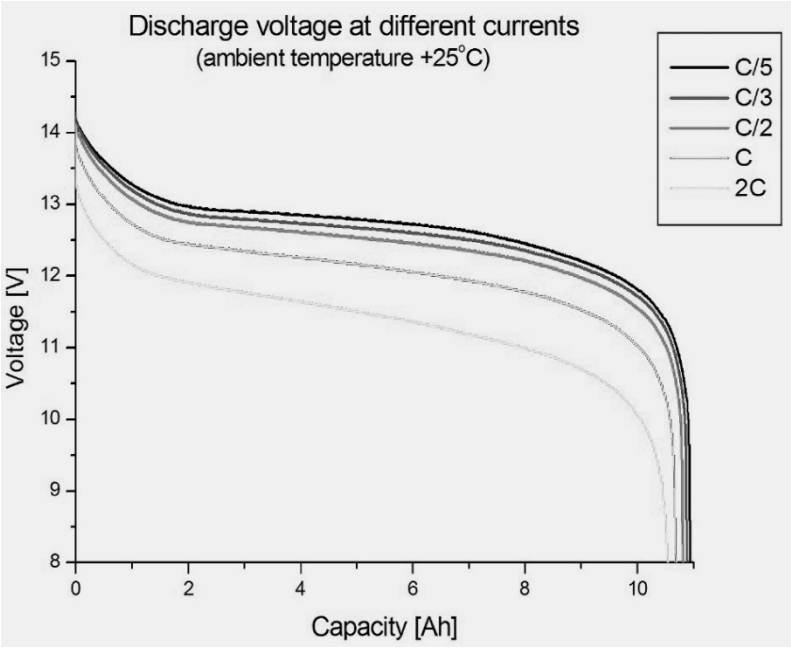

Figure 27: Discharge characteristics of the battery used in the physical prototype system (Nilar International AB, 2013)

The battery along with its supporting components is shown in Figure 28. There is a self-discharge resistance of 15 kΩ connected parallel to the battery, which has a low impact on measurements over short durations of time but may effect results over longer measurements, symbolizing self-discharge of the battery. To achieve full control of whether the battery is charging, discharging or neither, two digitally controlled switches are implemented: one only allows current going out from the battery while the

other only allows current into the battery. This is achieved by the operation of the diodes. Series resistance due to for example wiring is implemented at a value of 0.1 Ω for both directions. This effectively limits the current for a particular voltage, which may have benefits for numerical calculations performed by MATLAB. If there is nothing that limits current in transient conditions MATLAB will have trouble solving the system and may exit, returning an error.

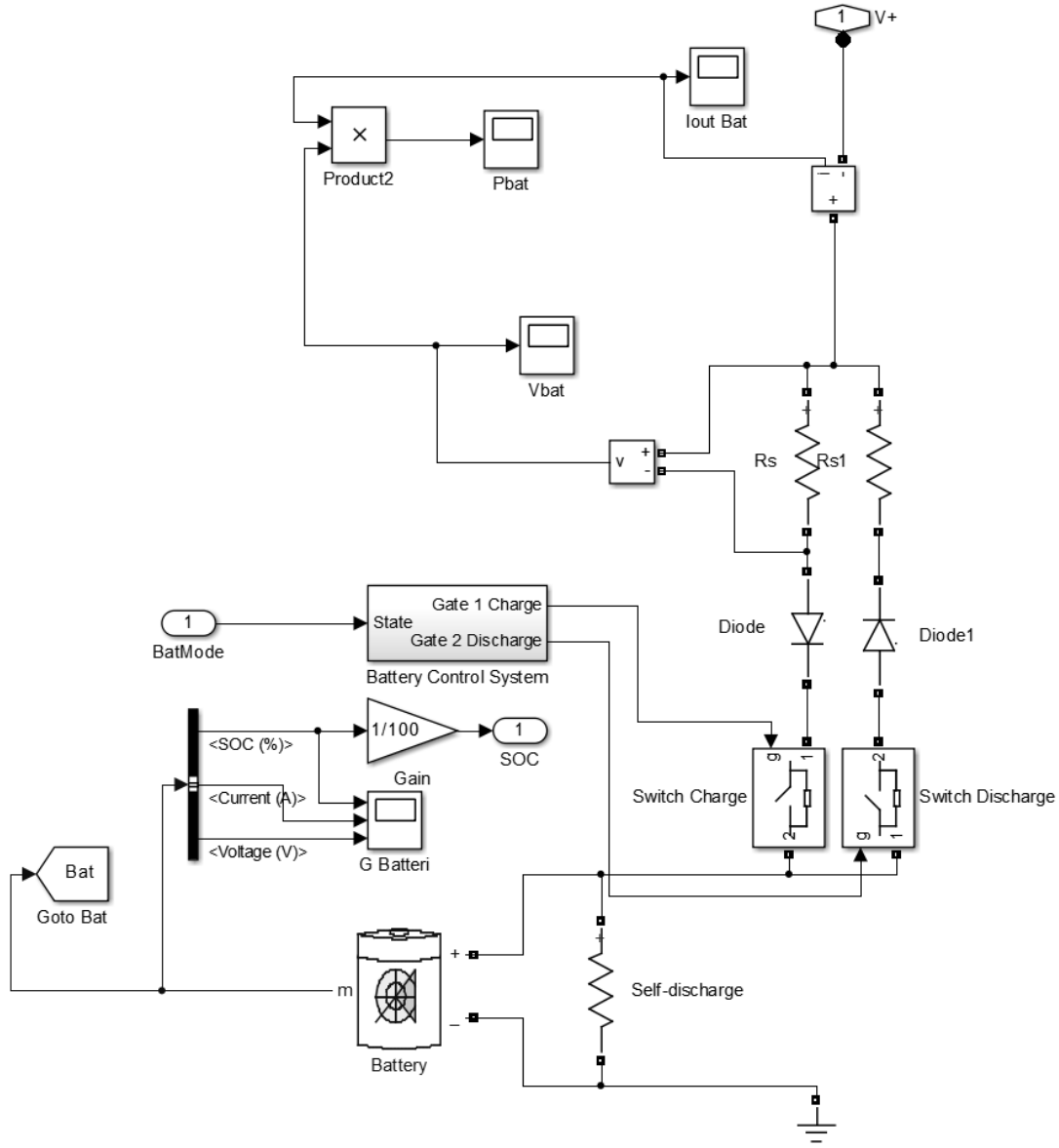

Figure 28: Simulink battery subsystem

There are two outputs from the battery subsystem: the battery state (voltage, current and SOC) and an electrical positive terminal. The negative terminal is connected straight to ground. SOC is effectively included in the "Goto Bat" component, but is also outputted separately for convenience in other parts of the system. The only input to the system is the battery mode, which can be one of three values. If the input is 1, the battery is in maintenance charge and the charging switch is closed while the discharge switch is open. For input 2 the battery is in charge mode and the charge switch is closed also in this case. For an input of 3 the battery is in discharge mode, and the charge switch is opened while the discharge switch is closed. The subsystem that is responsible for switching is shown in Figure 29.

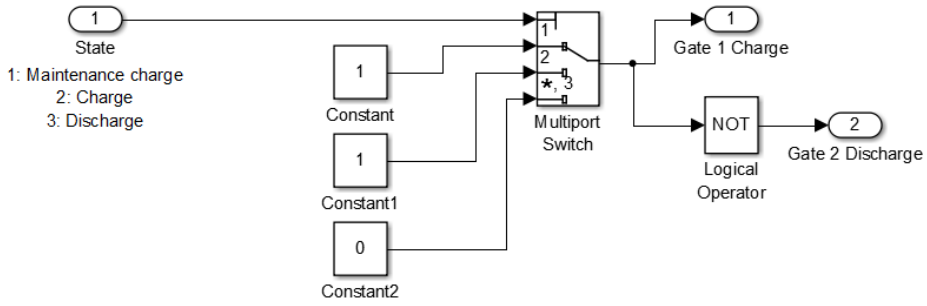

Figure 29: Simulink battery control subsystem

9.2.3 Inversion and load

The inverter is not specifically modelled in the Simulink model. Instead, a purely resistive load has taken its place (Figure 30). This symbolizes an inverter with a purely resistive input, feeding a semi-constant load. There are 4 resistors in parallel that can be switched on or off for simulation purposes, with the nominal power of 50, 100, 200 and 400 watts at a nominal voltage of 56.8 V. This allows the experimenter to choose any power divisible by 50 between 0 and 750 watts.

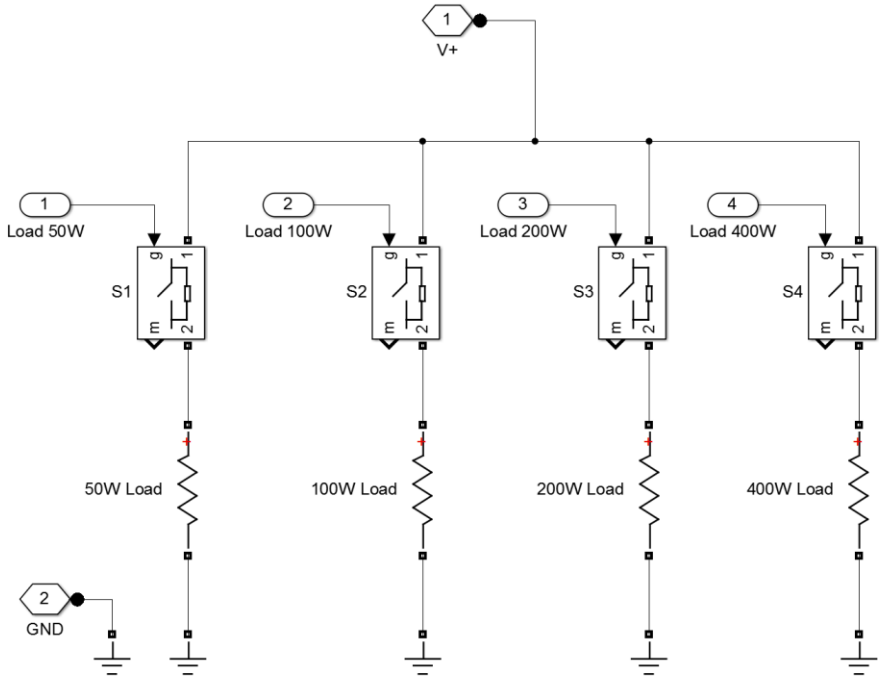

Figure 30: Load subsystem, used to simulate an inverter with load

9.2.4 Solar panels

The properties of the solar panels are modelled after the datasheet of the Stion STO–135 panel. In Figure 31 a comparison between the modelled panel (to the left) and the real panel (to the right, the darkest curve) can be seen. The real panel's curve has been taken from the panel's datasheet. Both plots show the behavior at STC.

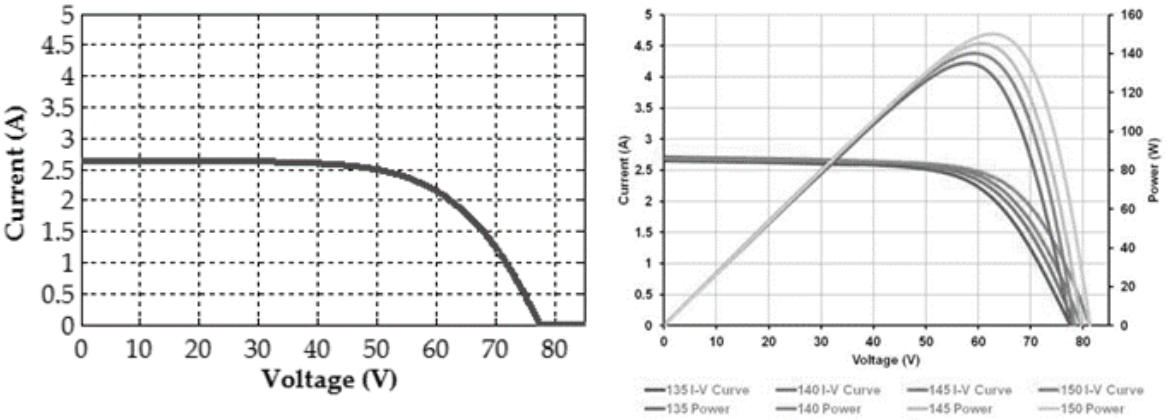

Figure 31: Simulink solar module model versus Stion STO–135 I–V curves (Stion Corporation, 2013)

The mathematical model was taken from a study by Walker (2001). Open-circuit voltage and short-circuit current at STC was directly taken from the datasheet and inserted into the model. Also given by the datasheet are coefficients for how much the open-circuit voltage and short-circuit current varies with temperature. This made it possible to determine those parameters for an arbitrary temperature, in this case 75 °C, and put those values into the mathematical model. The number of cells per module was determined by simply counting the number of cells on the physical panel. The slope of the I–V curve at STC was approximated visually from the manufacturer's graph to −5 V/A. Finally, the diode quality factor was chosen visually to give a knee that looked as much like the manufacturer's graph as possible, and was set to 2.5.

For each value of temperature, solar irradiance and output voltage listed in Table 1 a lookup table is constructed at runtime and determines the output current according to that model. A lookup table is also constructed for determining the MPP voltage at the different temperatures and irradiances.

Table 1: Values used to calculate different MPP's for the simulated solar model

	Minimum value	Interval	Maximum value
Irradiance [W/m²]	0	50	1,200
Temperature [°C]	0	2	74
Voltage [V]	0.0	0.1	90.0

The value returned from the lookup table is used to control a Simulink Power Systems current source representing the photovoltaic current generated by the solar panels that is directly connected to the output (which is in turn connected to the input of the solar charge controller). The voltage is measured at the output and fed back into the lookup table. This creates an algebraic loop, since the current depends on the voltage and the voltage depends on the current. MATLAB is able to solve the loop for normal operating conditions (i.e. the current is fed into the solar charge controller).

The subsystem has two inputs and three outputs. The two inputs are temperature in degrees Celsius and solar irradiance in suns (where one sun equals 1,000 W/m²), and is solely determined by the experimenter. One output is the MPP voltage from the MPP lookup table. The two remaining outputs are the electrical connections, where one is the positive terminal and one is ground. The whole subsystem is shown in Figure 32.

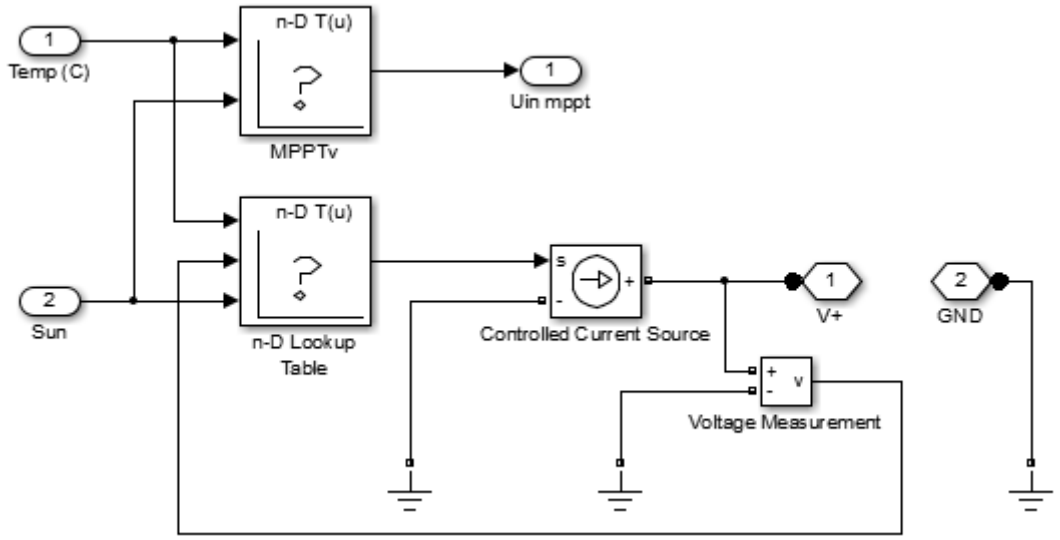

Figure 32: Simulink solar module model subsystem

9.2.5 Solar charge controller

A DC–DC buck converter (solar charge controller) was chosen for the simulated system, because the MPP voltage is generally above system voltage. The design of the buck converter was taken from the design discussed earlier in the literature review. Figure 33 shows the whole subsystem.

The electrical input to the solar charge controller is the solar panels defined earlier. Another input is system voltage, measured remotely after the cable that connects the DC–DC converter with the positive DC terminal. A reference voltage (Vmax) is also fed in to the subsystem, as well as the DC–DC mode where 1 stands for power terminal, 2 for slack terminal and 3 for shut-off.

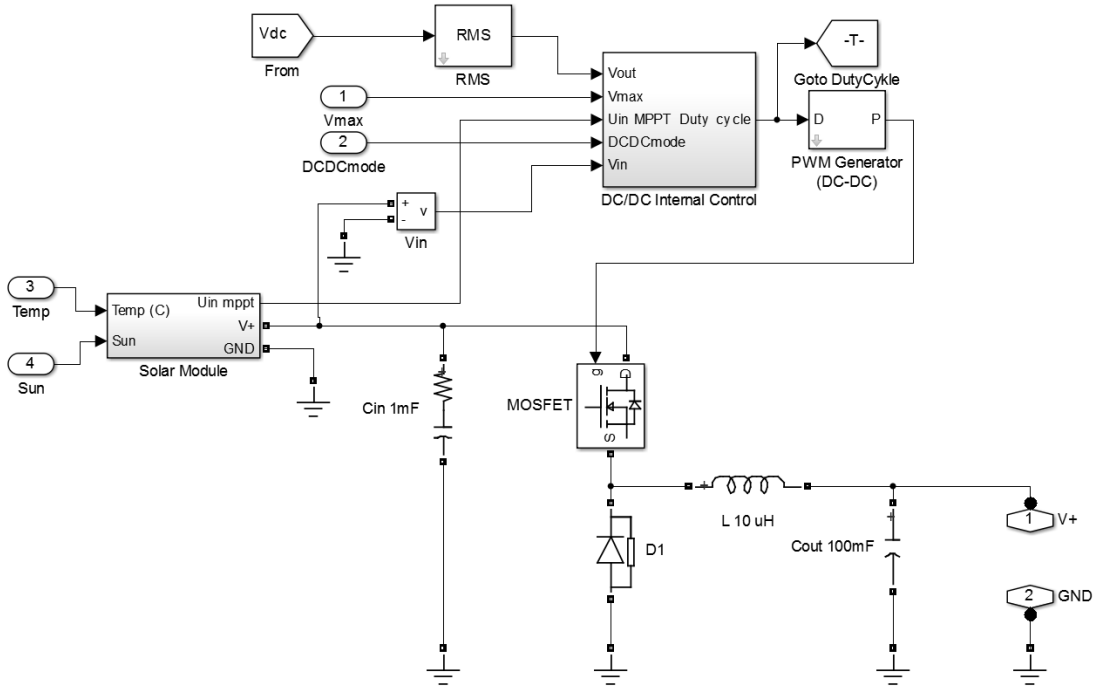

Figure 33: Simulink DC–DC converter subsystem

An input capacitor of 1 mF is used. It has an equivalent resistance of 0.02 Ω in order to limit transient currents and make the mathematical model well-behaved. The MOSFET has an on-resistance of 0.1 Ω, a diode resistance of 0.01 Ω and a snubber resistance of 100 kΩ. All other values are set to default, which are zero except snubber capacitance which is infinite. The diode D1 has a turned-on resistance of 0.001 Ω, a forward voltage drop of 0.8 V, a snubber resistance of 500 Ω and a snubber capacitance of 250 nF (default values). The output capacitor has a large capacitance of 100 mF to make the output smoother. In practice, more advanced filters are probably used.

The MOSFET is controlled by a Pulse Width Modulation (PWM) generator which takes a duty cycle value of 0 to 1 as input and operates at 10 kHz. The PWM generator is in turn controlled by the control system in Figure 34. When the DC–DC converter operates in power mode (DCDCmode is set to 1), the converter compares the RMS input voltage with the MPP voltage for the panels. The feedback is fed through a low-pass filter with a time constant of 1 ms and a PI controller that in turn feeds an integrator which holds the value of the duty cycle. The integrator output is limited to a value between 0 and 1. The PI controller was chosen and tested heuristically using trial-and-error; the goal was a fast rise time with no oscillations.

When the system switches mode to 2, the goal of the DC–DC converter is to fix the output voltage at the pre-set value of 56.8 V instead of achieving maximum power from the solar panels. This is achieved by comparing the system voltage with the reference maximum voltage Vmax. The difference is fed through a low-pass filter with a time constant of 1 ms and then a PD controller. As in mode 1, the controller was chosen and tuned heuristically. This signal feeds the same integrator as in mode 2, ideally leading to smooth transitions between states since the value of the integrator must be continuous by definition.

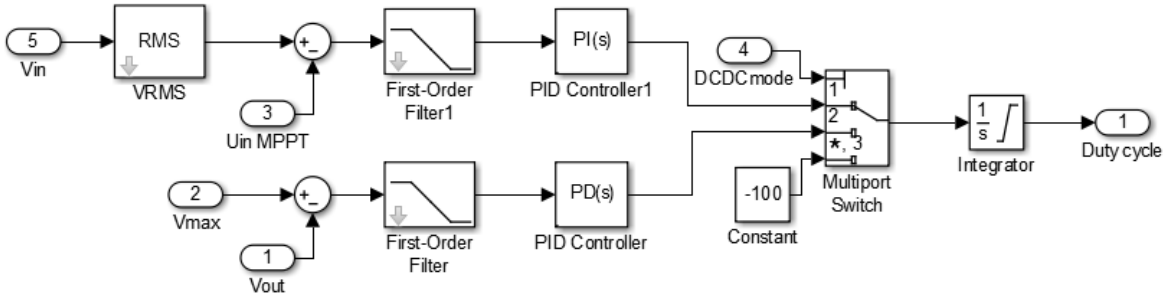

Figure 34: Simulink DC–DC control subsystem

Finally, mode 3 symbolizes turn-off and switches on a constant input of −100 to the integrator, making it quickly reach a zero state.

9.3 Experiments on the simulated system

Experiments on the simulated system were mostly of an exploratory nature. Prototyping was used to design the simulated system, which means that experiments were conducted in different stages of the system design as a part of the development of the model.

The experiments from the MATLAB model that are presented in this thesis are conducted on the final design of the Simulink system. They demonstrate the behavior and potential issues of the physical system, and were analyzed before the actual design of the physical prototype system. One of the experiments shows how the battery current varies with battery SOC, while the other shows how oscillations behave in the simulated system.

10 Method: Prototype system

In this section the design, measurement set-up and experiments related to the physical prototype system are presented.

10.1 Delimitations & Limitations

The scope of this study is to build a prototype system with all the principle components of both a UPS and a solar PV system in order to test the concept of a combined system. The entire system is scaled down significantly in order to make the system easier to conduct experiments on.

The difference in size between the prototype system and a full scale application is likely to result in changes in the relative sizing and design of the system. Since the aim of the prototype system was to test the concept, the conclusion of the conducted experiments is to be seen as a general indication. In-depth studies of a full-scale system are needed before such a system is put in operation. A similar limitation to the study is that only a basic UPS system was constructed, and thus the behavior of this basic system can differ from integrated UPS systems available in the market.

In general, large-scale commercially available UPS systems are designed to be of very high efficiency and with very high power quality. Since the components of a commercial UPS are designed to fit together, the power quality and conversion efficiency are likely to be higher than for the prototype system built as part of this study. This is due to both the efficiency and power quality parameters of the individual components (which were not designed for UPS systems) and the fact that the components were bought separately and not as a system. The absolute level of power quality and efficiency is thus not directly comparable with commercial UPS systems. However the aim of this study was to evaluate the relative effect of adding solar energy to the UPS system. Thus it is the relative difference in power quality that is the key focus in the study.

The inverter used has a maximum output power of 1000 W, because of the initial aim to have a typical load of 800 W. Because of the initially high current when starting to charge the battery, the load had to be decreased in order for the rectifier to handle the power demand. In a more advanced system the battery charging mode could have been designed as constant current charging using additional DC–DC converters, instead of the constant voltage charging strategy used in the prototype system. Building such a control system is however beyond the scope of this thesis. The oversizing of the inverter is not a major limitation as the maximum conversion efficiency of a typical inverter is reached when operating at around 30% of maximum load.

The DC–DC converter is similarly oversized, with a maximum capacity of 30 A at 48 V. This corresponds with a maximum output power of almost 1500 W, even though the installed PV panels have a combined rated power of 270 W. The conversion efficiency of the converter will thus not be at peak levels due to the maximum power output of the PV panels being only 20% of rated power of the converter. The choice of DC–DC converters was limited to a few standardized sizes and models, with the smaller models having received criticism for lower efficiency MPPT, which was considered of major importance.

A limitation of the experiment set-up is that the data acquisition unit (described later) used to collect the data only could handle taking measurements from one channel at a time, thus requiring to run each experiment several times in order to collect all data needed. The SOC of the battery is subjected to small changes in between subsequent runs of the experiment due to the charging or discharging of the battery during each run. The incoming power supplied by the solar panels is also continuously changing. This set-up introduces measurement errors due to the change in the system between runs and it is

thus possible that some changes observed between runs or between two experiments is due to this change in the system. The cause of observed changes in parameters will therefore be thoroughly discussed and analyzed.

10.2 The prototype system

In this section the different parts of the system are presented in detail, both regarding the components used, their electrical behavior and the design of the system with cabling and related minor components. A principal overview of the prototype system is shown in Figure 35 with a more detailed wiring diagram shown in Figure 36. Pictures of the prototype system are included below. Detailed technical information about all major components used in the system is available in Appendix 1.

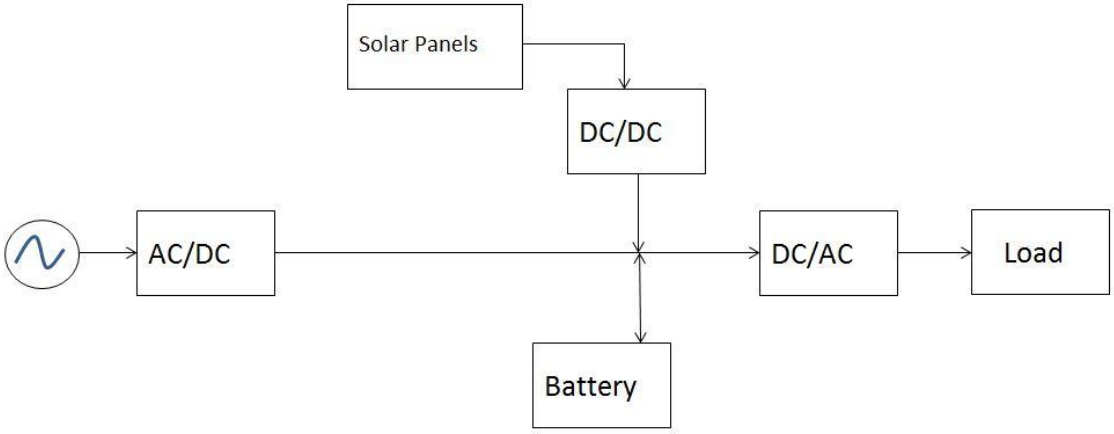

Figure 35: Overview of the prototype system

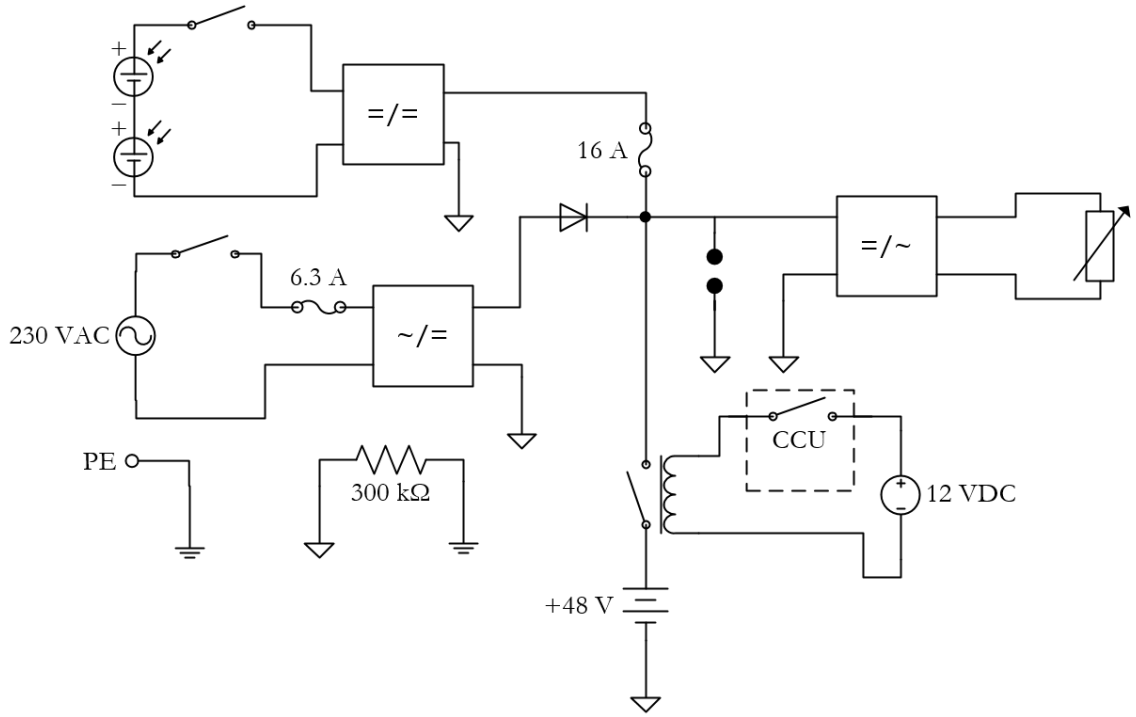

Figure 36: Wiring diagram of the prototype system

The system was designed to have a maximum load power of 400 W with the typical load being 300 W. The maximum output power of the inverter is 1000 W. The rectifier can supply 1200 W which is used to cover the power needed to charge the battery and load as well as the conversion losses in the invert-

er. The system was designed in order for the initial battery charge current to not surpass 2 C, and stabilize around 0.5 C. The unit C describes charging/discharging rates of batteries where 1C is defined as the amount of current that will completely charge/discharge the battery in 1 hour (MIT Electric Vehicle Team, 2008). This corresponds to a current of 11A for the battery used. The system is designed to have a nominal voltage of 48 VDC, resulting in the actual voltage of the DC-line being 56.6 V in order to charge the 48 V battery.

The experiments were conducted on the roof of the Department of Energy Technology at KTH, Royal Institute of Technology. The solar panels were placed outdoors and the rest of the system indoors in a small building on the roof of the laboratory.

10.2.1 Rectification of incoming AC power

The main source of electricity is from the grid via a one-phase AC-cable from a conventional 230 V wall-socket. The component furthest upstream is the main power switch which controls the power coming from the grid. Regardless of state of the switch, the protected ground of the power grid is utilized as the protective ground for the majority of the system.

After the power switch there is a fuse to limit the amount of current that the UPS system can draw from the power grid. The fuse used is a fast fuse with a maximum continuous current of 6.3 A, which with the voltage fixed at 230 V results in a maximum power of 1450 W, which is enough to supply the maximum power of the rectifier and its associated conversion losses and an added margin.

The final component of the grid AC-line is the rectifier used to transform the incoming AC power into DC. The rectifier used is a MeanWell MW-s 1200-60v, with an output power of 1200 W and a nominal DC voltage of 60 V (Figure 37). The rectifier has a typical conversion efficiency of 87% and provides a constant output voltage, which is mechanically set and cannot be adjusted during operation. The maximum rated ripple of the output voltage is 600 mV at peak power, with smaller ripples if the power is lower. The efficiency is lower than for typical large-scale UPS and the ripple factor higher, which likely results in a more unstable DC voltage than for a commercial full-scale system. These differences were not considered critical though, as the main objective of the prototype is to evaluate the effects of connecting the solar panels to the UPS system.

Figure 37: The rectifier used in the prototype system

As long as the main power switch is on, the rectifier is supplied with electricity. Since the rectifier is lacking an on/off switch of its own, the rectifier upholds the voltage of the DC-line.

10.2.2 The DC-line

The DC-line is where the components of the system are connected together through common-pole terminals. The terminals connects the rectifier, battery circuit, inverter and while plugged in the system also the solar charge controller with the solar panels. The entire DC-line with assorted components is shown in Figure 38.

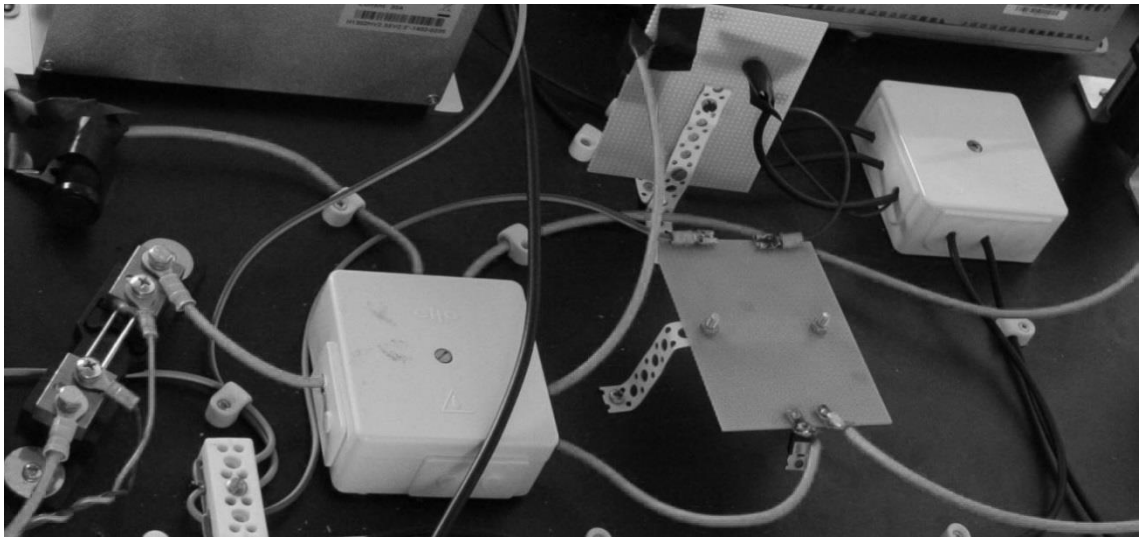

Figure 38: The DC-line with terminals, diode, resistor, fuse, current shunt and transient protection

Several additional components have been added to both enhance the performance of the system and for safety reasons.

On the positive side of the DC-line there is a diode between the rectifier and the terminal in order to eliminate the risk of current flowing back into the rectifier from the battery or solar charge controller. This also eliminates oscillations between the rectifier and other components, which minimizes the ripples in the DC voltage. The drawback of the diode is the voltage drop of approximately 0.6 V, corresponding to a power dissipation in the diode based on the current drawn from the rectifier. The power consumed by the diode is lost as heat, and lowers the total efficiency of the system.

The power flowing from the solar charge controller is limited by a fuse placed on the positive DC-line between the solar charge controller and the terminal. Since the voltage of the system is relatively low (minimal voltage before deep discharge shut-down is only 46 V) the fuse is dimensioned to handle a continuous flow of 16 A, which corresponds to approximately 150% of nominal peak power of the solar panels.

The battery circuit is connected to the positive terminal via a contactor which allows power to flow into and out of the battery only when this can be done safely. When the contactor is open, no power can enter the battery circuit and the battery is thus no longer connected to the DC-line.

The negative terminal is directly connected to the common negative terminal of all the components: the rectifier, battery, inverter and solar charge controller.

Additionally there are two safety components connected to the DC-line. The first is a transient protection which essentially consists of a capacitor and a resistance in series and which is connected between two cables of opposite polarity (Elko, 2014). In the case of a sudden voltage build-up on the DC-line, likely as a result of fast connection or disconnection of the load, the DC-spark over voltage is reached and the current will spark over the capacitor, essentially short-circuiting the system for a short duration

which allows the voltage to drop. The transient protection used in the circuit is rated at 90 V spark-over voltage.

A final protective component added to the system is a resistor between the negative terminal of the DC-line and protective ground. This was recommended by several experienced researchers to use as an added safety feature since the DC voltage otherwise would have no reference to protective ground. A resistance of 300 kΩ is connected between the negative terminal and protective ground, which is taken from the conventional AC-supply. This high-resistance connection prevents buildup of potentially hazardous voltages between the DC terminals and protective ground.

For measuring current, a shunt resistance is placed between the positive common terminal of the DC-line and the inverter. The shunt has a small voltage drop across it that varies linearly with current, with 25 A corresponding to a voltage drop of 65 mV. The shunt is used to acquire measurements of the current entering the inverter.

10.2.3 Battery circuit

The battery used in the prototype system is a Nilar Blåpack 48 V, 11 Ah Nickel Metal Hydrid (NiMH) battery. The rated capacity of 11 Ah is valid for a discharge current of C/5, with the capacity decreasing with increased current. Without the support of solar energy the battery can supply the nominal load of 300 W for approximately 40 minutes, which is enough for test purposes. In a full-scale system the battery capacity is designed based on the demands of the load. The relative high discharge rate of the battery makes NiMH batteries suitable. Another advantage of the battery is the fact that it is bi-polar; making it suitable for the higher DC-line voltages used in our system without the need for series connections of several separate batteries.

The battery circuit consists of a contactor with a primary and secondary circuit. In the primary circuit the positive terminal of the battery is connected with the positive terminal of the DC-line. In order for the primary circuit to be closed, there has to be a flow of current into the coil of the contactor through the secondary circuit. The contactor is thus controlled through the secondary circuit by a battery charge control unit. The principal operation of the battery circuit is presented in Figure 39.

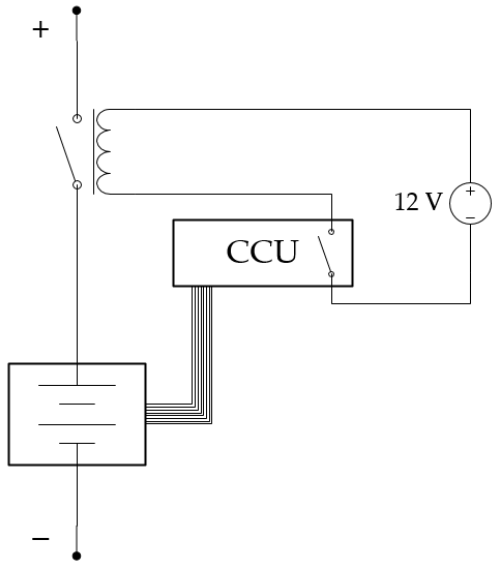

Figure 39: Principal diagram of the battery circuit

The battery charge control unit (CCU) is connected to the battery where data of voltage, pressure and temperature of the different cells in the battery is continuously monitored. The control unit operates

as a relay allowing current to flow through the relay as long as the values are normal. The control unit automatically detects changes in either the absolute values of battery voltage, pressure or temperature or in their rate of change, blocking current from passing the relay if any of the parameters leaves the pre-set ranges.

The switching of the control unit controls the flow of current in the secondary circuit of the contactor, thus effectively connecting or disconnecting the battery from the rest of the system. The contactor used in the prototype system has a secondary circuit voltage of 12 VDC, which is supplied by an external voltage source. The external voltage source is a Mascot type 719, which can supply the desired voltage very quickly after switching it on, thus making it suitable for frequent and fast switching of the battery circuit.

The negative side of the battery is directly connected to the negative terminal of the DC-line.

10.2.4 Inversion and load

The majority of the power supplied to the DC-line is transferred to the inverter and used to power the load with 230 VAC. The inverter used in the system is a MeanWell TS-1000-248, with a maximum power output of 1000 W (Figure 40). Since one of the major functions of the UPS is to ensure a high power quality, the inverter chosen is a true sine inverter with a total harmonic distortion (THD) of less than 3% at rated input voltage. The peak efficiency of the inverter is 92%, and the input voltage range of 42–60 VDC is adequate to function in all operating conditions of the designed system.

Figure 40: The inverter used in the prototype system

The output connection of the inverter is a standard power socket which is connected to a 3-connection power strip to enable several loads and instrument to be plugged into the AC-line at the output socket of the inverter.

The main load used is an electric stove (Figure 41) which can be manually set to six different heating levels, corresponding to power consumption between 130 W and 1200 W. The nominal power of the load is 300 W corresponding to the 3rd level of heating, with 130 W used to partially discharge the battery between experiments. The load is purely resistive, making it ideal to use in the experiment set up. All power is dissipated as heat in the stove.

Figure 41: The load consisting of a resistive stove

10.2.5 Solar panels and the solar charge controller

The parts of the prototype system described in the sections above constitutes the basic UPS with load. The solar energy is an addition to the system which is used in the experiments in order to analyze the impact of solar energy on the electrical behavior of the system.

The solar panels used in this study are Stion STN-135 CIGS thin film solar cells. The panels have conversion efficiency at STC of 12.4%. The nominal power from a panel is 135 W at STC, but under normal operating conditions this number is decreased due to lower solar irradiance. Two panels connected in series are the source of solar power used in the prototype system, resulting in a total area of 2.18 m^2 of solar cells. The nominal voltage at MPP is thus double that of a single cell since the cells are connected in series, and is 88.6 V – higher than the system voltage of the DC-line. The current is 3.05 A at MPP. The exact voltage level of the solar panels is not a key factor in the system as the solar charge controller can handle a span of incoming voltages, up to 150 V.

The panels are mounted on an aluminum framework preventing the panels to move in any direction. Since the panels are CIGS thin film they consists of many solar cells designed as thin, long strips parallel to the long edges of the panels. The panels are mounted facing south with an angle towards the horizontal plane of 13 degrees. This low angle is chosen partially due to simplifying the installation process and partially as the experiments are to be conducted in the middle of the day, where a low angle is beneficial to maximize the incoming solar radiation. The angle is also of less importance for thin film solar cells than traditional silicon cells (Kalogirou, 2014). The panels are mounted with the long edges bordering each other, thus mounting the panels with the individual cells placed vertically (Figure 42). In order to prevent the panels from moving due to heavy wind the frame is secured to the roof using lashing straps.

The panels are connected in series using solar contacts from Phoenix Contact. From the terminal the electricity is transported indoors to the rest of the system through 4 mm^2 wiring. The frames of the panels are not connected to protective ground by recommendation by the company providing the panels.

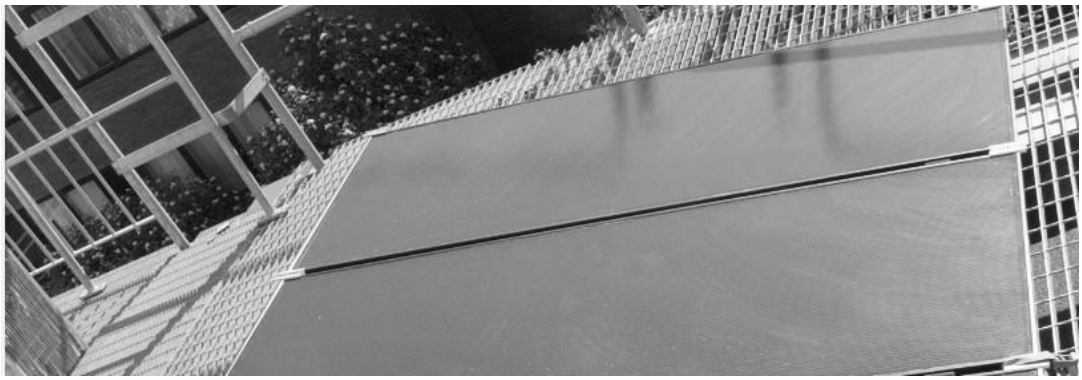

Figure 42: The solar panels used in the prototype system

The negative and positive wires are connected to a DC–DC converter in order to adjust the voltage of the incoming PV-power to the system voltage. The converter used is an ET3415 solar charge controller with MPPT from EP Solar. The converter is connected to the PV panels on one side and the DC-system on another (Figure 43). Between the solar converter and the PV panels is a switch which controls the power flow from the solar panels into the rest of the system. The switch is one-pole and thus is only used on the positive wire. When the switch is shut off there is no incoming PV power, and this switch is used for safe start-up and shut-down of the system. For experiments without solar panels the solar charge controller is completely separated from the rest of the system by disconnecting both the negative and positive wire from the respective terminal.

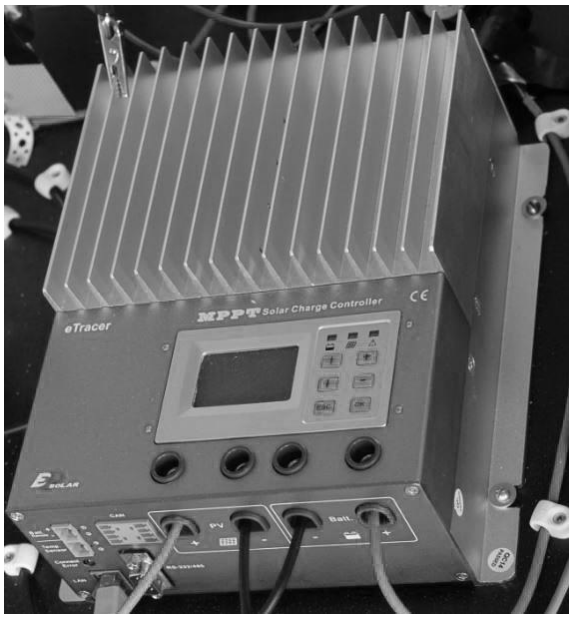

Figure 43: The solar charge controller used in the prototype system

Between the positive terminal and the DC–DC converter is a 16 A fuse designed to protect both the system and the converter in case of malfunctioning. The converter is not isolating, thus the negative pole of the DC-line is in direct contact with the solar panels. No fuse is placed between the solar charge controller and the PV panels since there is only one string of two panels and the rated short-circuit current is significantly lower than what the 4 mm^2 cables can handle.

The solar converter is programmed to supply the system with power of the constant voltage of 56.8 V, giving the solar power priority over the incoming mains power due to its higher electric potential. In the case of a disconnection from mains power the battery voltage will automatically set the system voltage if the solar panels are unable to supply the load by themselves. The DC–DC converter automatically detects the system voltage and adjusts its output in accordance.

10.3 Measurement set-up

In order to analyze the results of the experiments, measurements of voltage, current, power and harmonics were collected. The majority of the measurements collected were transferred to a computer through the use of a HP 34970 Data Acquisition Unit. The data acquisition unit (DAU) has 5 pairs of cables connected to it corresponding to 5 permanent measurements, where the data is acquired directly through analyzing the voltage across a pair of cables. The cables were spread out among the input channels of the data acquisition unit in order for the cables to fit, and the channels in use were number 1, 2, 5 and 7 (Figure 44). Channel number 4 was plugged in but not in use.

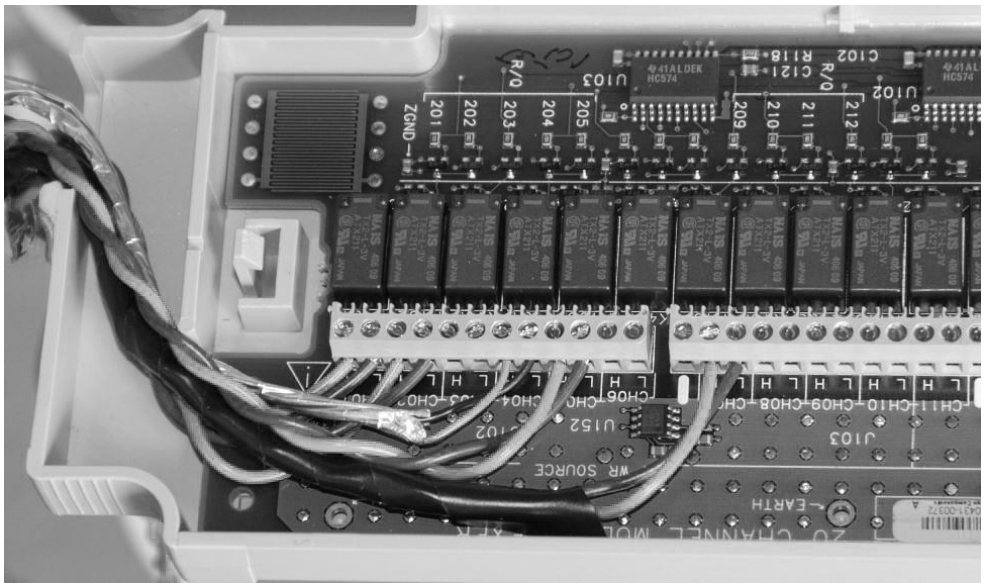

Figure 44: Channel layout for the data acquisition unit

Channel 1 measured the DC voltage on the DC-line, and was acquired directly by fixating cables to the positive and negative cable on the DC-side of the inverter.

Channel 2 measured the current entering the inverter by the voltage drop across the current shunt described above. The information was collected by measuring the DC voltage drop between a pair of cables placed on each side of the current shunt.

Channel 5 is different from the other channels as the measurement of this channel was taken by an external component, a FLUKE 80i-110s Current Probe. By moving the current probe measurements could thus be taken from any point in the system. The most common placement of the probe was on the positive cable on the DC-line, between the positive terminal and the contactor measuring battery current. The two additional points of measurement were the current from the solar charge controller when the solar power was connected to the system and the current from the rectifier when there were several sources of power. The current read by the probe corresponds to a voltage output of 10 mV/A and the output cable of the probe was connected to a pair of cables plugged into channel 5 of the data acquisition unit.

Channel 7 measured the AC voltage in the cables between the inverter and the load. The output voltage of the system is one of the most important parameters as stable power supply is a primary function of an UPS system. The measurement was taken directly by using a power cable plugged into the power socket after the inverter. The power cable was then divided and the individual cables for phase and neutral plugged into the DAU.

In order to see the fast oscillations in the system which was expected to have a frequency of 100 Hz, samples had to be taken every 4 millisecond. Due to the limited speed of the DAU only one channel could be active at a time in order to get measurements with the speed required. Thus all experiments were run several times over until data from all channels had been collected.

For every run of the experiment, 2000 data points were collected with 4 millisecond intervals by the DAU and saved as data points in a computer. The data was then transferred into MATLAB for further analysis.

The DAU was however unable to measure the AC voltage over channel 7 as fast as the DC-measurements. With the AC frequency of 230 Hz from the inverter the DAU could only manage to collect data from channel 7 at a rate of one sample per second. For channel 7 the amount of samples was therefore lowered to 30, with a 1 second interval. This measurement could thus only show major changes in voltage, and was unable to see high-frequency ripples.

In order to analyze the waveform of the current on the DC-line an oscilloscope was utilized. The oscilloscope used was a PicoScope 2104 capable of collecting measurements at a rate of 50 million samples per second. This allowed for analysis of very high-frequent noise in the waveform and was deployed during steady state operations. The measurements were taken on the current shunt.

In order to analyze the power quality in the electricity used to power the load the total harmonic distortion was measured using a FLUKE 80i-500s current clamp. The measurement tool was connected to the AC-line between the inverter and the load and measurements were read through the use of a Fluke 39 Power Meter. The THD was presented as a percentage number and recorded directly from the screen of the instrument.

Additionally, two power meters were used to measure the power flowing into the system from the power grid and out of the inverter to power the load. The measurements were taken using Maxxtro Power Calculators, but since only instantaneous values of the power drawn were required these components were not designed to log data. The instantaneous values were thus read manually from the display and put into a table. One power meter was placed between the power socket and the power cable into the system, and the other one directly at the output of the inverter.

10.4 Experiments

The experiments conducted were in general divided into two halves; with or without the addition of solar energy. Most of the experiments were first conducted without solar energy and then repeated with added solar power in order to compare the system performance to evaluate the effect of adding solar energy. Some experiments however were only conducted once, and the aim of these experiments was to test some specific system parameters unrelated to the addition of solar power. The experiments were conducted in steady state or were initially in steady state. Steady state refer to the system being in normal operation – that is the system has been powered on according to the specification of each experiment long enough to no longer be affected by transients related to the starting/shut off of the system. The system was not in a true steady state however as the SOC of the battery as well as the incoming power from the solar panels were subjected to constant changes, but the experiment aimed to minimize the effect of those changes.

For most experiments the general procedure was that the measurements were taken when the system had already been on for at least one minute in order to avoid the instabilities in voltage and current related to the starting of the system. Measurements for each individual channel of the DAU were collected in subsequent runs of the experiments. The measurements were always collected in the same order, starting from channel one with measurements taken in increasing channel order. For the current measurement of channel 5 the battery current was collected first, then solar current (if the solar power was used in the experiment) and finally the current from the rectifier as measured upstream from the diode. For the steady state experiments an oscilloscope was used in order to analyze the waveform of the current in the current shunt where measurement 2 was placed. The oscilloscope was used to analyze how the addition of solar power affects the DC waveform, and thus the noise and ripples, during steady state operation.

In order to compare the ripples between different experiments and configurations the ripple factor was calculated for steady state experiments. The ripple factor calculation was based on the assumption that the AC-part of the wave was a sine wave without overtones.

A brief description of the experiments are given here, the complete information of the experiment set-up is given in Appendix 2. In this section the main purpose is to describe the aim and the method used to conduct each experiment.

Experiment 1: The effect of load on system parameters
The aim of this experience was to be used as a benchmark to show how the load affects voltage drops, ripples and the response time of the system. The experiment was conducted using only the inverter, rectifier and load plugged into the system and was run twice – with no load (inverter powered on) and with the nominal load of 300 W. The experiment was conducted when the system had reached steady state and no parameters were changed during the experiment.

Experiment 2: Steady State
This experiment was conducted in steady state and was used to measure the ripples in voltage and current. In the first part the solar power was not connected to the system, and in the second part the solar power and solar charge controller was plugged onto the system and supplying part of the power required for the load. For this experiment the waveform of the current at the current shunt was also measured with an oscilloscope in order to find distortion and noise in the waveform. The results of the two set-ups were compared and discussed.

Experiment 3: Steady State Islanding Mode
This experiment was very similar to the previous steady state experiment with the difference that the system was in islanding mode with no connection to the electricity grid. The main switch on the incoming AC-line was thus switched off, resulting in the rectifier providing no power. The components plugged into the system was thus only the battery serving the inverter and load for the first part of the experiment, with the battery and solar charge controller combining to serve the load in the second half of the experiment. In this experiment, the waveform of the voltage over the current shunt was also measured with an oscilloscope in order to measure the amount of distortion and noise in the waveform. The aim of the experiment was to compare the ripples in voltage and current as well as the absolute level of outgoing AC voltage with and without the solar power plugged in.

Experiment 4: Starting the inverter
In order to measure the increases in current and voltage during system start-up an experiment was conducted with only the rectifier, inverter and load connected. At the start of the experiment the main switch was closed. The load and inverter were powered on from the start in order to start drawing current as soon as the main switch was closed, and the rectifier thus able to supply power to the system. The experiment aimed to show how the inverter affects current and voltage on the DC as well as AC side of the inverter during start-up.

Experiment 5: Stabilizing battery current after connecting the battery
Because of the chemical nature of the battery the current entering the battery is initially high, but stabilizing with time. The aim of the experiment was to analyze the time constant of the battery and how the battery current changes after connecting the battery to the system. Since measuring the effect of adding solar power was not the aim of this experiment the solar charge controller was disconnected from the system, and thus the rectifier was the only source of power. The rectifier and inverter was in steady state when the experiment started with the battery switch closing – allowing current to flow into the battery due to the higher voltage from the rectifier compared to the battery voltage. This experiment was conducted during approximately 10 minutes with only two measurements being collected per second. Due to the lower measurement speed, data from all channels were measured simultaneously.

Experiment 6: Entering Islanding Mode
While the steady states experiments were conducted in order to measure ripples and noise with and without the addition of the solar charge controller and solar panels, the following experiments were conducted in order to see how the system handles major changes. The aim was still to compare the results with and without solar power to evaluate the effect of solar power on the UPS functionality.

In this experiment the rectifier, inverter with nominal load and the battery was connected to the system and the system was in in steady state. At the start of the experiment the main power switch was turned off, equivalent to a situation when mains power fail. The experiment was conducted twice; first without solar and then with solar connected to the system. In the first part the battery was the single source of energy for the load, but with the solar power connected both sources supply power, with the solar charge controller as the primary source and the battery supplying what the solar panels cannot cover. The results were together with the AC voltage considered the most important parameter.

Experiment 7: Reconnecting to the power grid
This experiment is similar to experiment six, in that the experiment is divided into one half without solar power and one half when the solar charge controller was connected to the system. The difference is that in this experiment, the system had been in islanding mode long enough to minimize the effect of transients related to the starting of the system. At the start of the experiment the main power switch was closed and the rectifier was once again able to supply power from the power grid to the load and charge the battery. The effect of this sudden reconnection to the power grid on system voltage and current was analyzed and compared between the two scenarios.

Experiment 8: Switching off the load
The UPS system not only protects the load in cases of power failure in the conventional power grid but must also be able to handle sudden changes in the load without affecting the remaining load or the UPS system itself. This experiment aimed to analyze the effects of a sudden disconnection of the load. The experiment started with battery, rectifier and inverter with nominal load being powered on for enough time to avoid the effect of transient from the starting of the system. At the start of the experiment the load was suddenly lowered from nominal load to no load. Like previous experiments the experiment was conducted twice with the aim to compare the effects with and without having the solar energy connected to the system. The main parameter to evaluate was the outgoing AC voltage to the load.

Experiment 9: Switching on the load
This experiment is very similar to the previous one with the single difference that the effects of a sudden increase (instead of decrease) in load was analyzed. The system had thus been powered on with no load (but inverter connected to the system) in order to reach steady state. At the start of the experiment the load was increased to nominal load.

Experiment 10: Total harmonic distortion in steady state
In order to analyze the power quality of the outgoing AC power used to supply the load a power meter was used to measure the THD of the outgoing current. The THD was represented as a percentage and was measured using a current probe and then manually read from the screen of the power meter as described above. Measurements were compared with and without the solar energy connected to the system. All measurements were taken using both the nominal load of 300 W and a lower power of 130 W in order to capture the differences in THD based on the load power. The measurements were taken using only the battery, only rectifier and both rectifier and battery, with and without solar power. The results were presented as a table and the differences analyzed.

11 Method: Economic Analysis

In this section the model and method used to compare the investment cost and total system efficiency of either a combined system (UPS and solar combined) or two separate systems (UPS and solar separate) is presented.

11.1 Delimitations & Limitations

There are several delimitations and limitations related to the economic study, particularly related to the calculation of component costs. In order to make the two options comparable and scalable, all prices are recalculated using the common unit of $/W-peak, which is the industry standard.

The main delimitation of the economic analysis is that only the main components used exclusively in one of the alternatives were compared and calculated. The total cost for the system was not analyzed in detail as the majority of the components are used both in the combined and the stand-alone alternative, and thus unaffected of which option is chosen. Only the major components are compared in the model (i.e. solar inverter vs solar charge controller). To make a full comparison of both alternatives requires an in-depth analysis of a specific installation which is out of the scope of this thesis. However, as an indication of the profitability of the investment a basic payback-calculation was performed using industry standard data for system costs.

There are two available methods to use in order to find average prices per peak watt for solar inverters and solar charge controllers, either using prognoses of industry average prices, or check prices on products on the market. Since no prognosis is available which compare both solar inverters and solar charge controllers, and the span of the prices differ significantly between prognoses, it was judged that this source of data is not reliable. Instead prices have been taken as list prices from whole-sale companies. The main limitation with this method is that taxes, fees and the companies' added margin is added to the real cost of the component. In order to minimize the impact of these added prices, both solar inverters and solar charge controllers are taken from the same wholesaler, making the relative prices more reliable as the same margin is likely added to both components.

Another limitation of the study is that the prices of the individual components are calculated, when in reality UPS and solar power are commonly sold as a complete systems. The pricing for the individual components might thus differ from their share of the costs when sold as a system.

The unit used to enable comparisons between the systems in the economic analysis is $/W. The sizes of string inverters are commonly larger than for solar charge controllers, leading to a larger amount of components being used when using solar charge controllers. This can affect the costs of installation, mounting and wiring, but using only a $/W-approach the assumption is made that this does not have an impact of the total price. Similarly, when comparing the investment cost in $/W the costs for maintenance and similar is not included. An alternative would have been to use Levelized Cost of Energy (LCOE) but such a method is beyond the scope of this study, and left for future research.

Another assumption in the model is that the shape of the efficiency curves for the components used is the same regardless of size, and that the curves do not change due to degradation or other external factors. The peak and typical efficiency (euro efficiency) of the components are however calculated based on products in the market.

11.2 The economic model

In this section the model designed in Microsoft Excel is described.

11.2.1 Mathematical model

The model is based on the purpose of comparing two different systems, combined and separate. When separate systems are considered, the inverter is assumed to be connected directly to the power grid independent of the UPS system (Figure 45).

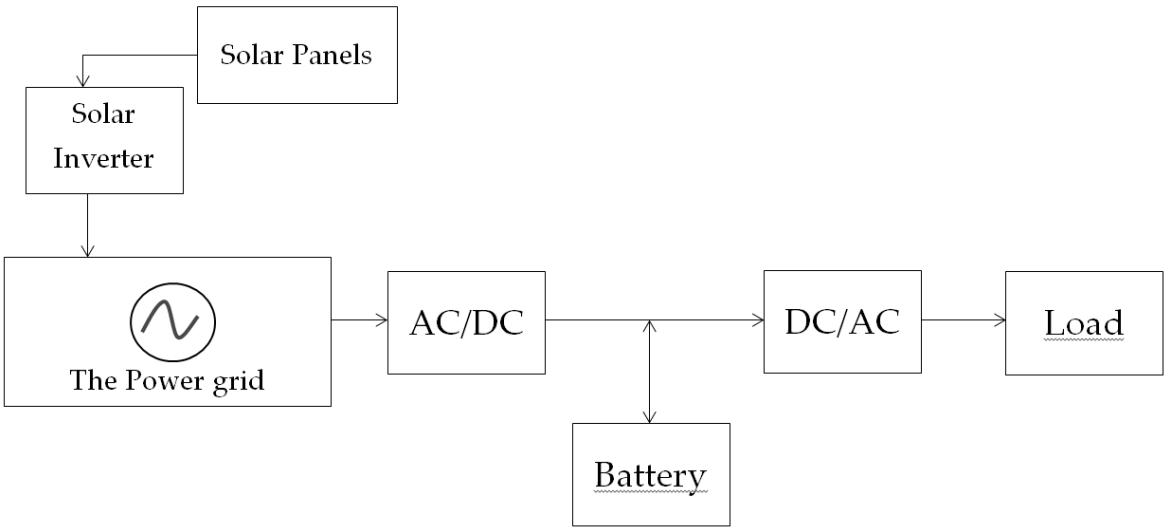

Figure 45: Principle operation, two separate systems

The inputs of the model are defined in Table 2. The inputs will be discussed further in their respective section.

Table 2: Input parameters to the mathematical model

Hourly Data		
Input	**Symbol**	**Unit**
Global Horizontal Irradiance (Hourly)	J_h	Wh/(h×m^2)
Dry Bulb Temperature (Hourly)	T_h	°C
Solar Modules		
Reference Temperature 1	$T_{ref,1}$	°C
Reference Temperature 2	$T_{ref,2}$	°C
Open-Circuit Voltage at Reference Temperature 1	$V_{OC,1}$	V
Open-Circuit Voltage at Reference Temperature 2	$V_{OC,2}$	V
Short-Circuit Current at Reference Temperature 1	$I_{SC,1}$	A
Short-Circuit Current at Reference Temperature 2	$I_{SC,2}$	A
Diode Quality Factor	D	—
Number of Cells per Module	$N_{C/M}$	—
Delta-Voltage / Delta-Current at Open-Circuit Voltage	k	V/A
Modules per String	$N_{M/S}$	—
Number of Strings	N_S	—
Cost per Module	C_M	
DC–DC		
DC–DC Nominal Power	$P_{in,DCDC,nom}$	W
DC–DC Cost	C_{DCDC}	US $
DC–AC (Solar Inverter)		
DC–AC Nominal Power	$P_{in,DCAC,nom}$	W
DC–AC Peak Efficiency	$\eta_{DCAC,peak}$	—
DC–AC Cost	C_{DCAC}	US $
AC–DC		
AC–DC Nominal Power	$P_{ACDC,nom}$	W
AC–DC Peak Efficiency	η_{ACDC}	—
Pre-Inverter Load Model		
Minimum Demand	L_{min}	Wh/h
Maximum Demand	L_{max}	Wh/h
Mode	L_{mode}	Wh/h

Solar Module Model

The model presented by Walker (2001) was used to calculate solar module current given the particular characteristics of the module, irradiance, temperature and output voltage. The function $I_{PV}(V_{PV}, T, J)$ is thus defined as the result of the MATLAB-function included in that study. The constants $T_{ref,1}$, $T_{ref,2}$, $V_{OC,1}$, $V_{OC,2}$, $I_{SC,1}$, $I_{SC,2}$, D and k are also included in the function. A detailed description of the calculations involved would be too extensive for this thesis, and interested readers are referred to the study.

All constants in the formula except the diode quality factor and the delta voltage–delta current are given from the datasheets for Stion STN 135W solar modules. Detailed technical data is given in Appendix 1. In order to arrive at a sufficiently accurate model of the solar modules, the two remaining constants are chosen to make the I–V curve at standard measurement conditions as similar as possible to the curve given in the datasheet. In Figure 46 the two curves are compared. The main difference between the two is that the real curve is slightly descending in the linear part at the lower voltages, while the modelled curve is totally flat. This is because the model used ignores the parallel equivalent resistance that leads to a leakage current, which in turn varies linearly with the voltage.

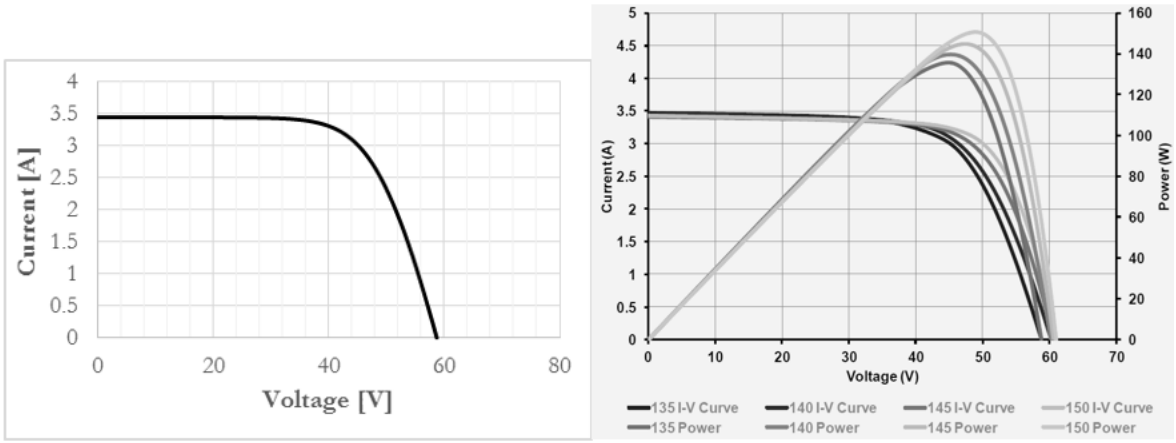

Figure 46: Solar panel efficiency curve (Stion Corporation, 2012)

In order to simulate a MPPT algorithm, voltages at the MPP are calculated for different temperatures and irradiances. This is done using a simple interval halving method. The values are stored in a table for lookup by functions in the model.

Load model

For the purposes of this thesis, the load is considered to be the pre–UPS-inverter load because that point and every point downstream in the system can be considered identical for both the combined system and two separate systems.

A triangular distribution is used to model the load. Random variates U_h are drawn from a uniform distribution in the interval $(0, 1)$ and the resulting load for that hour is calculated using Equation 2.

$$L_h = \begin{cases} L_{min} + \sqrt{U_h(L_{max} - L_{min})(L_{mode} - L_{min})}, & 0 < U_h < \dfrac{L_{mode} - L_{min}}{L_{max} - L_{min}} \\ L_{max} - \sqrt{(1 - U_h)(L_{max} - L_{min})(L_{max} - L_{mode})}, & \dfrac{L_{mode} - L_{min}}{L_{max} - L_{min}} \leq U_h < 1 \end{cases} \quad (2)$$

A random load is calculated for each hour of the simulation.

The triangular distribution is a good approximation if the underlying distribution is not known, but the maximum, minimum and most common values are known or can be estimated (Ngan, 2012). The probability distribution of a triangular distribution is seen in Figure 47. It can be seen that values around the mode are more probable than values close to the minimum and maximum.

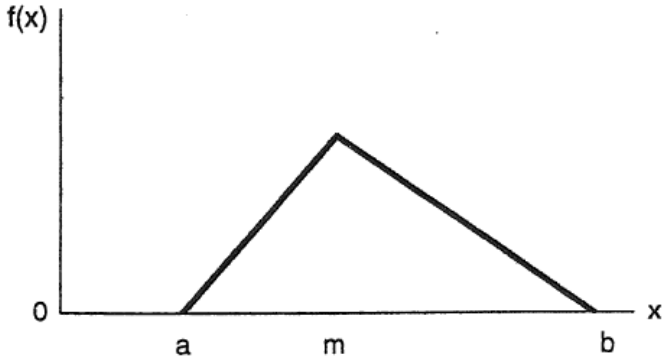

Figure 47: Probability density function of a triangular distribution (Ngan, 2012)

Efficiency models

Efficiencies of three components are included in the model: the DC–DC converter, the AC–DC converter and the solar inverter.

The DC–DC converter efficiency η_{DCDC} is modelled according to the efficiency curves given by the manual of the converter used in the prototype system, namely the EPsolar eTracer ET3415. The curve was adjusted visually to correspond to the curve given by the manufacturer. Figure 48 shows the modelled curve to the left and the curve given in the manual to the right (blue curve). The modelled curve display efficiency as a function of input power.

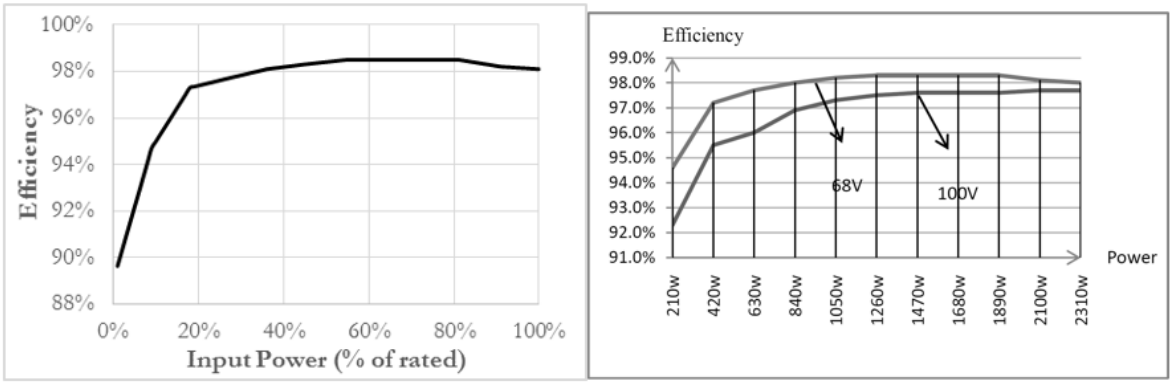

Figure 48: Solar charge controller efficiency curve (EP Solar, 2013)

The efficiency of the solar inverter is based on the efficiency model presented in the literature review. However, the voltage dependency is removed to simplify the model and to reflect the fact that voltage dependency differs among different inverters. The formula used in the model is described in Equation 3. The chosen inverter efficiency profile for modelling is the SMA SunnyBoy SMC 11000-10. Measured efficiencies for different powers were taken from the datasheet and curve fitted in MATLAB in order to determine the coefficients b_0, b_1 and b_2 used in the model.

$$\eta_{DCAC}\left(\frac{P_{in,DCAC}}{P_{in,DCAC,nom}}\right) = \frac{b_0}{\left(\frac{P_{in,DCAC}}{P_{in,DCAC,nom}}\right)} + b_1 + b_2\left(\frac{P_{in,DCAC}}{P_{in,DCAC,nom}}\right) \quad (3)$$

The coefficients that gave the best curve fit were:

$$b_0 = 1.589 \cdot 10^{-3},$$
$$b_1 = 7.679 \cdot 10^{-3} - \eta_{DCAC,peak},$$
$$b_2 = 2.188 \cdot 10^{-2}$$

The resulting curve is shown in Figure 49. The corresponding datasheet curve is shown in Figure 50. The 350 VDC curve were used for curve fitting.

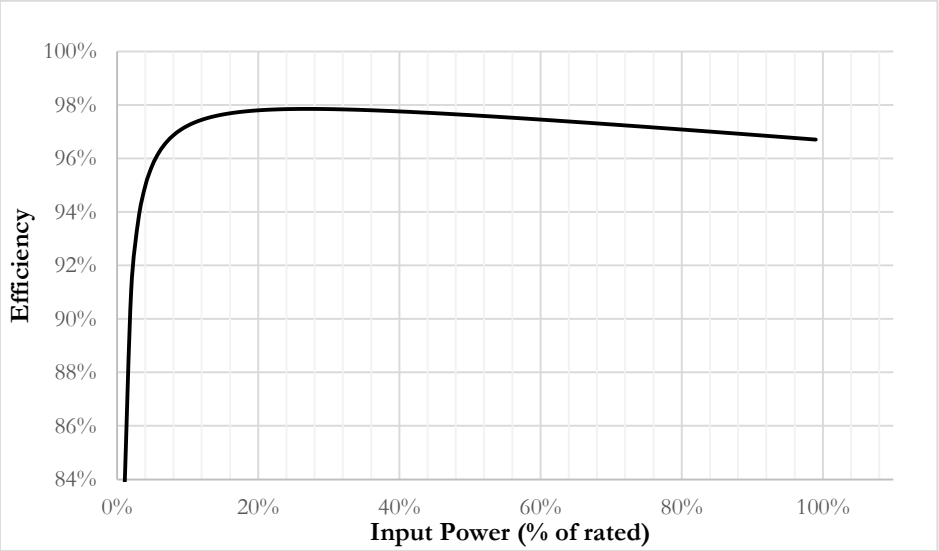

Figure 49: The simulated efficiency curve of a SMC 11000TL-10

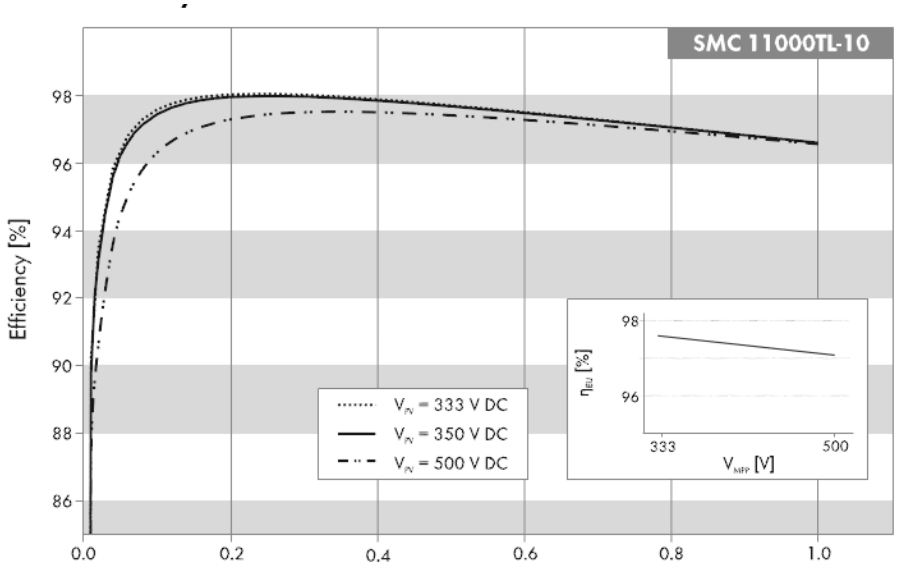

Figure 50: Efficiency curve of a SMC 11000TL-10 (SMA Solar Technology AG, 2013)

The efficiency profiles of different rectifiers vary depending on the rectifier design. For example Figure 51 shows the efficiency curves of different rectifiers depending on design.

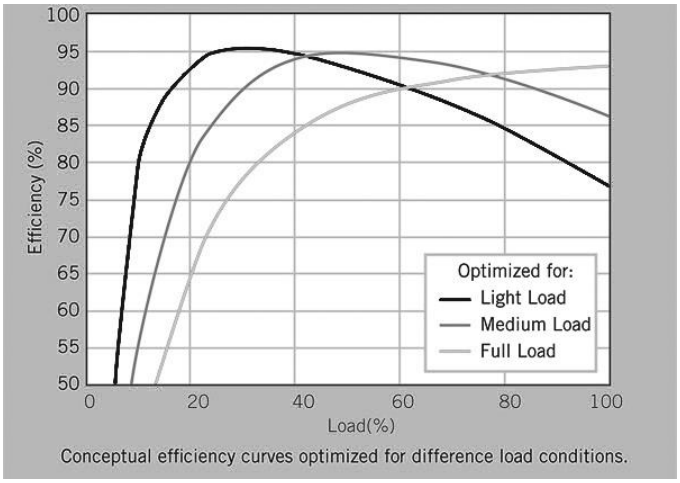

Figure 51: Rectifier efficiency curves depending on rectifier design (Strydom, 2012)

The rectifier efficiency profile used in the model is based on Figure 52. Based on efficiency curves for many different rectifiers, the chosen one was considered to best represent the average efficiency curve for the rectifiers on the market (Eaton, 2014). The lower end of the modelled profile was chosen arbitrarily; since the rectifier will be operating above 30% power for practically every hour it has a very small impact on the result of the model.

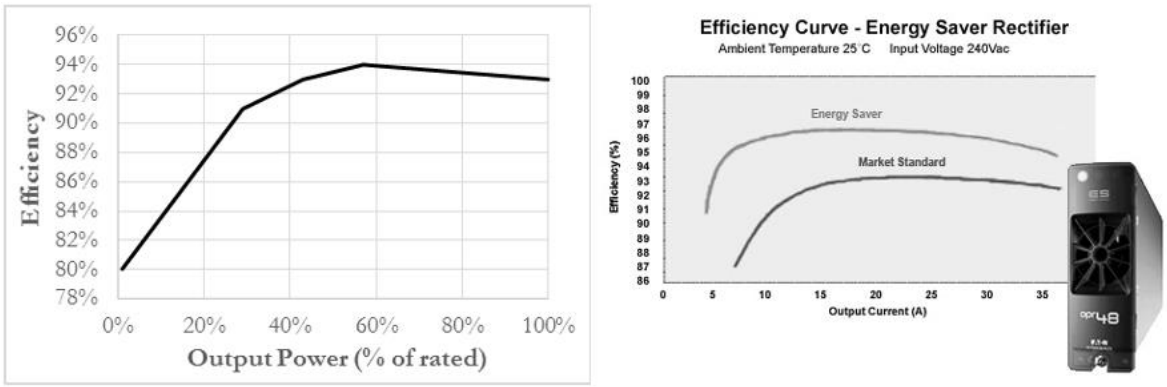

Figure 52: The rectifier efficiency curve (Eaton, 2014) and the curve used in the model

Hourly Calculations

Common for Both Cases

Hourly input data are global horizontal irradiance J_h, dry bulb temperature T_h and the randomized load L_h. Using this information and the table of MPP voltages calculated in the solar model, a simple table lookup function $MPP_{V,h} = MPP_V(J_h, T_h)$ is implemented to calculate the MPP voltage for each hour. The MPP current is then calculated with the previously defined function $MPP_{I,h} = I_{PV}(MPP_{V,h}, T_h, J_h)$. With the help of voltage and current the maximum power that can be extracted from the solar modules can be calculated: $MPP_{P,h} = MPP_{V,h} \cdot MPP_{I,h}$.

Specific for the Combined System

There are two reasons why the power from the DC–DC converter differs from the theoretical maximum power of the solar modules in the model. Firstly, losses are incurred in the converter itself, and are taken into account in the model by Equation 4. Secondly, if the load is less than the maximum post-converter power, the DC–DC converter transitions from being a power terminal into a slack terminal. This means that the DC–DC converter will produce just enough to feed the pre-UPS inverter

load L_h. Therefore the actual output power of the DC–DC converter for each hour is calculated using Equation 5.

$$P_{out,DCDC,h,max} = MPP_{P,h} \cdot \eta_{DCDC}\left(\frac{MPP_{P,h}}{P_{in,DCDC,nom}}\right) \tag{4}$$

$$P_{out,DCDC,h} = max\{P_{out,DCDC,h,max}, L_h\} \tag{5}$$

Next step is to calculate the AC–DC converter output, which is determined by the load and the DC–DC converter output according to Equation 6. When the output has been calculated, the input is calculated according to Equation 7 using the efficiency curve for the AC–DC converter defined earlier.

$$P_{out,ACDC,h} = L_h - P_{out,DCDC,h} \tag{6}$$

$$P_{in,ACDC,h} = P_{out,ACDC,h} \cdot \eta_{ACDC}\left(\frac{P_{out,ACDC,h}}{P_{out,ACDC,nom}}\right) \tag{7}$$

The net energy gain of the solar modules in the combined system is not the actual production of the modules, nor is it the delivered post–DC–DC converter energy. Instead it is considered to be the net difference in the input energy of the AC–DC converter compared to a system without solar power. In other words it is the energy that need not be purchased from the grid due to the PV installation. This has significance especially considering the varying efficiency in the AC–DC converter.

Specific for Separate Systems

For two separate systems, the solar power system is considered to be placed upstream of the UPS system as visualized in Figure 45. The power generated from the panels is fed through a solar inverter that always operates at the MPP. It is assumed that the power produced can always be either utilized by the downstream UPS-powered load or fed back to the utility and sold (in cases where the solar system produces more power than the load requires). The post-inverter power of the solar inverter is thus the maximum power extractable from the solar modules adjusted by the efficiency of the inverter (Equation 8).

$$P_{out,DCAC,h} = MPP_{P,h} \cdot \eta_{DCAC}\left(\frac{P_{in,DCAC,h}}{P_{in,DCAC,nom}}\right) \tag{8}$$

Summarized results

The net energy gain is summarized and compared in the end of the model. For the combined system, Equation 9 is used to calculate the net savings in energy going into the AC–DC converter due to the solar power. For separate systems, the post-inverter energy is simply summarized in Equation 10.

$$E_{savings} = \sum_{h=1}^{H}\left(L_h \cdot \eta_{ACDC}\left(\frac{P_{out,ACDC,h}}{P_{out,ACDC,nom}}\right) - P_{in,ACDC,h}\right) \tag{9}$$

$$E_{production} = \sum_{h=1}^{H} P_{out,DCAC,h} \tag{10}$$

The only component that differs between the two cases is the PV conversion device, which is either a DC–DC converter in the case of a combined system or a solar inverter in the case of two separate systems. Therefore the net reduction in investment costs can be calculated using Equation 11.

$$C_{savings} = C_{DCAC} - C_{DCDC} \tag{11}$$

11.2.2 System to be modelled

The full-scale system chosen to model is a data center since this type of application is one of the most common for UPS systems today (Ward, 2001). There are several characteristic features of a data center that is used in the model of the load. Firstly, the absolute majority of the power consumed in a data center is used by the servers and the cooling system for the servers (Pelley et al., 2009). The cooling system is generally not supplied by a UPS system as the cooling system is not in need of high power quality (Sheppy et al., 2011).

Since one of the key purposes of a data center is to provide around-the-clock access to its hosted servers, the load is usually never powered off. Similarly the load served by the UPS is usually close to constant as most of the power is consumed by the servers, with only a fraction, if anything, being used for other functions.

The load modelling is based on the publication by Sheppy et al. (2011) and a graph of their measurements of a real full-scale data center is shown in Figure 53. The total power consumption presented by the darkest line has some variations over the measurement period due to seasonal changes in cooling requirement, but the brighter line below representing the power to the servers, which is the only load fed through the UPS, is close to constant. The minimum to maximum variance in the IT-load is approximately 10%, over a 6-month period with no major changes detected for individual hours or days.

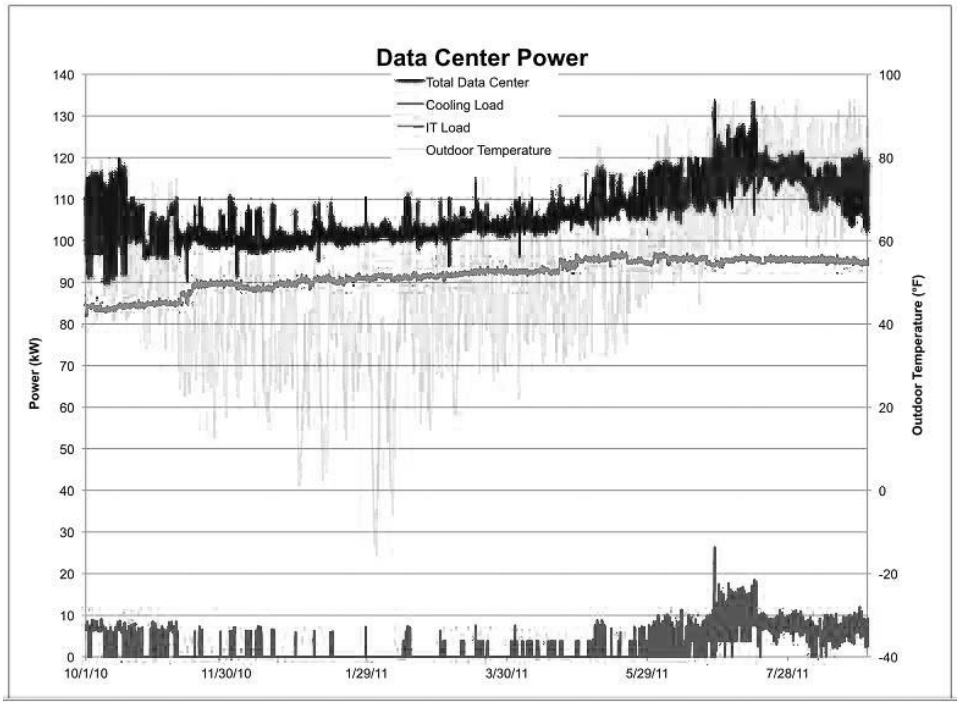

Figure 53: Data center power consumption, UPS load in red (Sheppy et al., 2011)

The sizes of a data center can differ significantly, but in this model the nominal load has been set to 100 kW of server power, as that is a common size (Sheppy et al., 2011). Only the part of the data center load fed via the UPS (i.e. the servers themselves) are included in the model, as other loads are not affected by the UPS or solar energy system.

The load is modelled using a triangular distribution, with the nominal power of 100 kW. Since the IT-power consumption in the data center load model presented by Sheppy et al. (2011) has an approxi-

mate variance of +-5% during a half-year measurement period the triangular distribution has a minimum load of 95 kW and maximum load of 105 kW.

When dimensioning the solar power in the economic model the main limiting factor is that for the combined system the power of the load has to exceed the power generated by the solar panels. This is because the UPS is not constructed to enable power to flow back into the grid. The surplus power from the solar cells would in such a situation be wasted and might affect the system in a negative way. The nominal power of the panels at STC was thus put below the minimum load (95 kW).

On the other hand, the more solar power installed, the greater the impact in the calculations in the model. Thus the solar power is dimensioned to produce approximately 80% of nominal load at STC. The number of solar panels used in the modelling is 600 - corresponding to 82 kW of installed solar power.

Since the model is based on prices per watt, the solar inverters and solar charge controllers can be scaled to any size. Since the nominal solar power in the model is 82 kW the maximum power for the inverters or solar charge controllers are scaled to handle this level of power with an added margin. In cooperation with representatives for a solar installation company this margin was chosen to 20%. The solar inverters and solar charge controllers used in the model is thus scaled to a total power of 98.4 kW.

11.2.3 Solar irradiance

The climate data used in the model is based on data for a typical meteorological year for Stockholm, Sweden. There are several different datasets for meteorological data available. In the model TMY2 is used, since it is a commonly used database with data for many locations.

TMY2 is a dataset based on hourly time-periods, and the data is based on measured data for the years 1961-1990 from the National Solar Radiation Data Base (Marion and Urban, 1995). TMY2 gives hourly data on many parameters, the ones used in the model is dry temperature and global horizontal solar irradiance. A minor limitation is that since the data used in this database is collected before 1990 the yearly irradiance might have changed slightly due to climate changes, but the effect of this is estimated to be low as the final result is in line with new measurements.

In order to evaluate the importance of geographical location in the economic model a sensitivity analysis is conducted using meteorological data for another city. Since the geographical scope of this thesis is limited to Sweden, meteorological data for the major Swedish city of Gothenburg are used in the sensitivity analysis. Due to the low amount of yearly irradiance in northern Sweden (Fraunhofer Institute, 2012) the geographical locations are both in southern Sweden.

11.3 Component cost

The economic analysis aims to evaluate the economic impact of combining solar energy and UPS systems by comparing the investment costs of components exclusively used in either the combined or the separate systems. Essentially these components are a solar charge controller for the combined system and a solar inverter for the separate system.

There are some prognoses for the cost of solar inverters (Clover, 2013, Solarbuzz, 2012), but this data is not coupled with data for solar charge controllers, and has therefore not been used to model the prices for the components.

Instead data of list prices, peak power, peak efficiency and typical efficiency (euro efficiency for solar inverters) has been collected from wholesale companies for components available in the market. The wholesale companies used for the comparison were chosen because of their wide selection of both solar inverters and solar charge controllers. List prices not only reflect the manufacturing cost of components but also taxes, shipping and the added margin of the wholesaler. Thus in order minimize the impact on the relative costs of inverters and solar charge controllers both components have been compared from the same website.

The type of inverter dominating the commercial and small scale solar industry is string inverters with sizes around 5-30 kW peak power (Fraunhofer Institute, 2012). In this model only data from inverters between 5 kW and 20 kW has been included. Since string inverters are generally larger than solar charge controllers all prices have been recalculated to the common unit of $/W in order to both enable comparison and scaling of the systems.

The solar inverters included in this study are from well-known manufacturers where the technical data is readily available and the panels have been tested in accordance to industry standards. All components used in the study have an integrated MPP tracker in order to maximize the generated power. The two wholesalers chosen are both American, and prices are listed without tax and shipping fees. Both wholesalers have a wide selection of models, of which several have been selected based on being classified as string inverters from well-known manufacturers. The wholesalers are Wholesale Solar (2014) and Alternative Energy Store (2013).

The prices for the solar inverters chosen are presented in Table 3 and the solar charge controllers presented in Table 4. The average price per watt for the two wholesalers is calculated and used in the economic model.

Table 3: Solar inverter prices from WholeSaleSolar and AltEstore

Brand	Name	Peak Power [W]	Price [USD] WholeSaleS	Price/watt WholeSaleS	Price [USD] AltEstore	Price/watt AltEstore
SMA	SunnyBoy 6000 TL	6,300	2,409	0.382		
SMA	SunnyBoy 8000 TL	8,300	2,965	0.357	3356	0.404
SMA	SunnyBoy 10000 TL	10,350	2,999	0.290	2995	0.289
SMA	SunnyBoy 11000 TL	11,500	3,450	0.300		
Schneider	Conext 5000 NA	5,000	1,935	0.387		
Fronius	IG PLUS 10.0	10,000	3,009	0.301	3499	0.350
Average				**0.3362**		**0.3479**

Table 4: Solar charge controller prices from WholeSaleSolar and AltEstore

Brand	Name	Peak Power [W]	Price [USD] WholeSale Solar	Price/Watt WholeSale Solar	Price [USD] AltEstore	Price/watt AltEstore
Schneider	XV Solar charge controller	3,500	475	0.136	497	0.142
Outback	Fleximax 60	3,750	499	0.133	539	0.144
Outback	Fleximax 80	5,000	549	0.110	549	0.110
Tristar	MPPT 45	2,400	415	0.173	410	0.171
Tristar	MPPT 60	3,200	530	0.166	499	0.156
Average				**0.1434**		**0.1445**

The average price for both wholesalers are 0.144 $/W for solar charge controllers and 0.342 $/W for solar inverters. These values are used in the economic model for the base scenario.

When comparing with both Chinese manufacturers and the prognosis by Clover (2013) the price difference for solar inverters are higher than for solar charge controllers – likely due to high-end inverters being chosen for the study. Therefore price data for solar inverters were also collected from the manufacturer Danfoss. The price for their respective models in the range 5 kW to 20 kW is presented in Table 5 along with average price per watt which is used as an alternative price for inverters in the economic model.

Table 5: Prices for Danfoss solar inverters

Modell	Peak Power [w]	Price [USD]	Price/watt
TLX+6k	6,000	1,810	0.302
TLX+8k	8,000	2,057	0.257
TLX+10k	10,000	2,477	0.248
FLX PRO 5	5,000	1,723	0.345
FLX PRO 6	6,000	1,810	0.302
FLX PRO 7	7,000	1,934	0.276
FLX PRO 8	8,000	2,057	0.257
FLX PRO 9	9,000	2,267	0.252
FLX PRO 10	10,000	2,477	0.248
FLX PRO 12.5	12,500	2,756	0.220
FLX PRO 15	15,000	2,789	0.186
FLX PRO 17	17,000	3,011	0.177
Average			**0.2258**

Data for solar inverters and solar charge controllers have also been researched from manufacturing companies in China via the sourcing website Alibaba. But the information regarding these products generally have not been adequate to compare different models and types due to ambiguity regarding test methods, if MPPT tracking is included, peak efficiencies, taxes, tolls and shipping fees. Therefore the choice was made to exclude this source of data.

The cost for solar inverters and solar charge controllers from Chinese manufacturers are however significantly lower than for the more widely spread models from for example SMA. But since the price gap between list prices for both inverters and solar charge controllers were approximately equal the relative price differences, and thus the impact on the economic comparison of the two options, is estimated to be small.

With price estimations in the unit $/W the systems can be scaled to any size in the model, and the economic study of component costs can thus be analyzed. In order to estimate the impact of individual parameters on the result all parameters are adjusted in a sensitivity analysis before comparing the result of the model.

11.4 Energy generation

The choice of design for the system does not only influence the investment cost for the components needed, but also influences the power flow and thus the conversion losses and the total system efficiency. In order to evaluate the two options (combined or separate solar power system) from an economic perspective the difference in total energy generation resulting from the potentially different conversion efficiencies also has to be discussed.

Most of the components in the system incurs some sort of conversion losses, but only the major ones which are also affected by the choice of system design is included in the model; the rectifier in the UPS, the solar inverter and the solar charge controller.

The efficiency curve of the solar inverter has already been included in the model, but the parameters left to decide is the typical efficiency (euro or CEC efficiency) and the peak efficiency. Data for these parameters were collected from the inverters used to model the component costs. Data is collected from technical datasheets by the manufacturers and average values are calculated in order to be used in the model. The data is presented in Table 6.

Table 6: Conversion efficiencies for some common solar inverters

Brand	Name	Peak Power [W]	CEC Efficiency	Peak Efficiency
SMA	SunnyBoy 6000 TL-US	6,300	98.0%	98.3%
SMA	SunnyBoy 8000 TL-US	8,300	98.0%	98.3%
SMA	SunnyBoy 10000 TL-US	10,350	98.0%	98.3%
SMA	SunnyBoy 11000 TL-US	11,500	98.0%	98.3%
Schneider	Conext 5000 NA	5,000	95.5%	96.7%
Fronius	IG PLUS 10.0	10,000	95.5%	96.2%
Average			**97.3%**	**97.8%**

The conversion efficiency of the solar charge controllers was collected with the same method as the solar inverters. The data is taken from the solar charge controllers used to calculate the components prices. Only data from peak efficiency is available as there is no standardized measure of typical conversion efficiency for solar charge controllers. The data is collected from manufacturers' datasheets and presented in Table 7, with the average value used in the economic analysis.

Table 7: Conversion efficiencies for some common solar charge controllers

Brand	Name	Peak Power [W]	Peak Efficiency
Schneider	XV Solar charge controller	3,500	99.0%
Outback	Fleximax 60	3,750	98.1%
Outback	Fleximax 80	5,000	97.5%
Tristar	MPPT 45	2,400	99.0%
Tristar	MPPT 60	3,200	99.0%
Average			**98.5%**

Since alternative prices were calculated from solar inverters from Danfoss, the average conversion efficiencies for these inverters were also calculated to be used in the economic model (Table 8).

Table 8: Conversion efficiencies for Danfoss solar inverters

Modell	Peak Power [w]	Euro Efficiency	Peak Efficiency
TLX+6k	6,000	96.5%	97.8%
TLX+8k	8,000	97.0%	97.9%
TLX+10k	10,000	97.0%	98.0%
FLX PRO 5	5,000	96.0%	97.6%
FLX PRO 6	6,000	96.4%	97.7%
FLX PRO 7	7,000	96.8%	97.8%
FLX PRO 8	8,000	96.9%	97.9%
FLX PRO 9	9,000	97.1%	97.9%
FLX PRO 10	10,000	97.1%	97.9%
FLX PRO 12.5	12,500	97.3%	98.0%
FLX PRO 15	15,000	97.4%	98.0%
FLX PRO 17	17,000	97.4%	98.0%
Average		**96.9%**	**97.9%**

The final component used in the efficiency calculations is the rectifier used in the UPS to convert incoming power from the electricity grid into DC power. As with the solar inverter and solar charge controller the efficiency curve shape had already been modeled, but the model was adjusted to fit the peak efficiency of the inverter.

There are many different topologies for rectifiying electricity, with a wide range of conversion efficiencies (Shepherd and Zhang, 2004). Many simpler topologies used in smaller applications have a peak efficiency well below 90% but since lower efficiency results in high conversion losses and thus higher electricity costs more advanced topologies is generally used in larger applications (Roth et al., 2002).

For a 100 kW data center application a relative high conversion efficiency is likely to result in lower overall costs because of the high amount of electricity bought from the power grid. This is supported by researching conversion efficiencies for commercially available large-scale UPS systems.

Based on data from the efficiency curves used to model the rectifier (Strydom, 2012) and data of rectifiers from Shepherd and Zhang (2004) the peak conversion efficiency of 94% was chosen as the standard case in the economic model.

In order to translate the energy generation into monetary value an electricity price is needed. The model uses a basic calculation of value of the electricity generated during one year, not during the lifetime of the system. This is because a complete prognosis of the future electricity price including governmental subsidies and taxes is needed to calculate net present value. Instead the electricity price for the first year is used as an indication of the monetary value of the generated energy.

The electricity price used in the model is based on the average Swedish spot market price during 2013 with the addition of the basic electricity tax and the variable part of the grid tariff. Since 2012 Sweden is divided into 4 different electricity price zons, with small changes in prices. Since the solar data used is from Stockholm, the price zon 3 – where Stockholm is situated is used to calculate the electricity price. For 2013 the electricity price in price zon 3 was 340.77 SEK/MWh (Nord Pool, 2014). The basic electricity tax excluding VAT was 293 SEK/MWh in 2013 (Elpriskollen, 2014). The grid tariff used in the model is based on prices from Vattenfall AB (2014) and is 200 SEK/MWh. The prices is heavily

depending on the amount of power bought, and can thus change considerably from the value chosen. The sum of the prices equals 833.77 SEK/MWh electricity.

Since all prices used in this thesis are U.S. dollars the cost of electricity is converted to $/MWh. The exchange rate used is taken from Google Finance 2014-05-29 where 1 SEK equals 0.15 dollars. The value of the generated money is calculated using the electricity price of 125.77 $/MWh.

As an indication of the profitability of solar energy and the combined solar energy and UPS system a basic payback calculation is included in the model. In order to calculate the investment cost of the components included in both the separate and combined solar energy system, standardized data from U.S Department of Energy (2010) is used. The costs are grouped into belonging to either solar modules or BOS/installation where the cost of modules for 2014 is interpolated to 1.27 $/W and costs of BOS/installation is interpolated to 1.14 $/W. No additional investment costs or maintenace costs is included in the calculation and the lifetime of the solar panels are assumed to surpass the payback time. The component cost for solar charge controllers (0.14 $/W) and solar inverters (0.34 $/W) is taken from the whole-salers as discussed above. The total investment cost summarizes to 2.75 $/W for the stand-alone system and 2.55 $/W for the solar part of the combined system.

The basic payback calculation uses the electricy price presented above and the price is considered to be constant over multiple years.

In Sweden, an additional source of variable revenue from renewable electricity generation is so-called electricity certificates. Producers of renewable energy receive certificates from the government that producers of non-renewable energy have to buy. This creates a market that stimulates investments in renewables. New solar PV installations receive certificates for 15 years. The number of certificates varies from year to year, increasing until year 2020 and then decreasing until 2035 which is the last year of the program. (Energimyndigheten, 2014)

In order to achieve a more realistic absolute payback time the effect of electricity certificates is also incorporated in the payback assessment. The average of future prices from year 2015 until 2019 is used as a constant addition to the revenue from produced electricity and amounts to 28.89 $/MWh (Svensk Kraftmäkling, 2014).

Results & Analysis

In this section the result of the three studies conducted in this thesis is presented. The result of each individual study is presented separately, together with an analysis of the results. The economic analysis also contains a thorough sensitivity analysis.

12 Result: Computer simulation

The main result of the MATLAB simulation is the learning gained from designing and testing the system, and not the actual output of the final system. However some outputs will be presented, that in short describes some insights gained in the simulation part of this thesis.

The final simulated system proved to be demanding in terms of computing power, which is why only shorter experiments can be conducted. For example, a ten-second experiment results in three million data points and takes several minutes to run. There are several reasons for why the system is computationally intensive, with the primary being numerical complexity in combination with a 10 kHz clock pulse from the solar charge controller.

First and foremost, the battery current needs to be closely monitored and thoroughly tested in order to ensure safe operation of the battery in the physical prototype system. The constant voltage of 56.8 V applied in the prototype system means that the battery current can be relatively high in certain cases, such as when the SOC approaches deep discharge. The risks of overcurrent are several. First of all, the CCU used in the physical prototype system would disconnect the battery often because of rising temperature and pressure in the battery, making the system dysfunctional. Secondly, decreasing battery health is a long term consequence of overcurrents. Finally, in extreme cases where extreme currents flow into the battery the CCU might not have time to react and the battery might get destroyed. In Figure 54, the battery current has been tested for two different SOC's, 90% and 5%. All other inputs are held constant. The load is set at full (750 W) and the solar modules operate at 1 sun and 20 degrees Celsius. The rectifier is at state 1 (on), the battery at state 2 (charge) and the solar charge controller is at state 1 (power terminal).

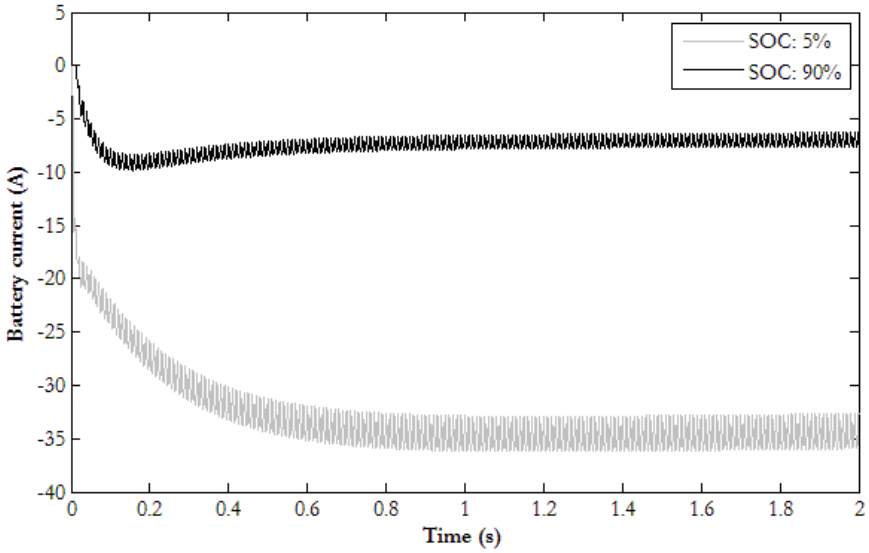

Figure 54: Battery charging current for different SOC's

It is clear that SOC has a very high impact on charging current. The reason is that the battery's voltage drops at low SOC's, leading to a higher difference in voltage between the system and the battery which in turn leads to a higher current according to Ohm's law. The current at 5 % SOC is considered too high for safe operation; therefore the conclusion of this experiment is that no experiments of deep discharge should be conducted on the physical prototype system. The likely consequence of such an experiment is that the fuse placed before the rectifier would blow since it cannot deliver enough current.

Another important factor in the system is how oscillations behave. Even with a purely resistive load, oscillations are present between the rectifier, the solar charge controller and the battery. Figure 55 shows the currents for all three components and the load. It can be seen that the current to the load is constant while the other three currents are oscillating. All four graphs are scaled equally to highlight the difference.

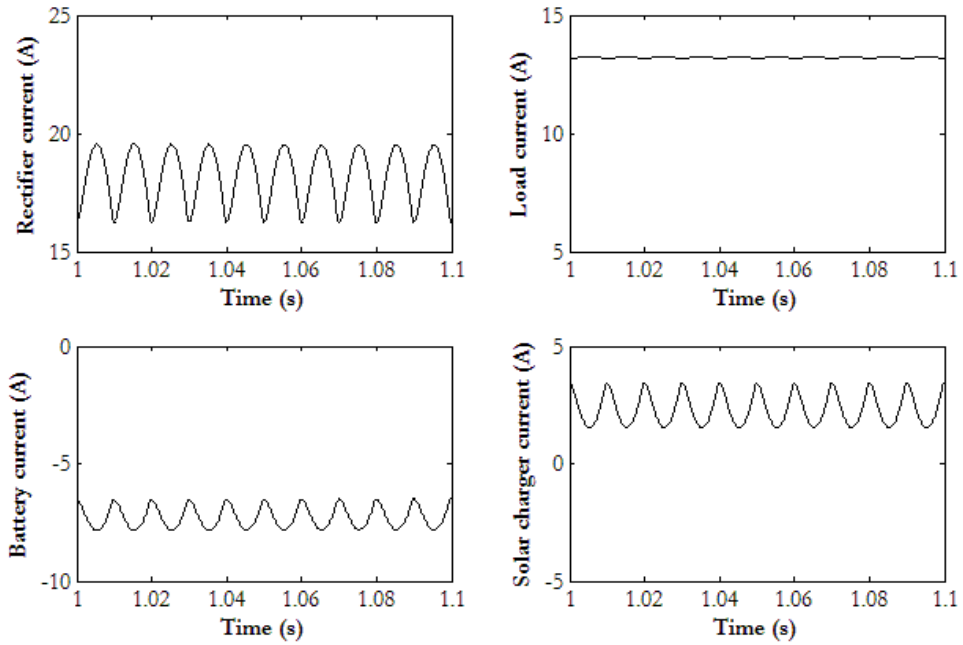

Figure 55: Oscillations in current for all four terminals

The result of the experiment displayed in Figure 55 led to the adding of a diode in the physical system after the rectifier. This will block any currents going backwards into the filter of the rectifier, for example in the case of islanding mode.

The conclusion of the Simulink simulation of this thesis is that much was learned about the system's behavior before building and experimenting with it physically. It also led to consequences in the physical system and the experiments: a diode was added, and experiments involving deep discharge in the physical battery were discarded.

13 Result: Prototype system

In this section the result from the experiments conducted on the prototype system is presented and discussed. The results for each individual experiment are discussed individually with a discussion of the combined results at the end of the section. The experiments are grouped together based on the purpose of the experiment.

13.1 Steady State

For the experiments conducted in steady state the main aim is to compare the level of ripples and noise in the steady state current and voltages. In order to compare the ripples between the configurations a ripple factor is calculated and presented. The result from measurements of waveform and ripples using an oscilloscope is also presented. The results of experiment 1, 2 and 3 are discussed in this section.

Experiment 1: The effect of load on system parameters

Both the rectifier and inverter have a drop in its output voltage based on the power produced. For UPS systems, supplying the load with stable power is a key functionality, and ideally the outgoing AC voltage should be independent on the power level. The ripples and voltage drop depending on the level of power required by the load are measured in the DC current over the current shunt and AC voltage respectively. The results are presented in Figure 56 and Figure 57.

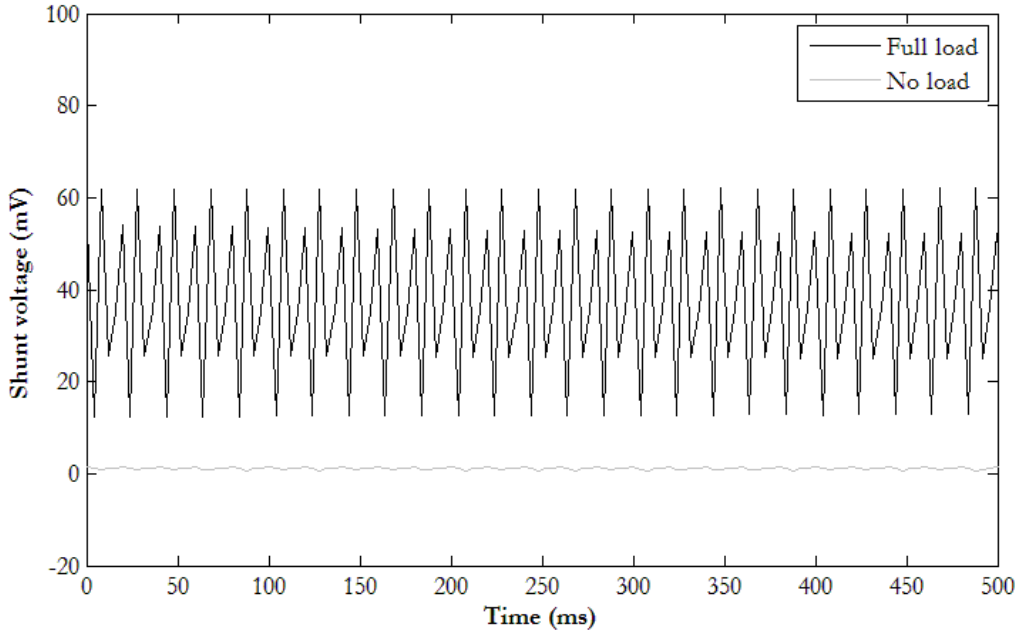

Figure 56: Experiment 1, DC current over the current shunt

With no load plugged in, all current passing the current shunt is used internally by the inverter. The no-load current level is thus low. With a nominal load of 300W the inverter draws more current from the rectifier – resulting in both a higher average consumption and a significant increase in ripples. The figure shows that even without load there are small ripples with the same frequency as the ripples generated with nominal load. Since neither battery nor solar power is plugged in it can be concluded that it is the inverter and rectifier that causes the majority of the ripples in current. In order to improve the voltage stability the inverter contains a high-capacitance filter. As has been explained by Rashid (2011) such a filter often introduces high oscillations in current in order to keep the voltage stable. Analyzing the graph it can be seen that ripples of two frequencies is present, namely 50Hz and 100Hz. The 100

Hz ripples are introduced by the rectifier, since a rectifying full-wave bridge injects ripples twice the frequency of the AC source (mains at 50 Hz). The 50 Hz ripples are presumably created by the inverter, since the output frequency is 50 Hz. The primarily cause of the large ripples in current is thus concluded to be the inverter with the rectifier responsible for a minority of the ripples.

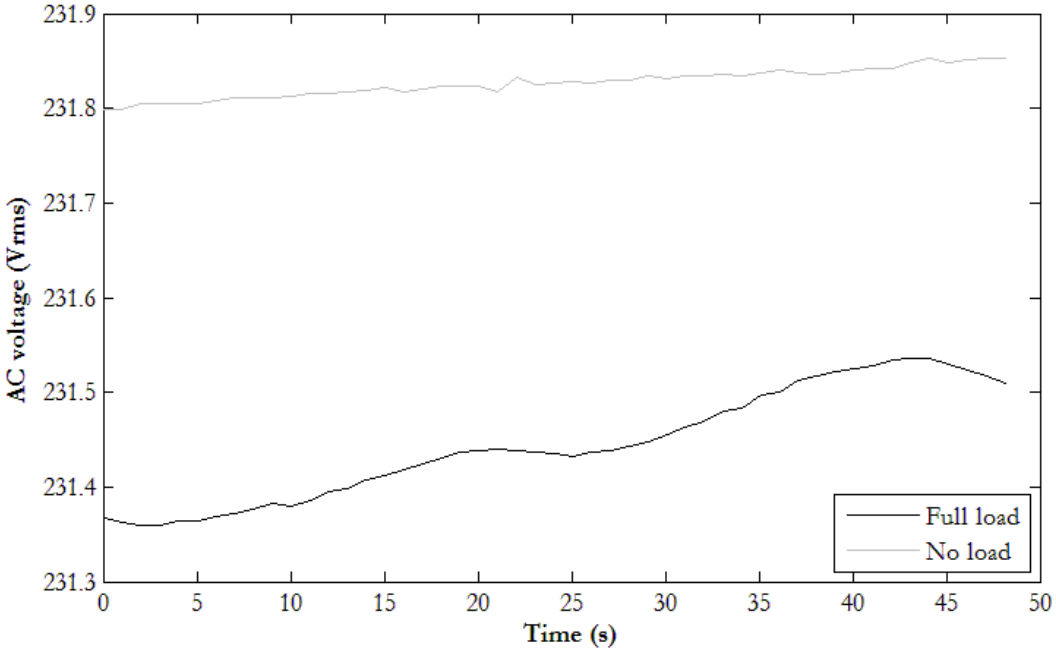

Figure 57: Experiment 1, AC voltage

The inverter is calibrated to supply an AC voltage of 230V at the maximum power of 1000W, and since there is a voltage drop associated with increasing load the inverter thus supplies load with a slightly higher voltage at lower levels of power. This is clearly shown in the graph where the output voltage with no load is approximately 0,4V higher than with the nominal load of 300W. Additionally it can be seen that the voltage without load is more stable than with load, even though the oscillations are small for both cases. The reason for the instabilities is likely that the load itself does not have completely flat power consumption.

Experiment 2: Steady State

Measurements are taken in steady state in order to analyze ripples in the voltage and current. Since the normal operating condition of the UPS is steady state operation with all components connected to the system, the impact on ripples by the solar power is considered a key parameter to evaluate the feasibility of the combined system. The result for measurements of DC voltage, DC current over the current shunt and AC voltage is presented in Figure 58, Figure 59 and Figure 60 respectively. Additionally an oscilloscope is used to analyze ripples in the current; the result from this measurement is presented below.

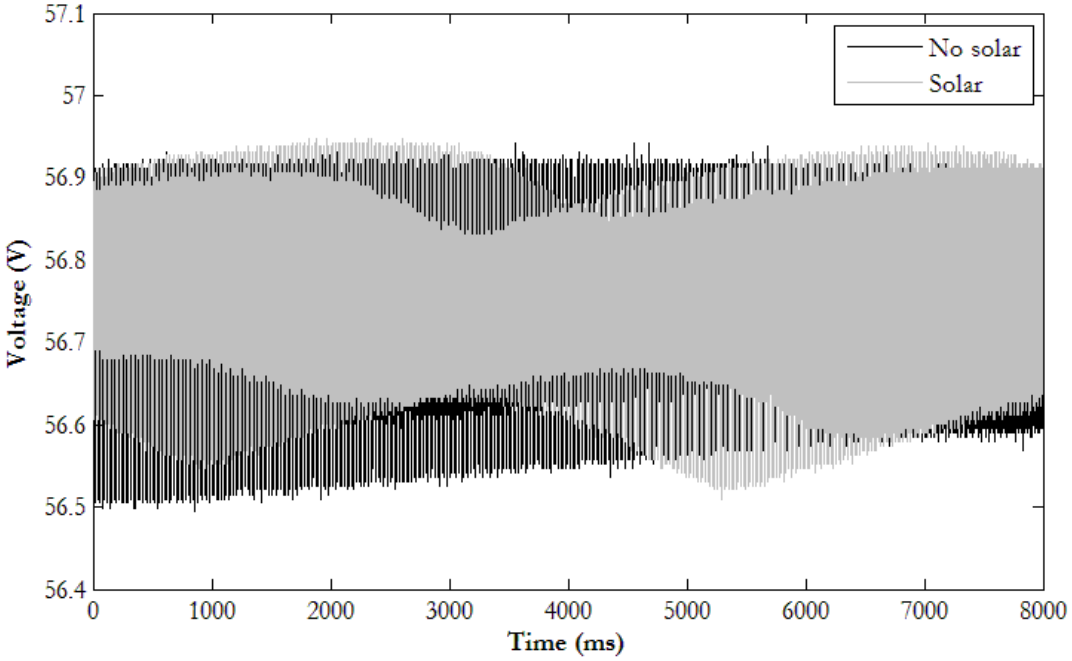

Figure 58: Experiment 2, DC voltage

Over the entire range of the experiment the voltage in both cases are oscillating around the average value of 56,6V to 56,8V which is in the range of the nominal voltage of the DC-line. From the graph it seems like the DC voltage is slightly higher in the case of added solar power. The addition of solar power does not seem to have any impact on the steady state voltage. The ripple factor is calculated for both cases and the result of 0,0027 without solar power and 0,0024 with solar power confirms that the ripples are low in both cases largely unaffected by the addition of solar power.

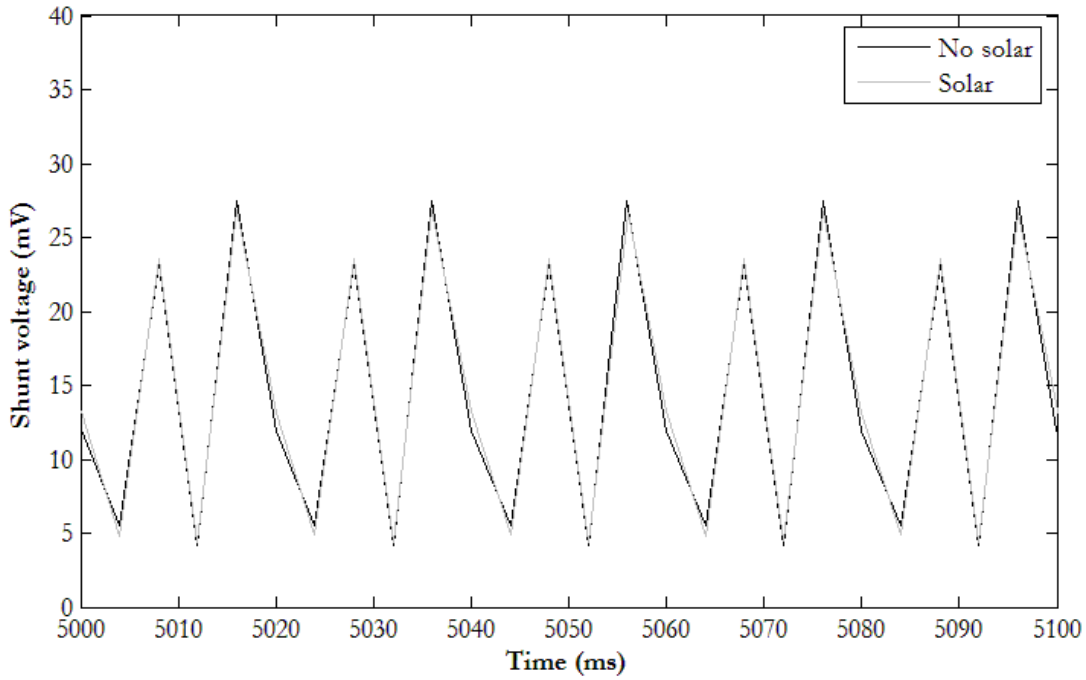

Figure 59: Experiment 2, DC current over the current shunt

As can be seen in the graph the ripples between the two cases are essentially equal. The ripple is thus not caused by the solar panels. The ripples are however high in both cases, with a ripple factor of 0,51 with solar and 0,47 without solar which likely affects the system in a negative way.

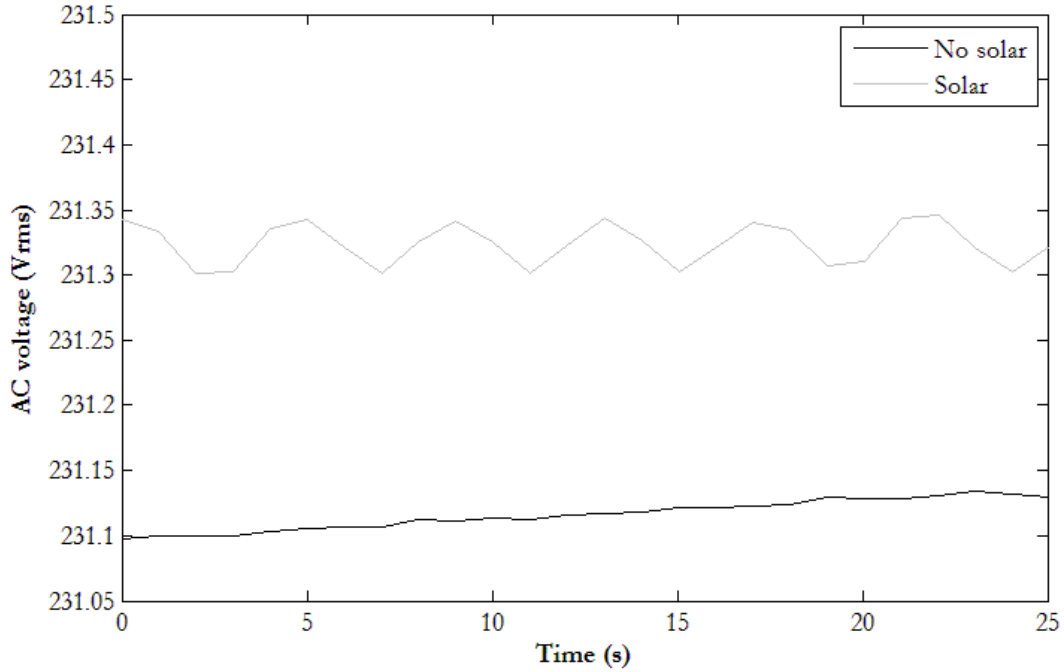

Figure 60: Experiment 2, AC voltage

There seem to be some small oscillations in the AC voltage in the case of added solar power, but the ripples are so small that they cannot be distinguished from measurement errors. For both cases the AC voltage is very stable, which is measured by calculating the THD during steady state in experiment 10. The voltage is approximately 0,2V higher with the added solar.

In Figure 61 the waveform as measured by the oscilloscope is presented without the added solar power, the result is compared with Figure 62 presenting the waveform with added solar power.

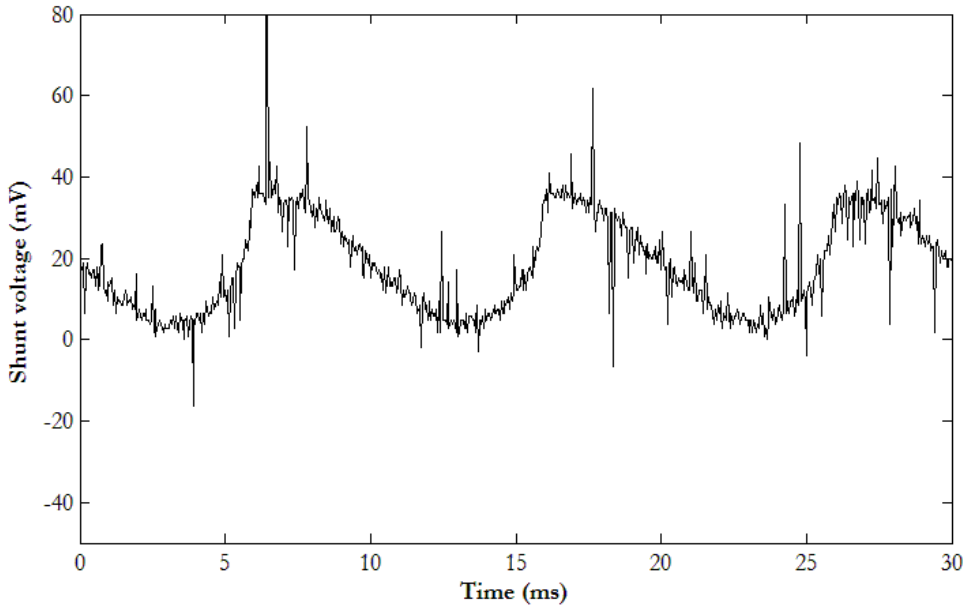

Figure 61: Experiment 2, oscilloscope measurement without solar power

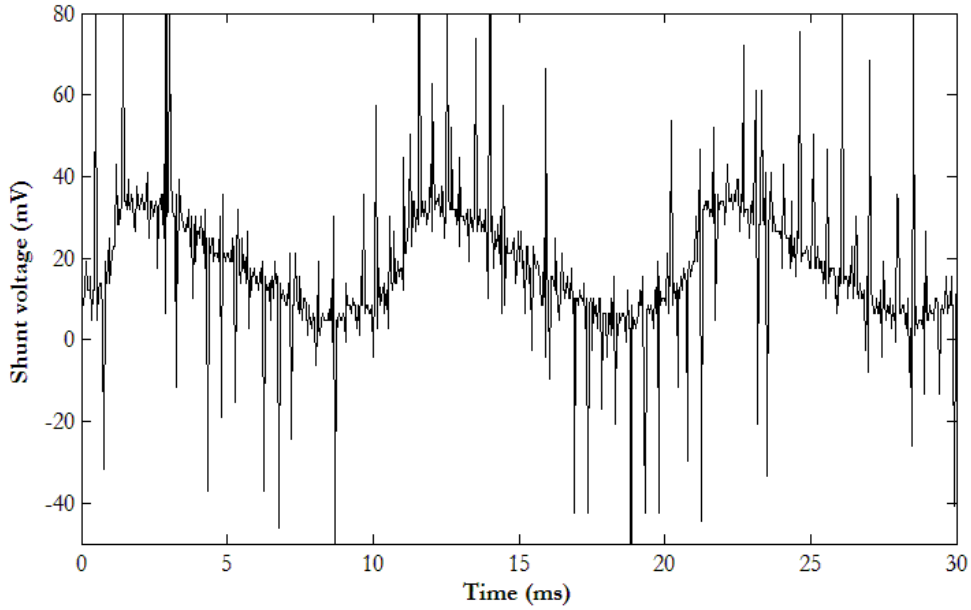

Figure 62: Experiment 2, oscilloscope measurement with added solar power

As can be seen when comparing the graphs the low-frequent waveform is similar between the two cases. In both cases there are significant ripples in the DC current. The oscillations have a fundamental frequency of 50Hz. What can also be seen is that there are also more high-frequent noise in the waveform, and this is significantly higher with added solar power – indicating that this noise is introduced by the solar charge controller. The ripples introduced by the solar charge controller are further analyzed in Figure 63 using much faster measurements in order to analyze high-frequency noise.

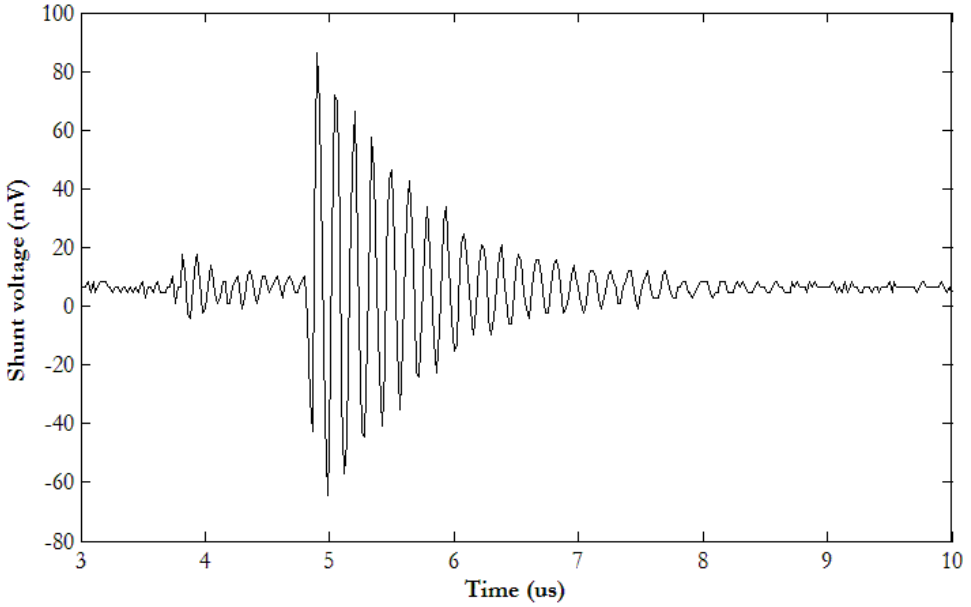

Figure 63: Experiment 2, ripples introduced by the solar charge controller

As can be seen in the graph there are very high-frequent oscillations present in the current waveform. The oscillations have a period of approximately 0,2µs – corresponding to a frequency of 5MHz. These oscillations have amplitude higher than the more low-frequent ripples introduced by the inverter and rectifier. These ripples are introduced by the solar charge controller and could potentially have a negative impact on overall system performance.

Experiment 3: Steady State Islanding Mode

Without the rectifier as the main supply of power the battery or the battery in combination with the solar power system must supply all power to the load. The ripples in steady state are analyzed with and without the addition of the solar power. The voltage ripple, current ripple and output AC voltage is presented in Figure 64, Figure 65 and Figure 66 respectively.

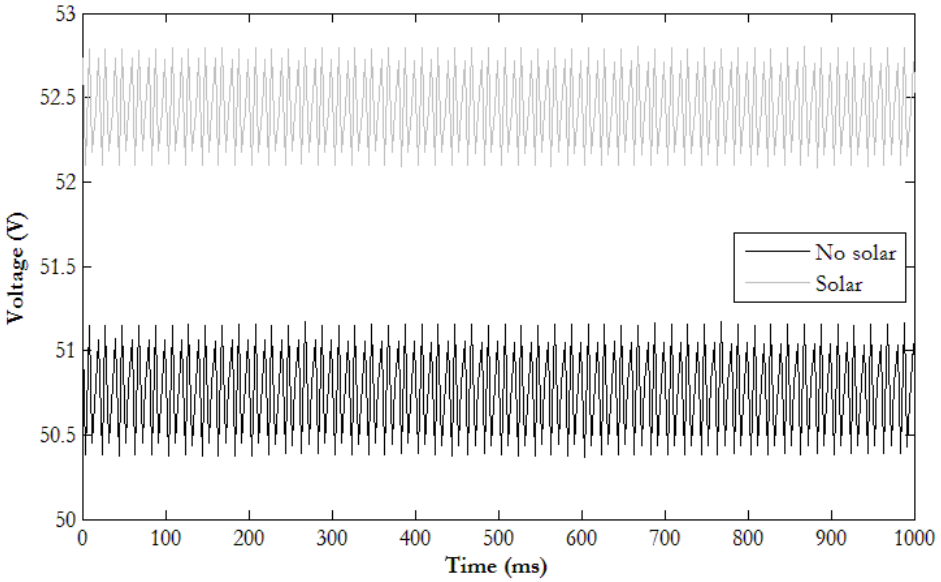

Figure 64: Experiment 3, DC voltage

As can be seen in the graph the voltage with solar is approximately 2V higher than without solar. The main reason for this is changes in the battery SOC – as it is the battery voltage that decides the system voltage a higher SOC corresponds to a higher system voltage. The ripples in the voltage are relatively small and are not affected significantly by the addition of solar power. The ripple factor without solar power is 0,0055 and 0,0048 with solar power.

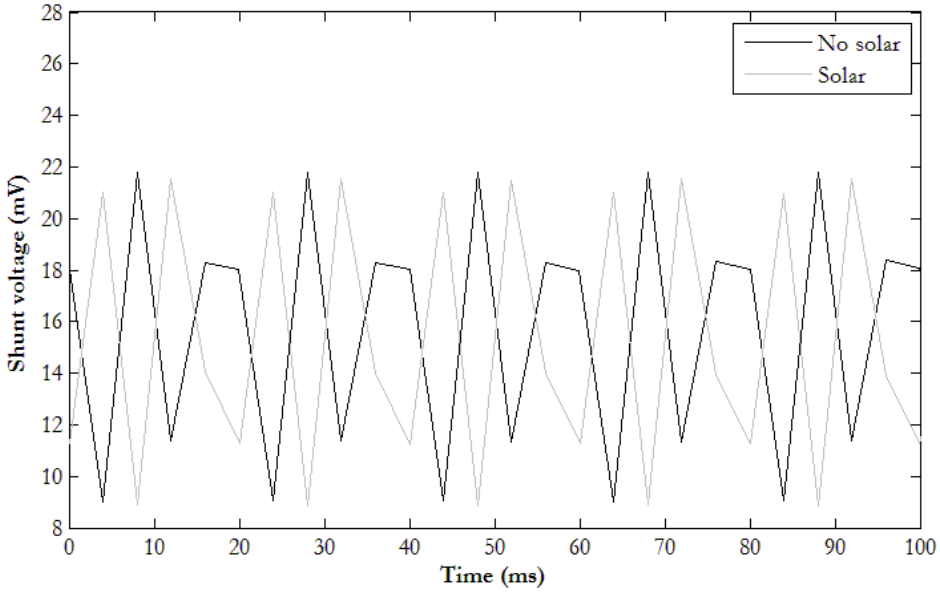

Figure 65: Experiment 3, DC current over the current shunt

The oscillations in the current over the current shunt are high both with and without solar power. The ripple factor without solar is 0,294 and with solar 0,298 indicating that there are no significant changes

between the two component configurations. Comparing to experiment 2 the oscillations, measured by the ripple factor is higher with all components connected to the system. This indicates that the rectifier introduces part of the ripples in the DC current, but that the inverter is the primary source of ripples.

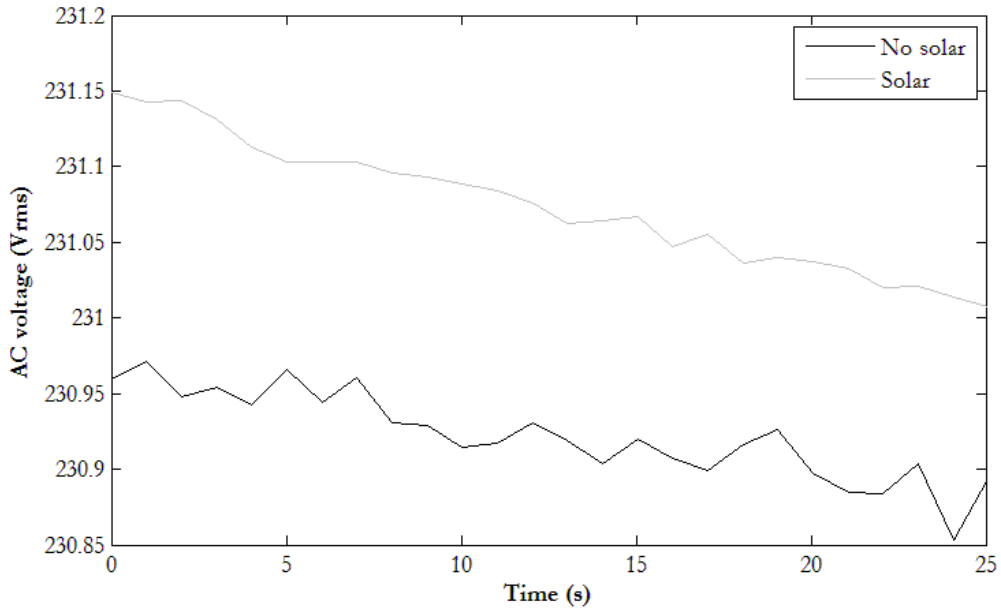

Figure 66: Experiment 3, AC voltage

The graph shows that the outgoing AC voltage is very stable, with little oscillations. After the start of the experiment the voltage seems to be slowly decreasing, both with and without solar power. This small decrease is likely to be either due to measurement errors (since the differences are very small) or part of a slow start-up stabilization.

13.2 UPS parameters

Apart from steady state operations the UPS system must be able to handle transitions to islanding mode in case of power failures in the electricity grid and changes in the load of the UPS. The result of such transitions is presented in this section. The focus of these experiments is to evaluate how the UPS maintains stable voltage and current during shut-off or switch-on of components.

Experiment 6: Entering Islanding mode

Since the main functionality of the UPS is to provide reliable power, even in the case of power failures in the main grid, an important analysis is how the system handles a shut-off of the main power supply. The effect of a sudden power failure in the rectifier is presented in Figure 67, Figure 68 and Figure 69 respectively.

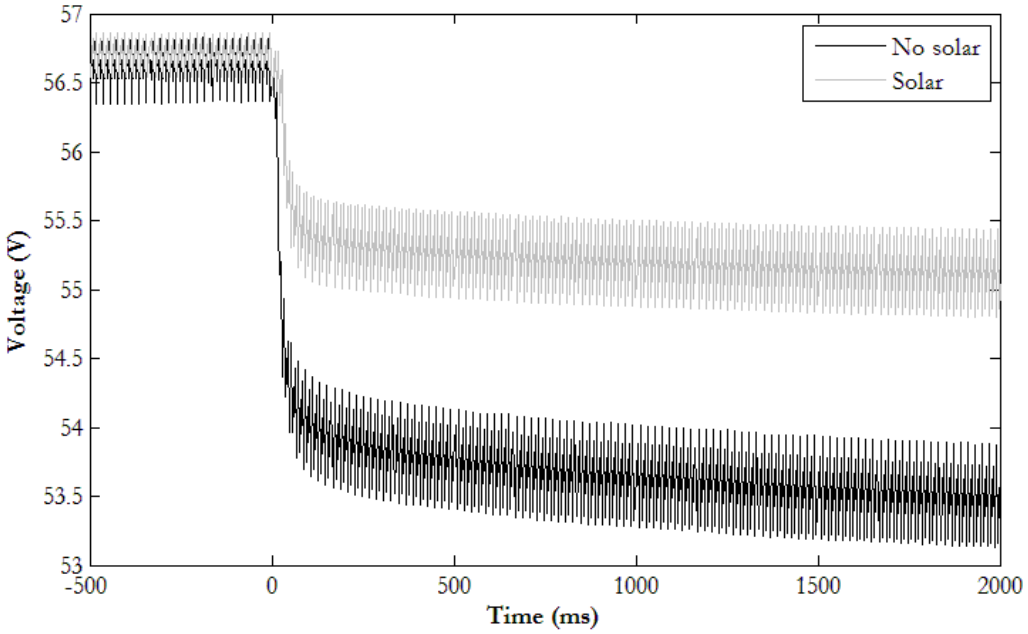

Figure 67: Experiment 6, DC voltage

The result clearly shows that the voltage drop following the disconnection of the rectifier is much larger in the case with no solar power. When the rectifier is disconnected the battery voltage becomes the new system voltage. The battery voltage depends both on SOC and battery discharge rate. It is likely that the SOC of the battery is higher in the case of connected solar, but that the added solar also affects the battery discharge current and thus has an impact on system voltage.

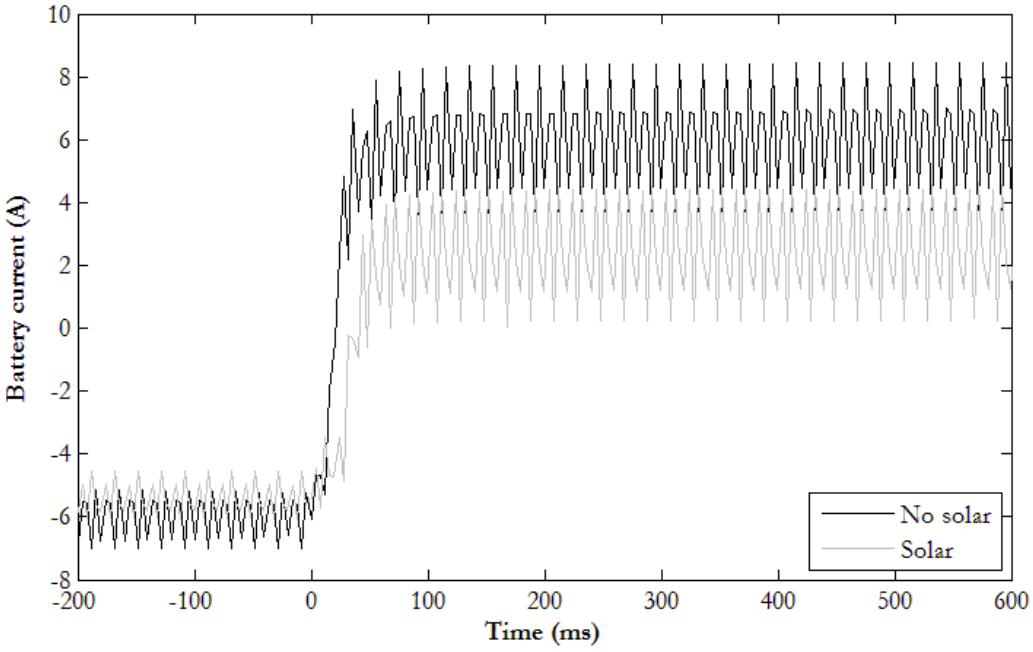

Figure 68: Experiment 6, battery current

As expected the current leaving the battery in order to power the load is higher without solar power, which has a positive impact on both total recoverable energy in the battery and battery lifetime. The ripples are significantly higher after disconnection of the load. This can be explained with the inverter – which is the primarily cause of the ripples – now drawing current from the battery and not the rectifier. With the rectifier connected to the system it supplies the current to the load, thus absorbing the ripples from the inverter.

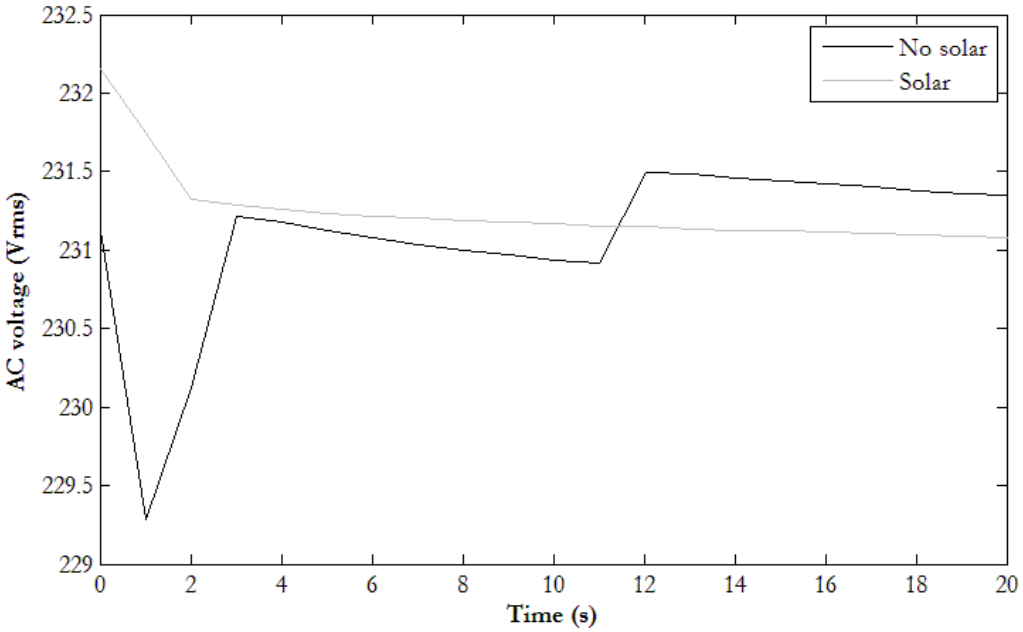

Figure 69: Experiment 6, AC voltage

Without the solar there is a significant voltage drop in the AC voltage following the disconnection of the rectifier. With the solar charge controller connected no such voltage dip occurs, even though the voltage is decreased to a level approximately 0,5V lower.

Experiment 7: Reconnecting to the power grid

When the power from the electricity grid is restored the rectifier can once again supply power to the load. The effect of the sudden flow of power from the rectifier on the DC voltage, battery current and AC voltage is presented in Figure 70, Figure 71 and Figure 72 respectively.

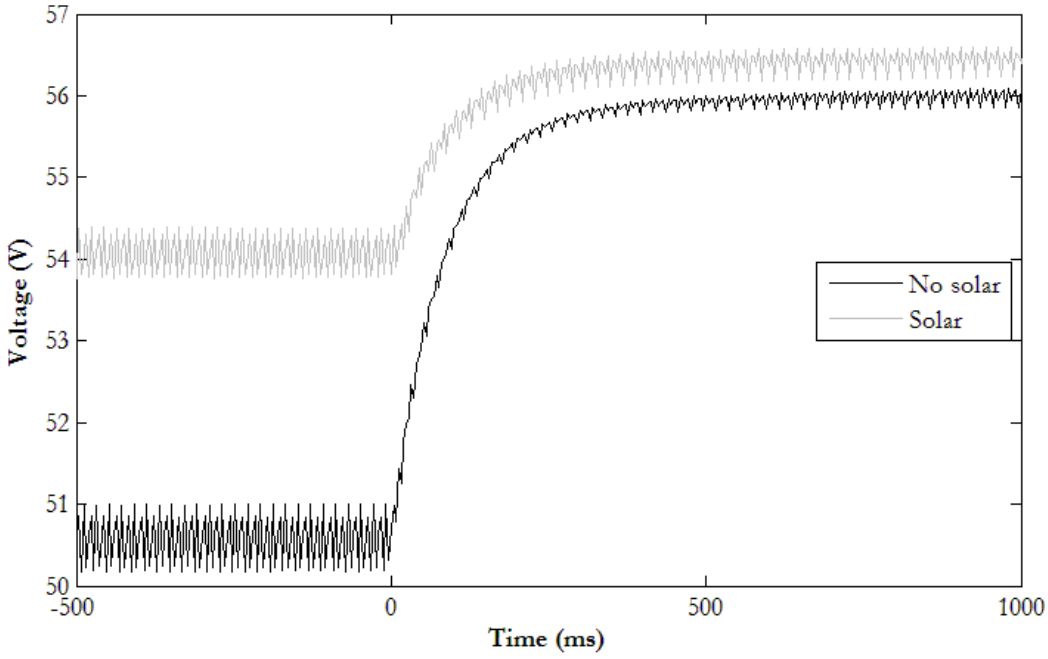

Figure 70: Experiment 7, DC voltage

The voltage on the DC-line at the start of the experiment, before the reconnection of the power from the rectifier, is significantly higher with solar power. This is because the solar charge controller supplies

part of the load, resulting in a lower battery discharge current which allows the battery to keep a higher internal voltage. The SOC of the battery also have an impact on the system voltage. After some time the rectifier is reconnected resulting in a higher system voltage since the rectifier now acts as the main power source, setting the system voltage.

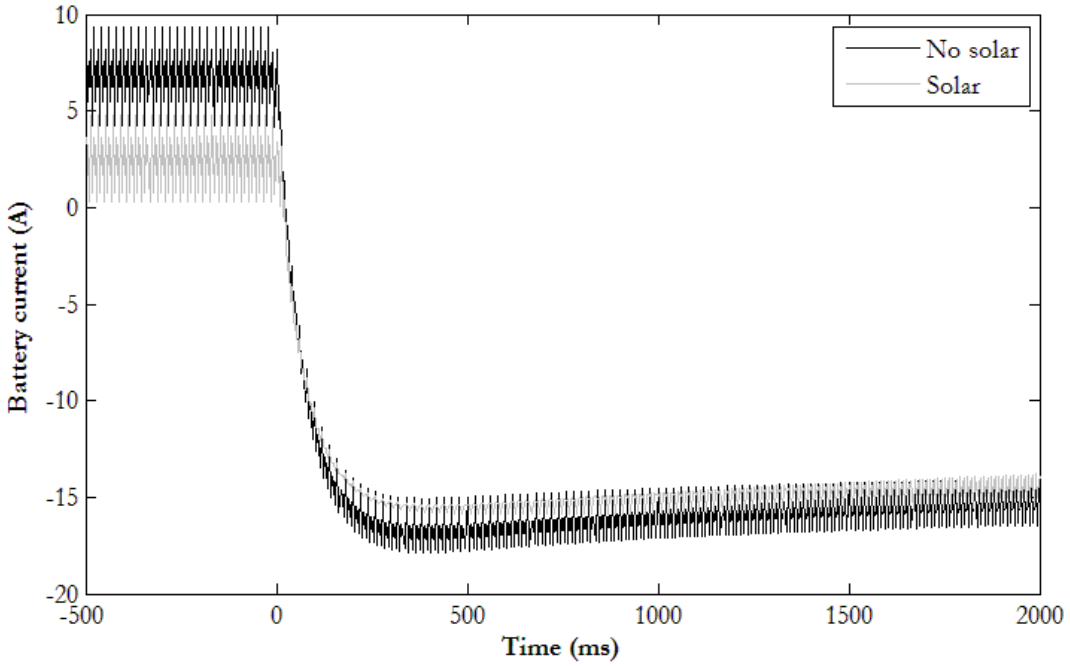

Figure 71: Experiment 7, battery current

When the main power supply is restored the battery is no longer needed to supply the load and the battery current is reverted from dis-charging to charging. With the added solar the discharging of the battery is slower prior to the restoration of the main power supply since the solar power can supply a portion of the load. The battery charging current after the reconnection of the rectifier is approximately equal regardless of the solar power, and is mainly depending on the battery SOC at the point of reconnection.

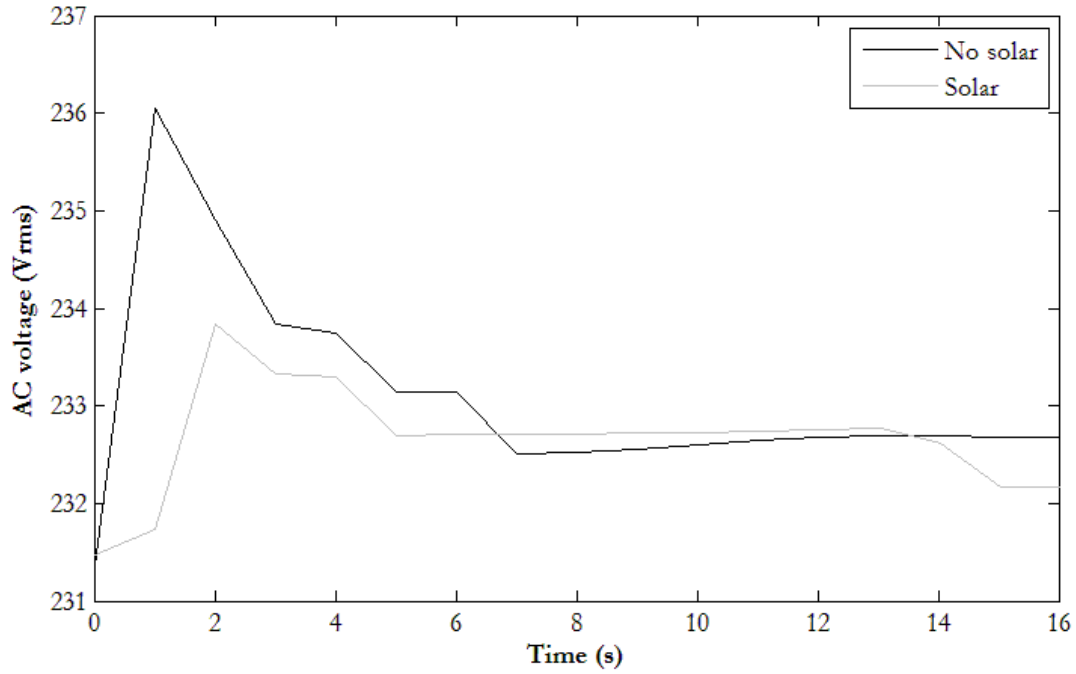

Figure 72: Experiment 7, AC voltage

For both cases the voltage level is stabilized at a higher level after mains is reconnected. This supports the observation that the voltage on the DC-line affects the AC voltage. Regardless of the addition of solar power there is a temporary voltage spike following the reconnection of the rectifier. However the voltage spike is higher without the solar power.

Experiment 8: Switching off the load

In this experiment the load is quickly lowered from nominal load to no load at the start of the experiment. The effect of this transitioning on the DC voltage, battery current and AC voltage is shown in Figure 73, Figure 74 and Figure 75 respectively.

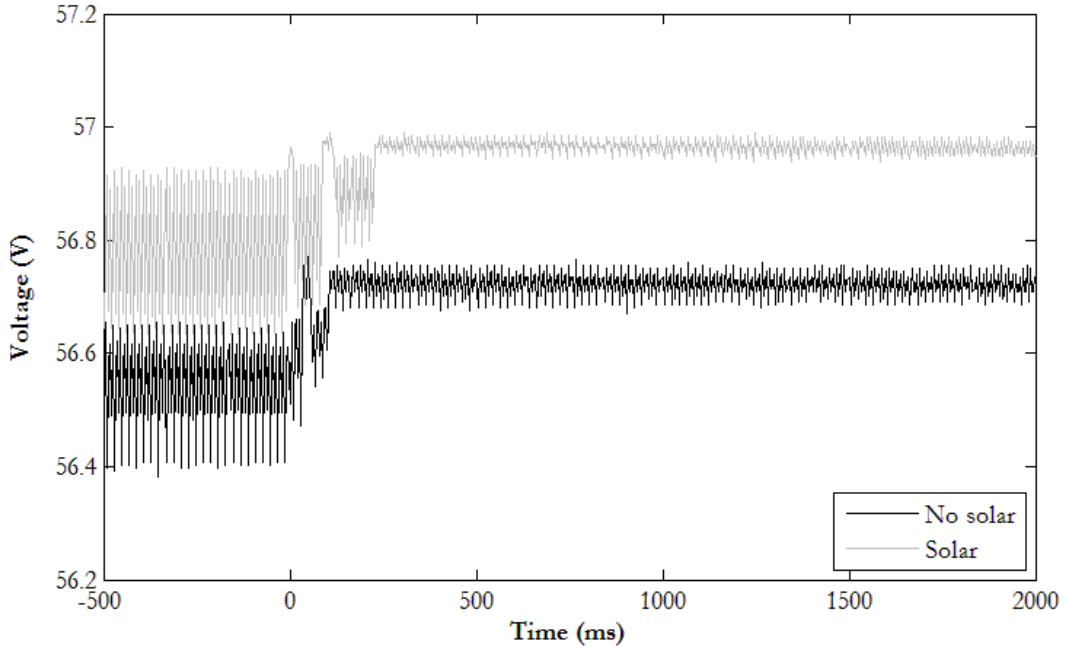

Figure 73: Experiment 8, DC voltage

Both with and without solar power the ripples in the voltage decrease significantly when the load is powered off. The higher load before the powering off is likely due to the rectifier being calibrated between the experiments with two configurations. What is more notable is that the increase in voltage at the switch-off of the load is higher without solar. The reason for this is likely that the rectifier has a voltage drop depending on the power it is delivering. With the solar panels connected the rectifier can split the power supplied and thus following the switch-off of the load the change in power supplied by the rectifier is lower than without solar power. Since stability on the DC-line is of major importance in UPS systems the addition of solar power has in this case a positive effect on the UPS-parameters.

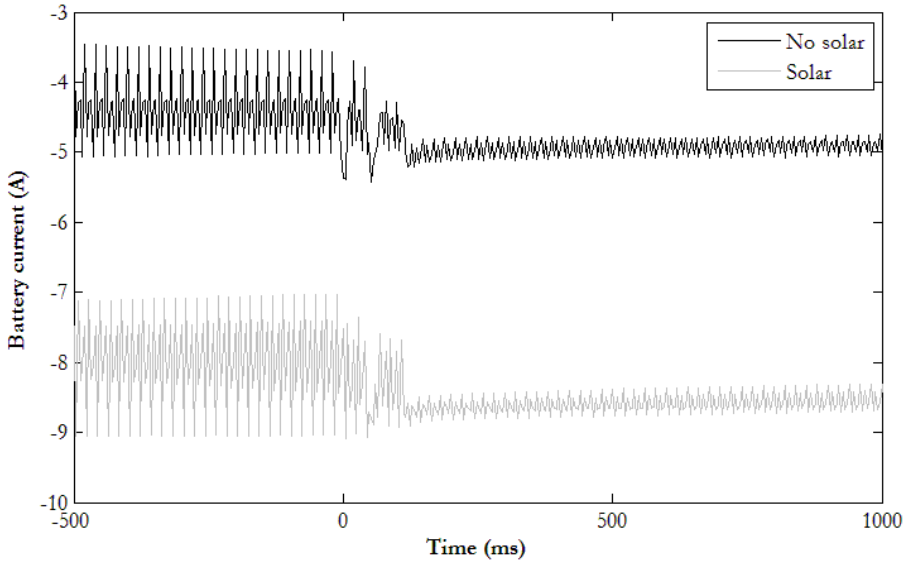

Figure 74: Experiment 8, battery current

The above graph clearly indicate that the inverter is the primarily cause of the oscillations in the current on the DC-line. When the load decreases the inverter decrease the current drawn, and the oscillations decrease significantly. The amount of current entering the battery is primarily dependent on the voltage difference between the internal voltage of the battery (i.e. the SOC) and the voltage on the DC-line. In the case with solar the battery SOC is lower or the rectifier voltage (which sets the voltage) higher, and this is the reason for the increased battery current.

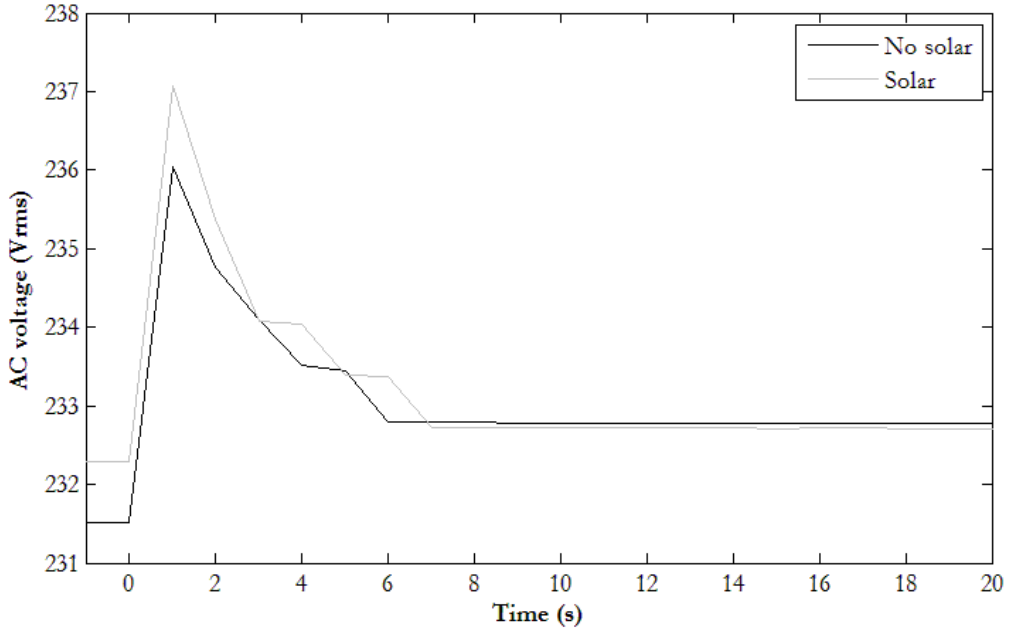

Figure 75: Experiment 8, AC voltage

It can be seen that the peak in AC voltage immediately after the load is shut off is higher with solar power, but that this is likely due to a higher AC voltage before the switch-off. The DC voltage before the switch-off is higher with solar power – mainly due to a higher SOC – and we believe that this can be the cause of the higher AC voltage.

Experiment 9: Switching on the load

The effect of a sudden increase in load on the DC system voltage, battery current and AC voltage is presented in Figure 76, Figure 77 and Figure 78 respectively.

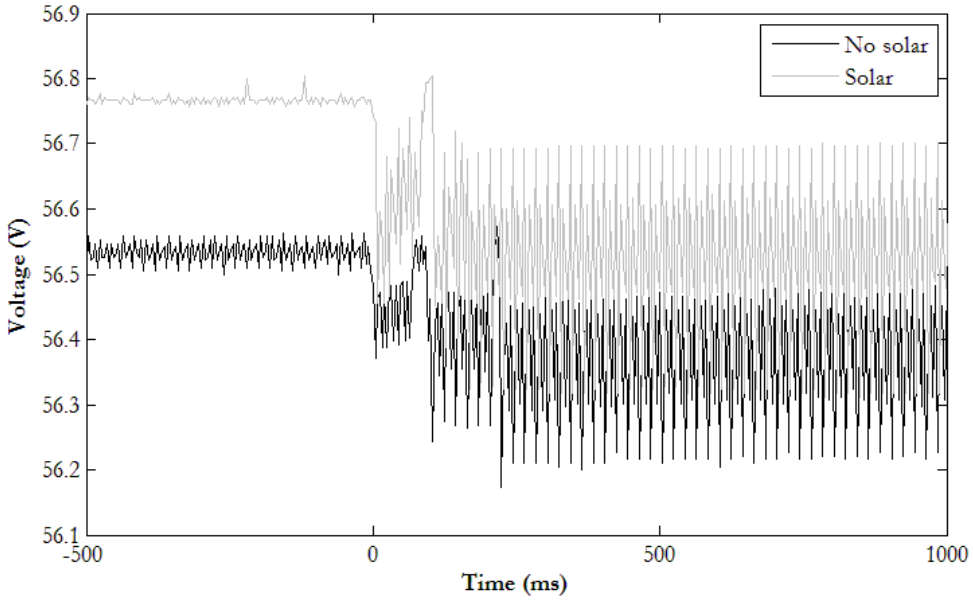

Figure 76: Experiment 9, DC voltage

The average value of the DC voltage is approximately 0,2V higher for the configuration with the solar power connected. This is likely due to a slightly higher output voltage from the rectifier. The voltage drop is slightly larger in the case of solar power, but this difference is small in comparison to the total

voltage of the DC-line. The ripples prior to switching on the load are smaller with solar but when the load is connected the ripples are similar.

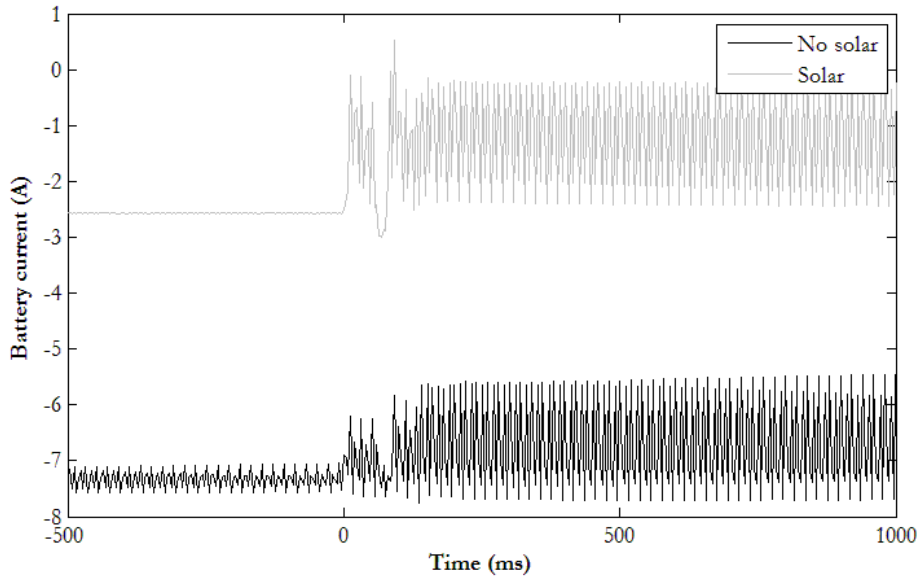

Figure 77: Experiment 9, battery current

As with the other experiments the difference in battery current is not judged to be dependent on the addition of solar power but on the SOC of the battery. Even though the DC voltage is higher with solar the battery current is lower, indicating a high SOC in the case with solar power. In steady state before the load is reconnected it can be seen that the ripples in the battery current are much lower with the addition of solar power. The solar current out from the solar charge controller is thus likely more stable than the current from the rectifier – which supplies all power to the battery in the case of no solar.

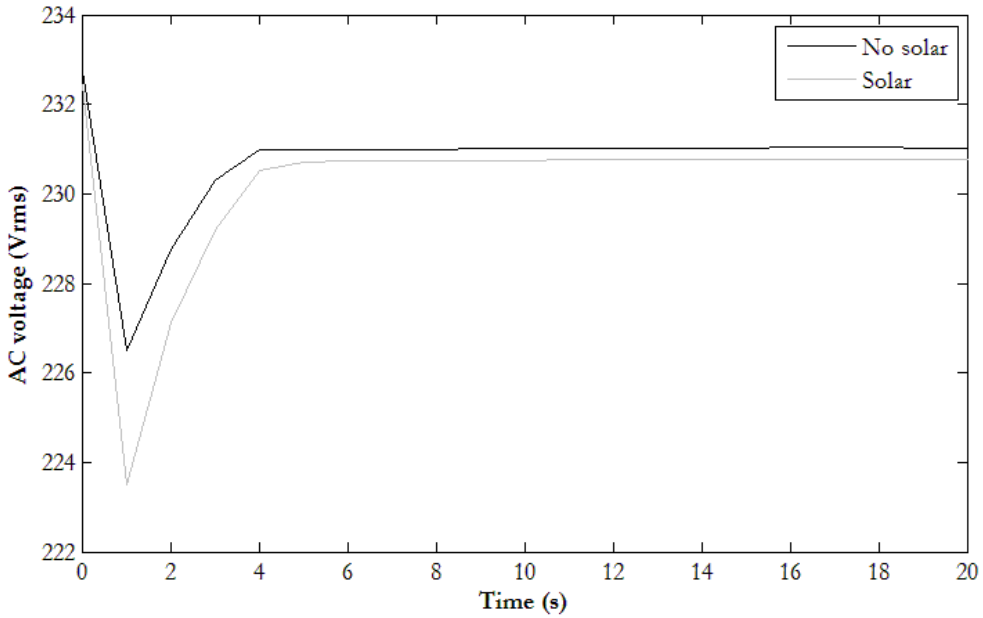

Figure 78: Experiment 9, AC voltage

In this graph the effect of the switch-on of the load on the inverter is shown. The voltage drop immediately following the increase in load is in both cases higher than what is acceptable in a real UPS system as a key role of the UPS is to provide stable power. The voltage drop is bigger with solar power

connected to the system. The reasons for this can be several, but the DC voltage also has a higher drop with solar panels connected and this can affect the voltage drop in the AC voltage. Another important factor for all AC-measurements is that data is collected at a rate of one sample per second. This slow rate of measurement means that fast changes might not be captured by measurements.

13.3 Other Experiments

Experiments not directly related to steady state or major transitions in operational modes are presented in this section.

Experiment 4: Starting the inverter

The current-profile of the inverter during start-up is presented as a graph in Figure 79 as measured at the current shunt, 65mV corresponds to 25A.

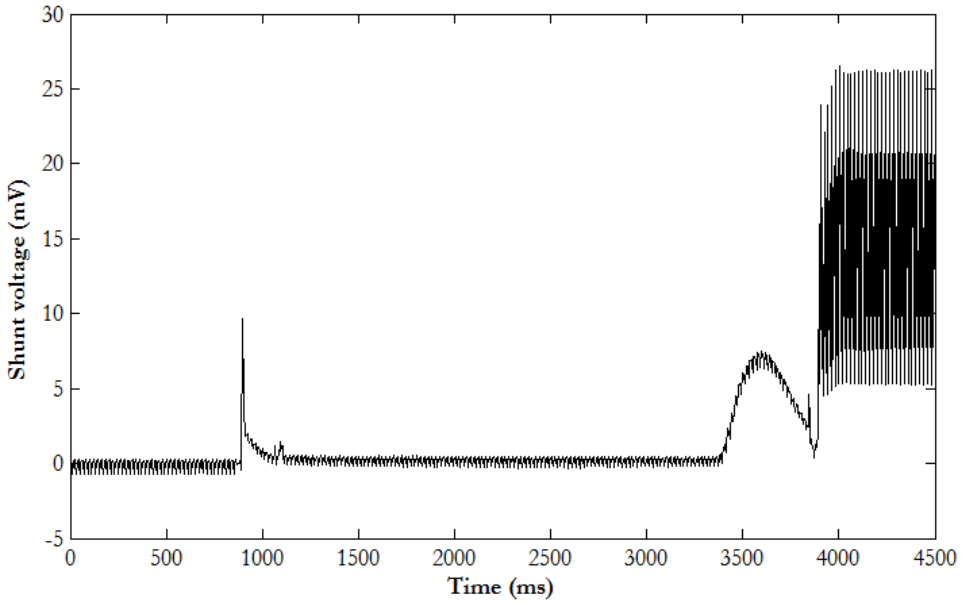

Figure 79: Experiment 4, DC current over the current shunt

The resulting graph shows that the starting time of the inverter is approximately 3000ms. The inverter starts by drawing a peak of current corresponding to approximately 3,8A at initialization of the start-up phase. No current is then drawn for 2500ms, until the inverter is almost fully started. As can be seen in the graphs the ripples in the current drawn is large after the inverter has entered normal conducting mode, even without the battery or the solar charge controller being connected to the system. The cause of these high ripples is thus likely the high-capacitance filter on the DC-side of the inverter.

Experiment 5: Stabilizing battery current after connecting the battery

The aim of this experiment is to analyze how the battery current stabilizes after connecting the battery. The graph of the battery current during the 12 minute long experiment is shown in Figure 80.

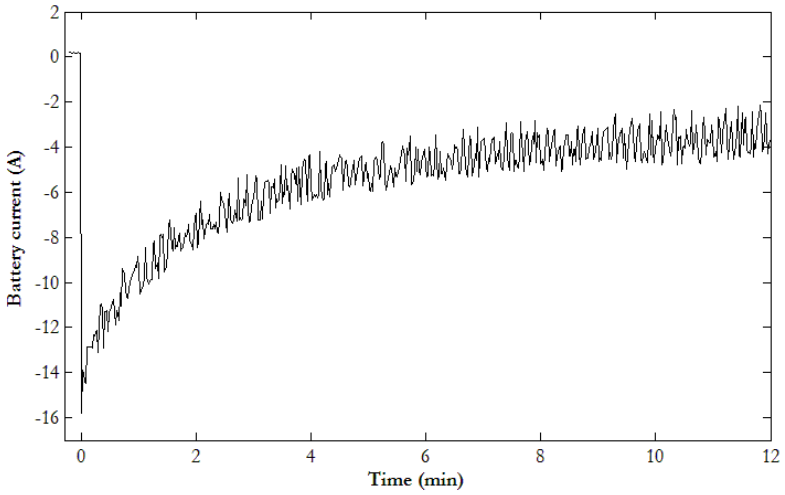

Figure 80: Experiment 5, battery current

The results shows that the battery current decreases logarithmically (negative values means current is entering the battery) over the duration of the experiment. Initially the current is above 1C, but after approximately 7 minutes the charging speed is below 0,5C – which is the recommended level for fast charge according to the manufacturer. As can be seen in the graph there are oscillations in the current, this is likely caused by the filter in the inverter and by ripples in the output of the rectifier.

The conclusion can be drawn that using a constant voltage instead of a constant current charge causes a high initial current entering the battery after connection, but that the battery used in this prototype system can handle such charging conditions. It is possible that such a charging algorithm decreases the total available energy in the battery however, and for a full-scale system a separate DC–DC converter could be used in order to allow a constant current charging.

Experiment 10: Total harmonic distortion in steady state

The results of the THD-measurements for several different component configurations are presented in Table 9. The values from the THD-measurements were not constant for all measurements, but since the variations were in the order of 0.3% an average value is presented in the table.

Table 9: Result from THD measurement

Condition	Without Solar	With Solar
Battery; Load 130W	2.7%	2.8%
Battery; Load 300W	1.15%	1.15%
AC–DC; Load 130W	2.6%	2.7%
AC–DC; Load 300W	1.2%	1.2%
AC–DC + Battery; Load 130W	2.6%	2.7%
AC–DC + Battery; Load 300W	1.2%	1.2%
Battery; More sun than load (130W)	-	2.6%

The results indicate that the addition of solar power into the system has a marginal effect on THD in the outgoing current. The minor changes seen in the table is more likely to result from measurement errors, as an average value was chosen if the THD-measurements were oscillating. What is more clearly indicated in the table is that the power used by the load has a significant impact on THD. With lower load the THD increases – the reason for this could be that the inverter is designed for a typical load of 1000W and not loads as low as 130W.

13.4 Analysis

Based on the experiments conducted with the prototype system some general results indicated by several individual experiments have been observed. The focus of this analysis is the comparison between the system with and without the addition of the solar charge controller and solar panels and its impact on the measurement results. The main differences between the small-scale prototype system and full-scale UPS system are also discussed in this section.

For most of the experiments the impact of solar power is low on the overall system performance, instead other parameters seem to have a major impact. The THD measurement for example shows that the effect of solar power on the THD of AC power from the inverter is negligible, but that the power drawn by the load has a significant impact. The THD doubled when the load was decreased from nominal 300 W to 130 W.

The main problem with the system seems to be unacceptably high ripples in the current entering the inverter. The ripple factor during steady state with all components connected and nominal load was 0.477 without solar and 0.545 with solar connected. The high-capacitance of the input filter in the inverter seems to be the main cause for these high ripples. The rectifier also affects the level of ripples in the current which is indicated by the higher ripples in steady state with all components connected than in steady state islanding mode. The impact of solar is negligible for higher loads. With no load the ripples decrease with solar power, indicating that it is not the solar charge controller that introduces ripples – instead the solar charge controller decreases ripples by allowing the rectifier to supply less power.

One of the most significant and important results is the effect of changes in the DC voltage on the AC voltage used to power the load. When the DC voltage decreased or the load increased the AC voltage experienced a dip lasting several seconds. In the case of an increase in DC voltage or a decrease or switch off of the load there is a spike in the AC voltage. The magnitude of the voltage dip or spike seems to be directly proportionate to the change in DC voltage. Even during steady state the absolute level of voltage in the DC-system directly affects the outgoing AC voltage. Our conclusion from this is that the conversion stability of the inverter is not sufficient for UPS applications.

When comparing the two cases – with and without added solar power – the results indicate that the system better handles cases of loss of a power source with added solar power. The voltage changes in the DC-system are smaller with an extra power source to supply the power – corresponding to smaller voltage spikes/dips in the AC voltage. In the case of changes in the load the result indicates that the system performance is slightly better without the added solar power. This can be due to a higher inertia in the system with an additional power source. The result is however less clear in this case. The factor with the highest impact on system performance in the case of changes in power sources or load is however not the addition of solar power but the SOC of the battery. The battery is the main determinant of the changes in the DC-system and thus has the main impact on the AC voltage.

The oscillations in current are unacceptably high for a UPS system, but the oscillations do not seem to be affected by the added solar power. The high capacitance filter in the inverter is likely the main cause of the ripples, with a part of the ripples introduced by the conversion in the rectifier. With low or no load and islanding mode the current is most stable, indicating that solar charge controller is more stable than rectifier.

As can be seen by the oscilloscope the solar charge controller introduces high-frequency ripples to the DC-system. The amplitude of these oscillations are high and might have a negative impact on the system even though the impact of this estimated to be low as the frequency is very high. The cause of these ripples is likely the clock-frequency of the DC–DC conversion in the solar charge controller. In order to minimize the effect of these ripples a common low-pass filter could be used as the frequency of the ripples from the solar charge controller are much higher than other oscillations.

From the result of the experiments with the prototype system we conclude that most parameters are not affected by the addition of solar power – this is clearly indicated by the THD measurement. With better components the impact on AC voltage would decrease or even completely disappear.

14 Result: Economic Analysis

In this section the results from the economic analysis is presented. The component costs and energy generation is compared between the two systems – the combined system with using solar charge controller and the separate systems where the solar power system is using inverters – and the results discussed. In order to evaluate the impact of the parameters used as input in the excel model a sensitivity analysis is conducted and the results from this is discussed individually. The section concludes with an overarching analysis taking both the results of the base case and sensitivity analysis into account.

Two cases have been used throughout the entire analysis using two different prices for solar inverters due to the big spread in inverter prices, as explained in the method section. Case 1 corresponds to solar wholesaler data of inverter costs and inverter efficiencies, with case 2 corresponding to the Danfoss prices and efficiencies.

14.1 Component cost

The initial investment cost is the dominating cost related to solar energy, and since a combined solar power- and UPS system would use different power electronic components than a stand-alone solar power system a comparison of these components has been made. The result of the comparison using a system with 82kW nominal solar power is presented in Table 10.

Table 10: Result component cost for the two base cases

Result	Case 1 Wholesaler	Case 2 Danfoss
Cost of solar chargers [$]	14 158	14 158
Cost of inverters [$]	33 649	25 168
Difference [$]	19 491	11 010
Difference [%]	57.9	43.7

The result clearly shows that regardless which provider of inverters is used the investment costs for solar chargers are significantly lower than for solar inverters. In case 1 the solar charge controllers are more than 50% cheaper than the inverters even though solar charge controllers generally have higher peak conversion efficiency.

14.2 Energy generation

The energy generated by solar power systems is mainly depending on the solar irradiance at the specific location of the installation. This is unaffected by the choice of system in this study. However, the conversion efficiency of the components also affects the generated energy. The conversion efficiencies of the components depend on the efficiency curve of the component and the actual level of power flowing through them at every instant. In the case of the combined system the energy supplied by the solar panels does not have to pass the rectifier – with its assorted conversion losses – and thus is affected by the choice of either combined or separate systems. The energy generated in the combined system has been scaled up to include this saved conversion in the comparison between the generated energy in the two systems. The result for this comparison is presented in Table 11 for both cases of inverter supplier.

Table 11: Result energy generation for the two base cases

Result	Case 1 Wholesaler	Case 2 Danfoss
Produced energy, separate system [kWh]	77 520	77 599
Saved energy, combined system [kWh]	84 361	84 361
Difference [kWh]	6 842	6 762
Monetary value first year, separate system [$]	9 695	9 705
Monetary value first year, combined system [$]	10 551	10 551
Difference [$]	856	846
Peak PV production [kW]	68.6	68.6
Combined average system efficiency	93.486%	93.486%
Separate systems UPS & solar average efficiency	93.354%	93.362%
Inverter average efficiency	97.295%	97.395%
Solar charger average efficiency	97.260%	97.260%

The first result from the economic model is that the produced energy in both inverter cases is higher for the combined system than the separate systems. The difference is approximately 8%, regardless which case is used.

The difference in produced energy is a consequence of different total system efficiencies – corresponding to variations in conversion efficiency in the components used. As can be seen in the table the average efficiency of the inverter was higher than for the solar charge controller, even though the peak efficiency for the inverter being lower. This is another important result. This is due to the shape of the efficiency curves of the components, with inverters having higher conversion efficiency for the typical amount of power generated by the solar panels. The higher total system efficiency of the combined system is explained by the lower losses in the rectifier used in the UPS system. For the stand-alone system all power used by the load has to pass the rectifier whereas only the part not supplied by the solar panels pass the rectifier in the combined system.

To translate the energy saved to a monetary value over the lifetime of the solar power system requires forecasting of electricity prices which is outside of the scope of this study. However, as an indication of the monetary value, the value for one year and a simple payback calculation using a fixed Swedish electricity prices was calculated. The result shows that for an 82 kW system the combined system generates and saves energy to a value of approximately $850 more than a stand-alone solar power system every year.

The result of the payback calculation for both the separate combined solar power system is presented in Table 12.

Table 12: Result payback calculation

Post	Separate System	Combined System	Difference	Difference %
Yearly Cash Flows				
Yearly Generation [MWh]	77.52	84.36	6.84	8.83%
Revenue, Energy Price [$]	9 695	10 550	856	8.83%
Electricity Certificates [$]	2 240	2 437	198	8.83%
Yearly Cash Flow [$]	**11 934**	**12 987**	**1 053**	**8.83%**
Investment Costs				
Modules [$/W]	1.27	1.27	-	-
BOS/Installation [$/W]	1.14	1.14	-	-
Power Electronics [$/W]	0.34	0.14	−0.2	−57.92%
Investment Cost [$/W]	**2.75**	**2.55**	**−0.2**	**−7.21%**
System Size [kW]	82	82	-	-
Total Investment [$]	**225 391**	**209 146**	**−16 244**	**−7.21%**
Payback				
Total Investment [$]	225 391	209 146	−16 244	−7.21%
Yearly Cash Flow [$]	11 934	12 987	1 053	8.83%
Payback [years]	**18.9**	**16.1**	**−2.8**	**−14.73%**

As can be seen in the table, the yearly cash flows of the combined system are 9% higher for the combined system, corresponding to approximately $1,050 with the added revenue from the electricity certificates. The payback time for the combined system is calculated to 16.1 years and the stand-alone solar system has a payback time of 18.9 years. For both cases the payback time is high compared to industry estimates, which can be explained by the high costs taken from U.S Department of Energy (2010). The difference between the alternatives are however of more interest to this study. The combined system has a payback time of 2.8 years or 15% lower than a standard stand-alone system. This indicates that the profitability of the combined system is higher, and that the combined system thus can be seen as a more attractive investment alternative.

The summarized results from the base case of the economic analysis clearly indicate that the combined system has economic advantages over a stand-alone system due to both lower investment cost and higher energy yield. The yearly energy generation is 8% higher for the combined system corresponding to a monetary value of $850. The payback calculation indicates that the payback times for both alternatives are quite high but significantly lower for the combined system. Thus, the profitability of an investment in a combined system is higher than for a stand-alone solar power system.

14.3 Sensitivity analysis

In order to evaluate the impact of individual parameters on the result a sensitivity analysis is conducted where the most important parameters are altered. The parameter is adjusted stepwise and the final result calculated again. The sensitivity analysis is conducted for both cases and presented as graphs. If the parameter adjusted is unaffected by inverter prices and efficiencies only the result of case 1 – prices from wholesalers - is presented. Most of the parameters adjusted only affect either the generated energy or the component cost – and thus only the affected results are shown.

The parameters adjusted in the sensitivity analysis are the geographical location, the price for inverters and solar charge controllers, the efficiency of the inverter, solar charge controller and rectifier and the number of solar panels.

Different geographical location

Since the solar irradiance is heavily dependent on the specific geographical location where the system is constructed an important sensitivity analysis is to change the location. This is done by changing the weather data to Gothenburg instead of Stockholm. Since the change of data does not affect component costs only the result for energy generation is presented.

The results with the new location are presented in Table 13 including the difference compared to the base case.

Table 13: Sensitivity analysis – different locations

Result	Case 1 Whole-salers	Change from base Case 1	Case 2 Danfoss	Change from base Case 2
Produced energy, separate system [kWh]	83 893	8.22%	83 807	8.11%
Saved energy, combined system [kWh]	91 200	8.11%	91 200	8.11%
Difference [kWh]	7 307	8.06%	7 393	8.06%
Monetary value first year, separate system [$]	10 492	8.22%	10 481	8.11%
Monetary value first year, combined system [$]	11 406	8.11%	11 406	8.11%
Difference [$]	914	8.06%	925	8.06%
Peak PV production [kW]	69.6	1.47%	69.6	1.47%
Combined average system efficiency	93.53%	0.04%	93.53%	0.04%
Separate systems UPS & solar average efficiency	93.39%	0.03%	93.38%	0.03%
Inverter average efficiency	97.43%	0.04%	97.33%	0.04%
DC–DC average efficiency	97.36%	0.11%	97.36%	0.11%

As can be seen the geographical location of the system – or more specifically the solar irradiance at that location – has a major impact on the total energy generated by the solar panels. Moving from Stockholm to Gothenburg which has a slightly higher yearly irradiance level increases the generated electricity by approximately 8%. The impact on system efficiency is however much more limited, resulting in that the relative difference between the alternatives are largely unchanged.

Cost of solar inverter

The prices for inverters are adjusted to span from 0.18 $/W (the lowest forecast found) to 0.4 $/W (the highest price found on the whole-sellers pricelists). The resulting total cost of inverter and the

difference in total investment cost between the combined and stand-alone system is presented in Figure 81.

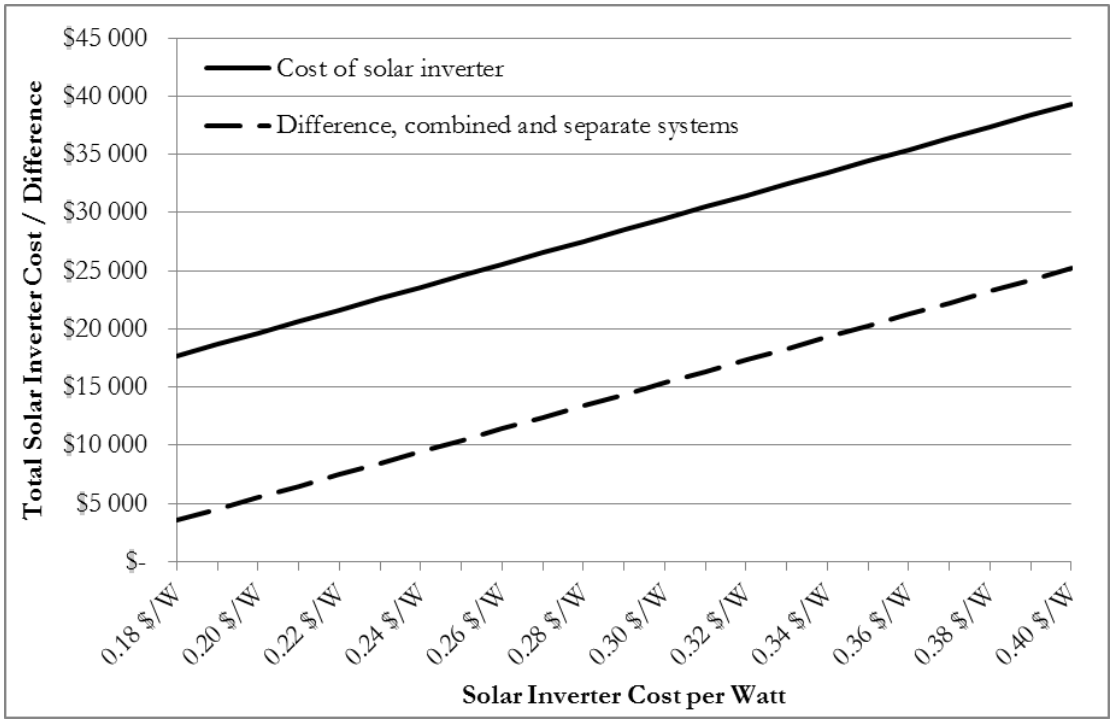

Figure 81: Sensitivity analysis, cost of solar inverter

The figure shows that the prices of inverters affect the difference between the two alternatives. But not even with the inverter cost of 0.18 $/W, which is close to half of the prices in case 1 and significantly lower than in case 2, is the inverter the cheaper alternative.

Cost of solar charge controller

The cost of solar charge controllers is varied between 0.12 $/W and 0.3 $/W. The resulting total cost for solar charge controllers and difference in cost for the two systems is presented in Figure 82 for case 1 and Figure 83 for case 2.

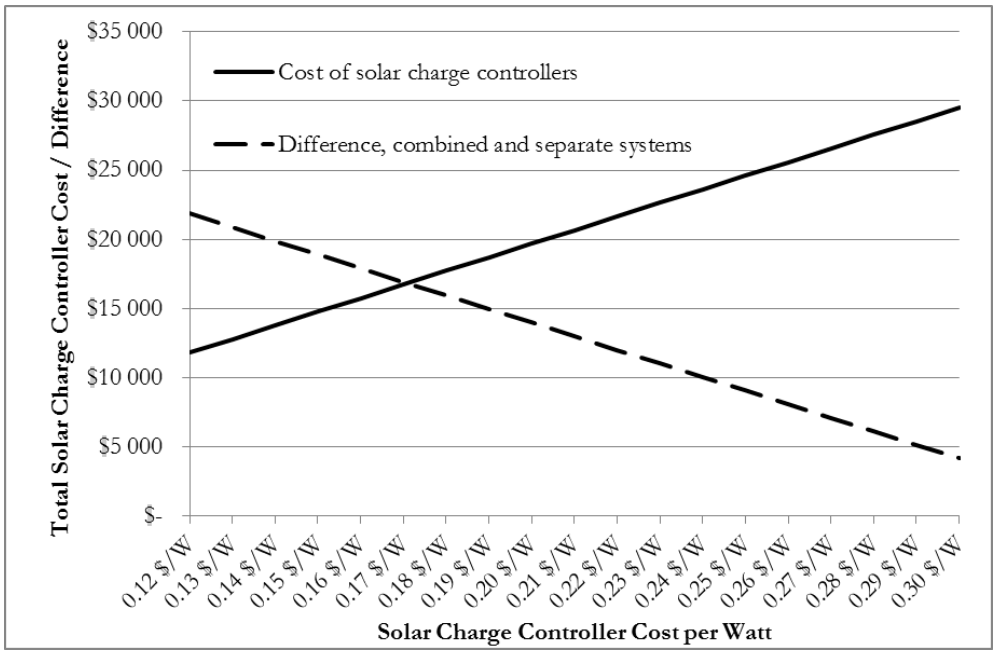

Figure 82: Sensitivity analysis, cost of solar charge controller – Case 1

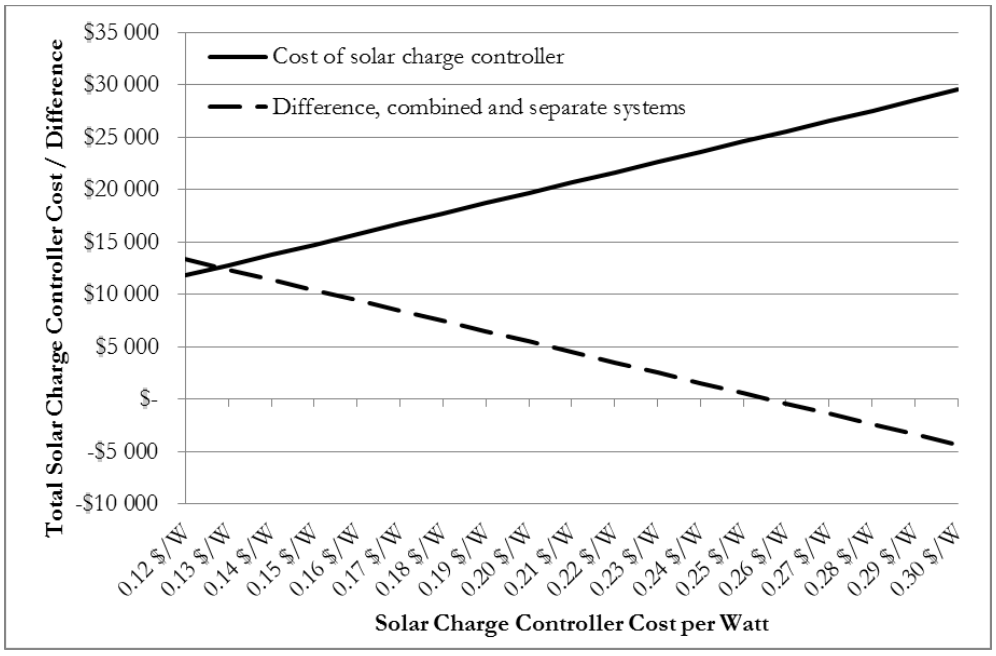

Figure 83: Sensitivity analysis, cost of solar charge controller – Case 2

In both cases the total cost for solar charge controllers is lower than for solar inverters for the majority of prices. The point of intersection between the curves corresponds to solar inverters having a total cost double that for solar charge controllers. For case 1 this intersection point is to the right of the base case.

For case 1 the total cost of solar charge controllers are the cheaper alternative even with a doubling of the prices compared to the base case. For case 2 the inverters become the cheaper alternative at a cost of solar charge controllers approximately double that for the base case. The results clearly indicate that the prices of solar charge controllers need to increase drastically – to levels which are considered unlikely – in order to make the stand-alone system cheaper.

Solar inverter peak efficiency

The peak efficiency of commercially available solar inverters varies within the range of a few percent. In order to evaluate how the choice of peak efficiency affects the total generated energy in the stand-alone system the inverter efficiency is varied between 96.5% and 98.5% with the results presented in Figure 84 together with the difference between the combined and separate systems.

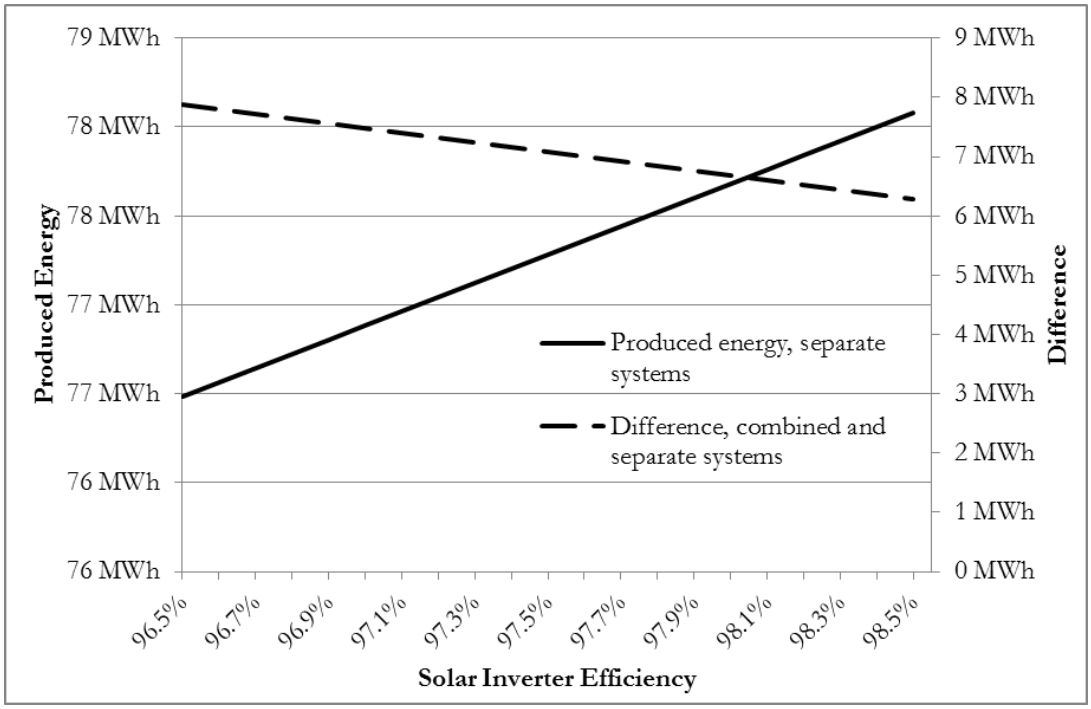

Figure 84: Sensitivity analysis, solar inverter efficiency

The results show that the impact of peak efficiency does affect the total generated energy, but that since the range of inverter peak efficiency is only a few percent the differences are small. The solid line (left axis) shows that the difference between a low-performance solar inverter with a peak efficiency of 96.5% and a top-of-the-line inverter with an efficiency of 98.5% is only 1500kWh – approximately 2%. The difference in generated energy between the combined and separate systems is shown on the right axis and indicates that the system efficiency of the combined system is higher for all types of solar inverters.

Solar charge controller efficiency

As with the case of solar inverters the peak efficiency of solar charge controllers are varied to cover the span of typical efficiencies for components commercially available. The peak efficiency is varied between 97% and 99%. The resulting total energy saved with the combined system and differences between combined and separate systems are presented in Figure 85.

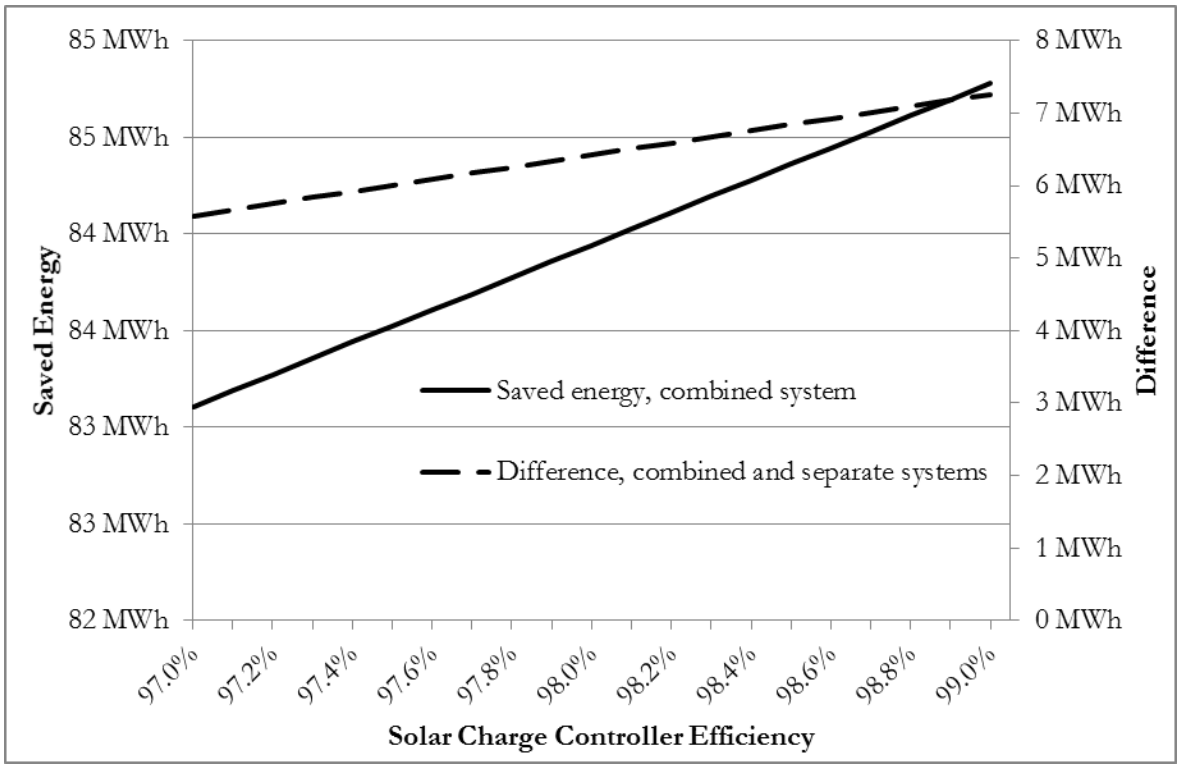

Figure 85: Sensitivity analysis, solar charge controller efficiency

The resulting total energy saved using the combined system is represented by the solid line (left axis) indicating a change of only approximately 2% over the span of conversion efficiencies. The difference in total energy generated by the two systems is shown by the dashed line (right axis) and is favoring the combined system for the full range of efficiencies.

Rectifier efficiency

The third component affecting the total system efficiency is the rectifier in the UPS since the combined system can bypass this conversion with the energy from the solar panels. The range of efficiencies for rectifiers has a higher variation due to different conversion typologies available – but for UPS applications only high-performance components is chosen. The rectifier efficiency is varied between 88% and 96%, with 94% used in the base case. The resulting saved energy with the combined system is presented in Figure 86 together with the difference between the combined and separate systems.

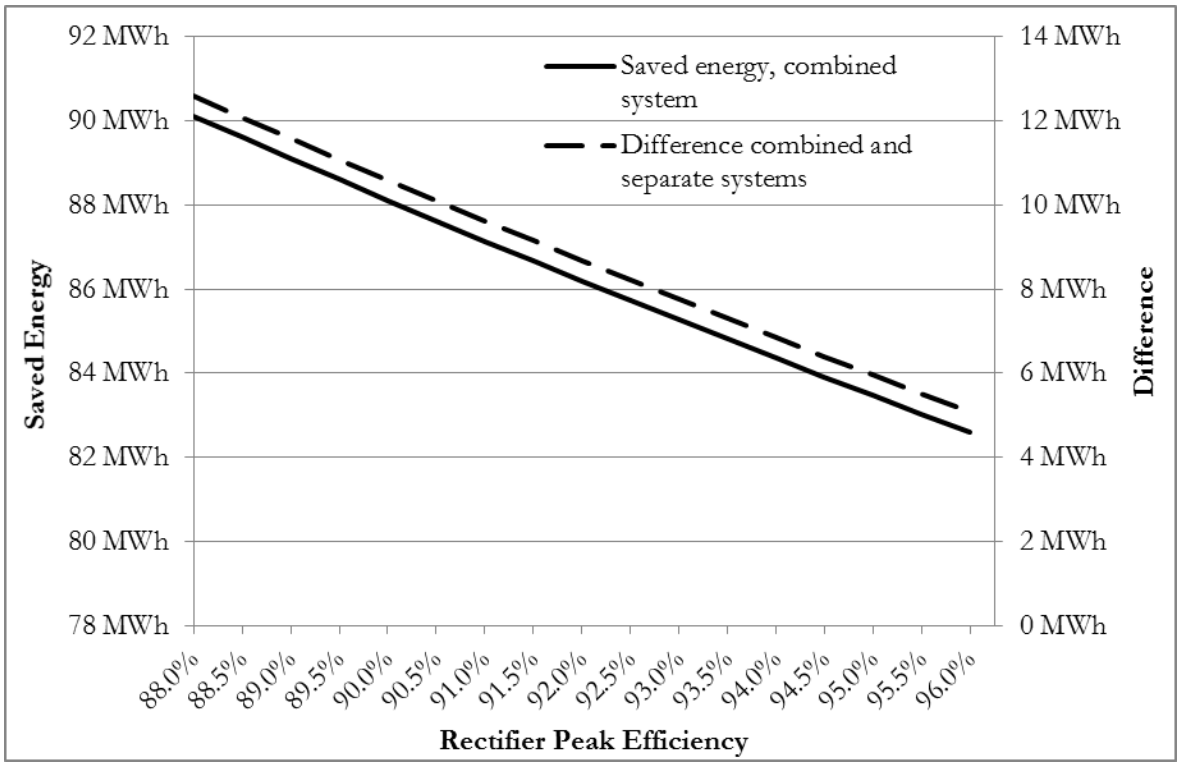

Figure 86: Sensitivity analysis, rectifier efficiency

As can be seen in the graph lower conversion efficiency favors the combined system over the separate as the increased losses in the rectifier partially can be avoided using the combined system. The total energy saved (left axis) varies with approximately 10% over the range of rectifier efficiencies. The difference between the systems (right axis) has the same changes in absolute numbers, but a higher percentage change. The result clearly indicates the importance of a high-performance rectifier in UPS applications.

Number of solar panels

The number of solar panels used with the fixed nominal load of 100 kW directly affects the cost and energy generation of the system. The more solar panels installed the bigger share of total power is supplied from the solar – and thus less power has to be converted in the rectifier for the combined system. Since UPS systems are not designed to enable reversed power flow (from the solar panels back into the grid in the case of more solar than load) having excess solar power capacity leads to energy being wasted. The number of solar panels in the base case is 600, and the range in the sensitivity analysis is 100 to 1400 panels. The resulting energy generation is presented for case 1 in Figure 87 and the resulting component cost presented in Figure 88.

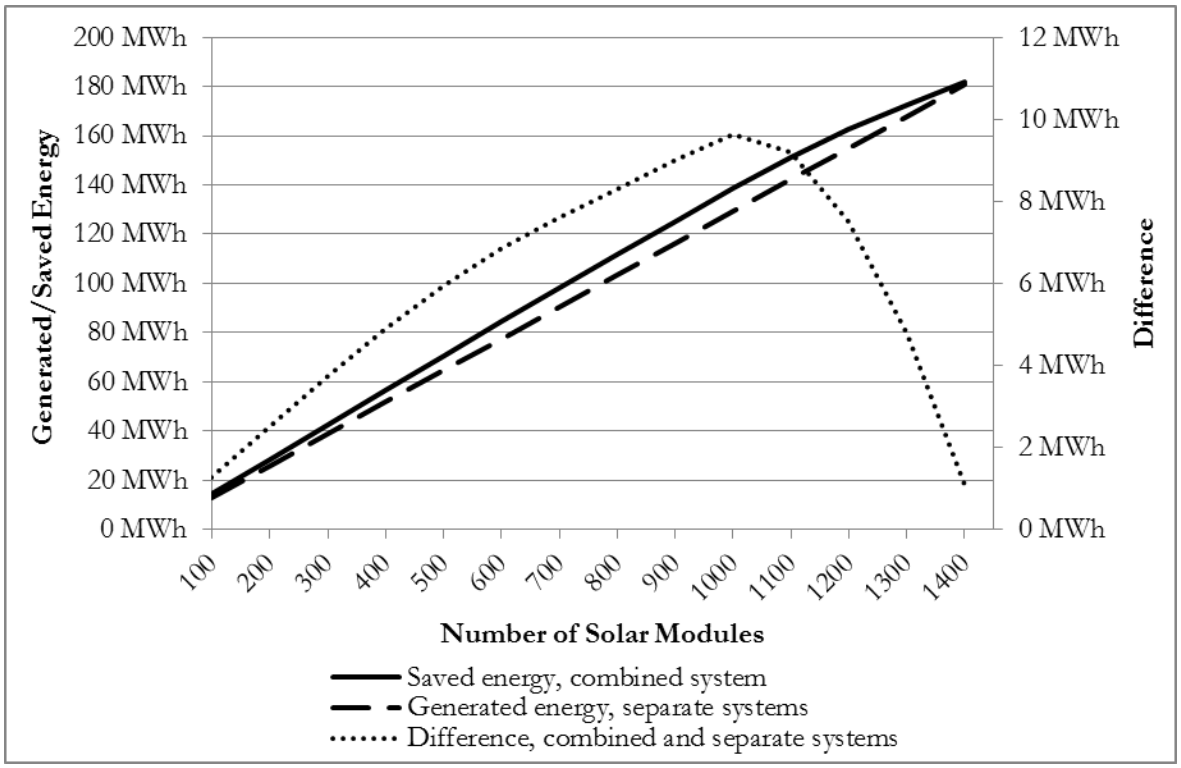

Figure 87: Sensitivity analysis, number of solar panels – energy generation

The lines for energy generated in the combined system and stand-alone system is shown on the left axis of the graph. The combined system has a higher energy generation for the entire range of solar panels. However, the difference between the two alternatives (the dotted line on the right axis) reaches a maximum value at around 1000 panels and adding additional solar panels results in a smaller difference. The reason for this is that when using more than 800 panels the total nominal power of the solar installation is higher than the nominal power consumption of the load, resulting in situations where energy is wasted in the combined system. The benefit of the combined system is decreased sharply as more panels are added and consequently a larger share of the total energy is wasted. The stand-alone system does not have this problem as all energy is sent into the power grid. The graphs are not linear as the efficiency curves of the components vary with solar irradiance. If more than 1400 panels would have been added the combined system would generate less total energy than the separate system.

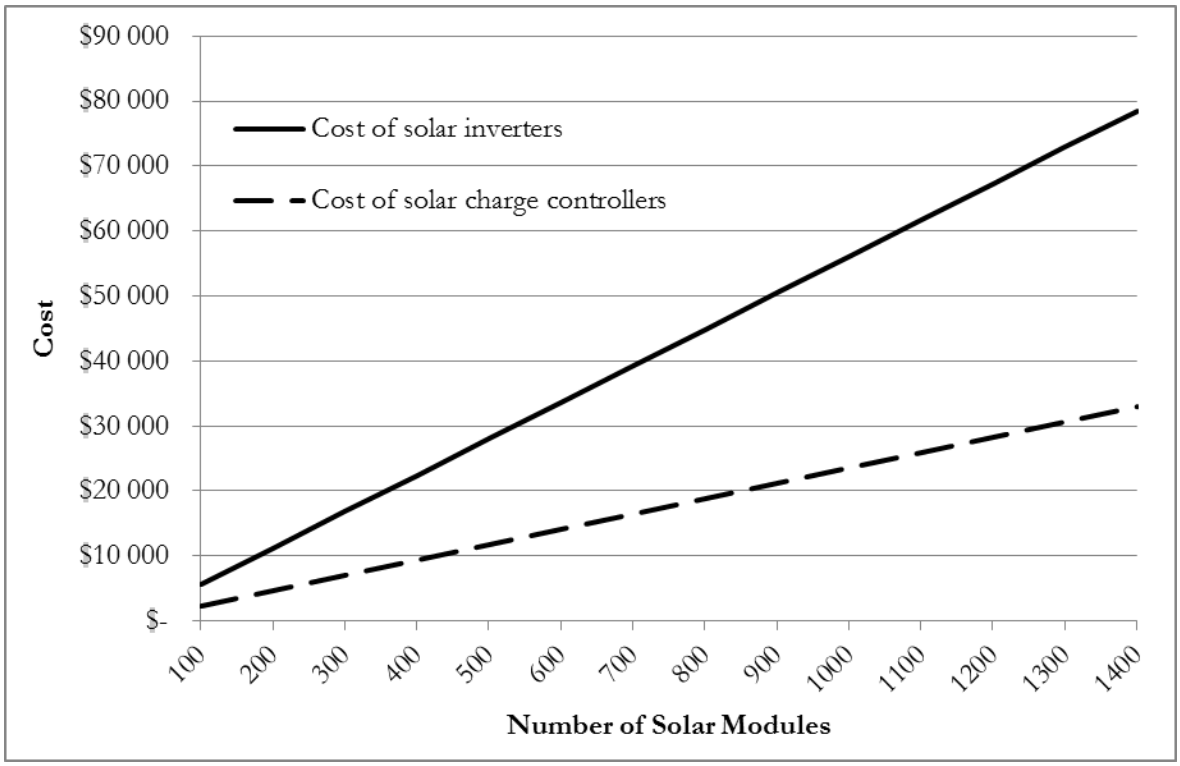

Figure 88: Sensitivity analysis, number of solar panels - component cost

As with the generated energy the total cost for inverters or solar charge controllers are directly depending on the number of solar panels installed. If the number of solar panels is doubled, so is the cost for inverters or solar charge controllers as the cost of the components are calculated per watt. Since the cost per watt for inverters is approximately double the cost for solar charge controllers in case 1 the total cost is always approximately double for the separate system.

14.4 Analysis

The economic analysis clearly shows that the combined system – using solar charge controllers instead of solar inverters – has a significantly lower component cost. The main cost associated with solar energy is the initial investment cost, and a lower investment cost directly impacts the overall profitability and attractiveness of solar energy.

Additionally the results indicate that the energy generation is higher in the combined system. The average efficiency is higher for inverters than solar charge controllers, but the conversion losses in the rectifier can partially be avoided in the combined system – resulting in a higher total system efficiency for the combined system. With bigger share of power supplied by the solar panels instead of coming from the power grid the benefits of the combined system increases up to the point where the nominal solar power is higher than the load.

The difference in cost per watt of installed power between inverters and solar charge controllers is large. For the wholesaler data in case 1 the price of inverters are double the price for solar charge controllers. In case 2 using Danfoss inverters the price was approximately 66% higher than for solar charge controllers. In the sensitivity analysis with varying prices for solar charge controllers the inverter becomes the cheaper alternative only in case 2. This only happens with prices for solar charge controllers doubled compared to the base case – and only for case 2. The sensitivity analysis changing prices on inverters down to 50% of base case indicated that the combined system is cheaper except in the most extreme changes of price. In order to evaluate the lifecycle costs of the alternatives a study of a

real installation would have to be made to see if there is other cost associated with solar charge controllers which could affect the outcome. The result of this model indicates that the price difference is very large. The difference in overall investment cost has been calculated as part of the payback method and amounts to approximately 7.2%. The payback time of the combined system is thus lower.

The sensitivity analysis also indicates that the impact of different conversion efficiencies is limited – the range in peak efficiency is only a few percent for commercially available inverters and solar charge controllers. The overall impact on generated energy using a cheaper component or a top-of-the-line component is small. The impact on total system efficiency and generated energy is higher for rectifiers – results indicate that low conversion efficiency favors combined system. Even though the range in conversion efficiency is wide for commercially available rectifiers, large-scale UPS applications utilize high-performance rectifiers. Conversion efficiency below 90% is thus not realistic for UPS applications and the impact of the rectifier efficiency is thus more limited.

The analysis also shows that the location of the installation is of key importance for the energy generated. The difference between Stockholm and Gothenburg is high, and thus the solar irradiance at the specific location of the installation has to be carefully measured to evaluate the potential energy generation.

As is shown clearly in the sensitivity analysis the number of solar panels used are directly affecting the cost and energy generation of the systems. As the nominal solar power is increased for a fixed load the difference between the combined and separate systems decreases due to excess energy being wasted in the combined system. There is thus a fixed number of solar panels corresponding to a maximum difference between the alternatives and a number of solar panels where the two alternatives has the same generation. Increasing the number of panels past that amount results in the separate system having a higher total energy yield.

The combined results of the economic analysis indicate that in general the combined system has a higher performance and is cheaper than stand-alone system. Thus economic synergies exist in the combination of solar power and UPS system.

Discussion and Conclusions

In this section the results of the combined studies are discussed. The impact of the delimitations and limitations of the studies are analyzed together with the implications of the results. The conclusions of the study are presented together with suggestions for future research.

15 Discussion

In this section the overall results of the combined studies are discussed and evaluated. The delimitations and limitations of the three studies are discussed together with a comparison of the results of this study with previous studies presented in the literature review.

15.1 Result combined studies

The aim of this thesis has been to evaluate if the combination of solar energy and UPS is technically feasible and have any economic synergies compared to a stand-alone solar power system and separate UPS system. The results from the prototype system indicate that the main cause of ripples is not the addition of solar power but from other components. The impact of solar power on critical parameters—especially the THD of output AC voltage—is largely unaffected by the addition of solar power. In the case of power outages the solar power can even be beneficial compared to a regular UPS system. The solar charge controller does however introduce some noise into the system, and the addition of new components make the overall architecture more complex, requiring some adjustments of the original UPS system. The economic analysis clearly shows that the investment cost of solar charge controllers is significantly lower than for solar inverters. During the work with this thesis the impact of the combined system of total system efficiency was also discovered to be an important synergy. By using a combined system less power has to be rectified by the UPS and thus the conversion losses decreases. This discovery accounts for the main part of the difference in generated energy between the combined and the stand-alone system. The payback calculation indicates that the payback time of the combined system is significantly lower. In summary the combined system has a high potential as an alternative to stand-alone solar energy for companies or investors that are also in need of reliable power.

The experiments with the prototype system indicate that connecting a solar charge controller to the DC-line of the UPS introduces some high-frequency ripples and thus can potentially affect the power quality. Additionally the components need to be compatible with each other in order for control systems and similar function to work properly. The high-frequency noise can be filtered out by adding extra filters and the control system can be adjusted to compensate for the added components but since some adjustment of the system is required the potential to retrofit existing UPS systems with solar power could prove difficult.

The two main causes for the high current ripples in the prototype system are concluded to be the high-capacitance filter in the inverter and the low-performing rectifier. High capacitance filters are a cheap type of filters used to smooth the voltage, but generally at the cost of instability in the current. The rectifier used has a very simple topography which is not suitable for UPS purposes. The high ripples and the resulting low power quality could have been mitigated by the use of higher quality components specifically designed for high power quality. A result from the study is thus that a UPS system is a complex system requiring high-performance components and careful design to work properly. In order to make the combined system fulfill the strict requirements of a UPS system the two components (UPS and solar energy) would need to be integrated and the system carefully tested before being used in a real application.

The combined system proposed and evaluated in this thesis is different from what has been treated in previous studies. In the literature no system has been encountered which combines UPS and solar energy for large-scale applications. Previous studies such as Jawaid et al. (2012) and Cavallaro et al. (2009) have explored the possibilities for solar energy to charge batteries to be used as a back-up energy storage. These studies have however been focused on using solar energy as an insurance against unstable power from the grids in locations where power outages are common. No study known to us

has had the aim to integrate solar energy and UPS in order to minimize the electricity bought from the grid when the normal power grid is functioning. The results of this study indicate that there are economical synergies when combining solar energy and UPS systems even in locations with a stable power grid.

15.2 Delimitations/limitations

The main limiting factor related to the experiments and the evaluation of the technical feasibility of the combined system is that this study has been conducted on a prototype system instead of a commercially available UPS system. The components used are designed to be working individually and not as a system, leading to the power quality being significantly lower compared to a UPS. If the study could be conducted on a functional UPS system the resulting power quality would likely have been significantly better for both the combined and separate systems. The relative difference between the UPS with and without the addition of solar energy is still the main focus, but without the high amount of noise introduced by other components in the prototype system the measurements would likely be better at showing small changes introduced by the solar.

The economic study has focused on the relative investment costs for a combined versus a stand-alone solar power system. The results indicate that the combined system has a lower total investment cost, and the basic payback calculation shows that the payback time is 14.7% (2.8 years) lower for the combined system. However the net present value (NPV) of the system has not been calculated. The results of the study are thus more valid as a solution to *how* to install solar power, not the question *if* solar power should be installed.

The study has been geographically limited to Sweden, using climate- and electricity data for Sweden. The implications of this geographical delimitation for the investment cost of the system or electricity data are judged to have a marginal impact on the results of the study. The impact of using solar irradiance data for Sweden on the total energy generation is however very high. On a global scale Sweden is not considered to be a country very suitable for solar energy. The yearly available energy, and thus the energy generation and profitability of solar energy could be significantly increased by using climate data for other geographical locations.

One critical aspect of this study is the design of the combined UPS and solar system. In this case, the design was chosen for a couple of reasons: because current UPS and most other DC systems are designed for constant DC voltages, and because of simplicity in finding the right components for the design in order to conduct physical experiments. However, if the combined system is designed from scratch, one interesting alternative is to use a non-constant DC voltage. This would allow the whole system to track the MPP; no DC–DC converter is thus needed for the solar panels. However this would require redesign of the battery part of the system, since a battery would not handle such varying voltages as most solar panels need to track the MPP.

In the case of NiMH batteries, a bidirectional DC–DC converter is probably preferable in any case to achieve constant current charging. If such a converter is used, it can be designed along with the rectifier and the inverter to work at a larger range of voltages. This leads to harder design and probably costlier components, but the solar DC–DC converter can be eliminated altogether which might prove to save more than the extra cost of the other components. The control system would also have to be reconsidered for a system where the voltage varies.

15.3 Implications

The attractiveness of a combined solar energy and UPS system is closely related to the overall attractiveness of solar energy. This is mainly influenced by the investment cost of solar energy compared to the yearly energy generation. Even though the results of this study indicates that a combined system is both cheaper and generates more energy than a stand-alone solar energy system the ultimate factor affecting the investment is if the solar energy system is cheaper than buying all electricity from the power grid. With prices for solar energy continuing to decrease the attractiveness of solar energy increases. In the future the investment calculations made by potential investors will be increasingly favorable and thus the interest for the proposed combined solar energy- and UPS system will likely increase accordingly.

A topic raised in the introduction and literature review is the growth of the concept of microgrids. A grid based on small networks of power able to operate independently if needed is indeed a realistic concept for the future. UPS systems can be seen as microgrids, since they have loads, connection to utility, energy storage and in some cases generation. A transition from viewing UPS systems as simple back-up power stations to viewing UPS systems as microgrids would certainly lead to more dynamic and smarter systems, where the generation might even be able to support the critical load for a much longer time than what is now possible. Actors with critical loads might even become part of microgrids incorporating other nearby facilities, while designing the system to ensure uninterruptible power. The possibilities for microgrids are large, and the concept is still under development.

For a company having a sensitive load in need of protection and looking into the potential of solar energy the result of the study implicates that the two systems could favorably be combined for a lower investment cost and increased energy production. The lower cost compared to a stand-alone solar energy system implicates that the combined system could lead to that an installation of solar energy which previously was unattractive becomes profitable. From a broader perspective, this would in turn lead to more installed solar power which would benefit the environment. For a manufacturer of UPS solution the implication of the study is that combining UPS and solar energy is technically feasible. A combined solution would require some integration of the systems, for example extra filters, but would likely result in a new product offering for the UPS manufacturer which does not exist today.

16 Conclusions & Future Research

16.1 Conclusions

The conclusions drawn regarding the technical feasibility of the combined system is that it is technically possible (with minor modifications) to combine solar energy and UPS systems on a common DC-line. The addition of solar energy does not have any significant impact on the power quality of the UPS system. In the case of power outages in the electricity grid solar power can benefit the system with both less impact on power quality at the point of disconnection from the grid and also increase the autonomy time of the UPS.

The economic synergies related to the combination of solar power and UPS systems are two-fold: the investment cost of the system and the total generated energy. Based on prices for commercially available inverters and solar charge controllers the conclusion is drawn that the investment cost of the combined system is significantly lower than for separate systems. Using wholesaler data the cost for inverters was higher throughout all sensitivity analysis with inverters from Danfoss only becoming the cheaper alternative when the prices for solar charge controllers were doubled.

In the solar generation model the combined system is concluded to have higher total system efficiency than a stand-alone solar power system. This is due to the decreased need of power to pass the rectifier resulting in decreased conversion losses in the combined system and thus a higher total energy yield.

16.2 Future Research

An interesting aspect when combining solar panels and UPS is the possibility to utilize the energy storage capacity in the batteries of the UPS to store excess energy from the solar panels. Dedicating a predetermined amount of battery capacity to be used by the solar panels would enable a higher nominal solar power installation, and thus a higher percentage of total load demand to be supplied by the solar energy system. The control system for such a solution would however need to be able handle more complex charging algorithms in order to optimize the system. The construction of such a system and an analysis of its impact on energy generation and profitability are left for future research.

This study has focused on the relative benefits of a combined system compared to having UPS and solar energy separate. In order to fully evaluate the proposed system a full study of the net present value of the system could be conducted, instead of the basic payback calculation conducted in this study. The NPV of any solar power system depends on the future electricity prices and the addition or removal of governmental subsidies and taxes along with the specific costs associated for every specific installation. The complexity of such a study makes it unable to fit into the scope of this thesis. A full LCC-calculation of all costs associated with the combined solar energy and UPS system in order to calculate the NPV of the system is thus left for future research.

The results from the prototype system indicate that the combined system is technically feasible. The prototype system has however been constructed from principle components with the aim to build a combined system. Since there are many UPS systems in operation an interesting aspect would be if solar energy could be retrofitted to existing UPS. A retrofitted application requires studying the possibilities of integration into a specific commercially available UPS system. Such a study would require a close cooperation with an existing UPS manufacturer and is left as a future research.

List of references

ACTENERGY. 2014. *The principle charactistics of a photovoltaic system* [Online]. Available: http://actenergy.it/?lng=us&ms2=61&ms3=53&ctm=64 [Accessed 14th July 2014 2014].

ALTERNATIVE ENERGY STORE. 2013. *Alternative Energy Store* [Online]. Available: http://www.altestore.com/store/ [Accessed 8 May 2014].

BADAWY, W. A. 2013. A review on solar cells from Si-single crystals to porous materials and quantum dots. *Journal of Advanced Research*.

BRANKER, K., PATHAK, M. J. M. & PEARCE, J. M. 2011. A review of solar photovoltaic levelized cost of electricity. *Renewable and Sustainable Energy Reviews,* 15**,** 4470-4482.

CAVALLARO, C., MUSUMECI, S., SANTONOCITO, C. & PAPPALARDO, M. Smart photovoltaic UPS system for domestic appliances. Clean Electrical Power, 2009 International Conference on, 9-11 June 2009 2009. 699-704.

CHATTOPADHYAY, S., MITRA, M. & SENGUPTA, S. 2011. *Electric Power Quality,* London, Springer.

CHEN, C. J. 2011. *Physics of Solar Cells,* Hoboken, New Jersey, John Wiley & Sons, Inc.

CHOW, N. C. L. 2012. Standby generator and UPS description. Lecture in Electrical Services Elective I City University of Hong Kong, 16 November 2012.

CIRCUITSTODAY. 2014. *Capacitor Input Filter* [Online]. Available: http://www.circuitstoday.com/wp-content/uploads/2009/08/Capacitor-Input-Filter-Circuit.jpg [Accessed 25 May 2014].

CLOVER, I. 2013. IHS cuts global inverter market forecast in face of dramatic price drops. *PV Magazine* [Online]. Available: http://www.pv-magazine.com/ [Accessed 8 May 2014].

CO, T. B. 2004. *Ziegler-Nichols method* [Online]. Available: http://www.chem.mtu.edu/~tbco/cm416/zn.html [Accessed 02 June 2014].

DONG, C. & LIE, X. 2012. Autonomous DC Voltage Control of a DC Microgrid With Multiple Slack Terminals. *Power Systems, IEEE Transactions on,* 27**,** 1897-1905.

DRIESSE, A., JAIN, P. & HARRISON, S. Beyond the curves: Modeling the electrical efficiency of photovoltaic inverters. Photovoltaic Specialists Conference, 2008. PVSC '08. 33rd IEEE, 11-16 May 2008 2008. 1-6.

DUBEY, S., JADHAV, N. Y. & ZAKIROVA, B. 2013. Socio-Economic and Environmental Impacts of Silicon Based Photovoltaic (PV) Technologies. *Energy Procedia,* 33**,** 322-334.

EATON. 2014. *Efficiency - Energy Saver Rectifier* [Online]. Available: http://dcpower.eaton.com/3G/ESR-efficiency.asp [Accessed 10 May 2014].

EIKELBOOM, J. A. & JANSEN, M. J. 2000. Characterisation of PV modules of new generations: results of tests and simulations. The Netherlands: ECN.

ELECTRONICS PROJECT. 2014. *Ripple Factor of bridge rectifier* [Online]. Available: http://electronicsproject.org/ripple-factor-of-bridge-rectifier/ [Accessed 27 May 2014].

ELKO. 2014. *Transientskydd* [Online]. Available: http://www.elko.se/oevrigt/transientskydd-article1644-542.html [Accessed 10 May 2014].

ELPRISKOLLEN. 2014. *Energiskatt* [Online]. Available: http://www.ei.se/sv/elpriskollen/vanliga-fragor-och-svar-elpriskollen/min-faktura/ [Accessed 20 May 2014].

ELTAWIL, M. A. & ZHAO, Z. 2010. Grid-connected photovoltaic power systems: Technical and potential problems—A review. *Renewable and Sustainable Energy Reviews,* 14**,** 112-129.

ENERGIMYNDIGHETEN. 2014. *Om elcertifikatsystemet* [Online]. Available: http://www.energimyndigheten.se/Foretag/Elcertifikat/Om-elcertifikatsystemet/ [Accessed July 13th 2014 2014].

EP SOLAR 2013. eTracer Series Operation Manual.

FALK, H. 1990. Uninterruptible power supplies. *Electronic Library, The,* 8**,** 5.

FEIST, R., MILLS, M., ROZEVELD, S., WOOD, C. & THOMPSON, K. Thermal degradation and light capture performance of CuInGaSe2 (CIGS) and c-Si photovoltaic devices. Photovoltaic Specialists Conference (PVSC), 2010 35th IEEE, 20-25 June 2010 2010. 003411-003416.

FEIST, R., MILLS, M., THOMPSON, K. & RAMESH, N. Comparison of solar cell device thermal degradation and low-irradiance performance. Photovoltaic Specialists Conference (PVSC), 2011 37th IEEE, 19-24 June 2011 2011. 002301-002304.

FONASH, S. J. 2010. *Solar Cell Device Physics,* Boston, Academic Press.

FRAUNHOFER INSTITUTE 2012. Photovoltaics Report. Germany: Fraunhofer Institute.

FTHENAKIS, V. 2009. Sustainability of photovoltaics: The case for thin-film solar cells. *Renewable and Sustainable Energy Reviews,* 13**,** 2746-2750.

FUCHS, E. F. & MASOUM, M. A. S. 2011. *Power Conversion of Renewable Energy Systems*, Springer.

GLUNZ, S. W., PREU, R. & BIRO, D. 2012. 1.16 - Crystalline Silicon Solar Cells: State-of-the-Art and Future Developments. *In:* SAYIGH, A. (ed.) *Comprehensive Renewable Energy.* Oxford: Elsevier.

GRUNOW, P., LUST, S., SAUTER, D., HOFFMANN, V., BENEKING, C., LITZENBURGER, B. & PODLOWSKI, L. 2004. Weak Light Performance and Annual Yields of PV Modules and Systems as a Result of the Basic Parameter set of Industrial Solar Cells. *19th European Photovoltaic Solar Energy Conference.* Paris.

HARVARD UNIVERSITY OFFICE FOR SUSTAINABILITY. 2013. *Life Cycle Costing* [Online]. Available: http://www.green.harvard.edu/theresource/new-construction/life-cycle-costing [Accessed 11 2013].

IPCC 2013. Summary for Policymakers. *Climate Change 2013: The Physical Science Basis. Contribution of Working Group I to the Fifth Assessment Report of the Intergovernmental Panel on Climate Change.* Cambridge, United Kingdom and New York, NY, USA: IPCC.

ISHAQUE, K., SALAM, Z. & LAUSS, G. 2014. The performance of perturb and observe and incremental conductance maximum power point tracking method under dynamic weather conditions. *Applied Energy,* 119**,** 228-236.

JAWAID, H., EHSAN, N., MIRZA, E. & BHATTI, M. W. 2012. Solar powered UPS. *Procedia Technology,* 1**,** 217-224.

JÄGER-WALDAU, A., SZABÓ, M., MONFORTI-FERRARIO, F., BLOEM, H., HULD, T. & LACAL ARANTEGUI, R. 2011. Renewable Energy Snapshots 2011. Luxembourg: European Commission Joint Research Centre.

KALOGIROU, S. A. 2014. *Solar Energy Engineering,* United States of America, Academic Press.

KOMIYAMA, H. & KRAINES, S. 2008. *Vision 2050: Roadmap for a Sustainable Earth,* United States of America, Springer.

KUMAR CHINNAIYAN, V., JEROME, J. & KARPAGAM, J. 2013. An experimental investigation on a multilevel inverter for solar energy applications. *International Journal of Electrical Power & Energy Systems,* 47**,** 157-167.

LIDULA, N. W. A. & RAJAPAKSE, A. D. 2011. Microgrids research: A review of experimental microgrids and test systems. *Renewable and Sustainable Energy Reviews,* 15**,** 186-202.

MARION, W. & URBAN, K. 1995. User's Manual for TMY2s Typical Meteorological Years. Golden, Colorado: National Renewable Energy Laboratory.

MIT ELECTRIC VEHICLE TEAM 2008. A Guide to Understanding Battery Specifications.

MORENO-MUNOZ, A., DE LA ROSA, J. J. G., PALLARÉS-LOPEZ, V., REAL-CALVO, R. J. & GIL-DE-CASTRO, A. 2011. Distributed DC-UPS for energy smart buildings. *Energy and Buildings,* 43**,** 93-100.

NAKICENOVIC, N. 2000. Energy Scenarios. *World Energy Assessment: Energy and the Challenge of Sustainability.* New York: United Nations Development Programme.

NASIRI, A. 2011. 24 - Uninterruptible Power Supplies. *In:* RASHID, M. H. (ed.) *Power Electronics Handbook (Third Edition).* Boston: Butterworth-Heinemann.

NGAN, S. 2012. Lecture 2. Lecture in Systems Modelling and Simulation, City University of Hong Kong, 15 October 2012.

NGUYEN, M. Y. & YOON, Y. T. 2014. A Comparison of Microgrid Topologies Considering Both Market Operations and Reliability. *Electric Power Components and Systems,* 42**,** 585-594.

NILAR INTERNATIONAL AB 2013. Nilar 12V Energy Module Datasheet.

NONAKA, S. & HARADA, K. 1997. Application of utility interactive photovoltaic power generation system for UPS. *Solar Energy Materials and Solar Cells,* 47**,** 271-279.

NORD POOL. 2014. *Elspot prices* [Online]. Available: http://www.nordpoolspot.com/Market-data1/Elspot/Area-Prices/ALL1/Hourly/ [Accessed 20 May 2014].

PELLEY, S., MEISNER, D., WENISCH, T. F. & VANGILDER, J. W. Understanding and abstracting total data center power. Workshop on Energy Efficient Design (WEED), 2009.

PRICE, B. J. 1989. Uninterruptible Power Supplies. *Library Hi Tech,* 7**,** 21 - 47.

RASHID, M. H. 2011. *Power Electronics Handbook: Devices, Circuits and Applications,* USA, Elsevier Inc.

RAU, U. & SCHOCK, H. W. 2013. Chapter IC-3 - Cu(In,Ga)Se2 Thin-Film Solar Cells. *In:* MCEVOY, A., CASTAÑER, L. & MARKVART, T. (eds.) *Solar Cells (Second Edition).* Elsevier.

RAZYKOV, T. M., FEREKIDES, C. S., MOREL, D., STEFANAKOS, E., ULLAL, H. S. & UPADHYAYA, H. M. 2011. Solar photovoltaic electricity: Current status and future prospects. *Solar Energy,* 85**,** 1580-1608.

REICH, N., VAN SARK, W., ALSEMA, E., KAN, S., SILVESTER, S., VAN DER HEIDE, A., LOF, R. & SCHROPP, R. Weak light performance and spectral response of different solar cell types. Presented at: 20th European Photovoltaic Solar Energy Conference and Exhibition, 2005. by: Publication date: ECN Solar Energy 1-6-2005, 10.

REICHELSTEIN, S. & YORSTON, M. 2013. The prospects for cost competitive solar PV power. *Energy Policy,* 55**,** 117-127.

ROTH, K. W., GOLDSTEIN, F. & KLEINMAN, J. 2002. Energy Consumption by Office and Telecommunications Equipment in Commercial Buildings. Massachusetts: Arthur D. Little.

SHEPHERD, W. & ZHANG, L. 2004. *Power Converter Circuits,* New York, Marcel Dekker

SHEPPY, M., LOBATO, C., VAN GEET, O., PLESS, S., DONOVAN, K. & POWERS, C. 2011. Reducing Data Center Loads for a Large-scale, Low-energy Office Building: NREL's Research Support Facility. Golden, Colorado: National Renewable Energy Laboratory.

SHERWANI, A. F., USMANI, J. A. & VARUN 2010. Life cycle assessment of solar PV based electricity generation systems: A review. *Renewable and Sustainable Energy Reviews,* 14**,** 540-544.

SIMS, R. E. H., SCHOCK, R. N., ADEGBULULGBE, A., FENHANN, J., KONSTANTINAVICIUTE, I., W. MOOMAW, NIMIR, H. B., SCHLAMADINGER, B., TORRES-MARTÍNEZ, J., TURNER, C., UCHIYAMA, Y., VUORI, S. J. V., WAMUKONYA, N. & ZHANG, X. 2007. Energy supply. *Climate Change 2007: Mitigation. Contribution of Working Group III to the Fourth Assessment Report of the Intergovernmental Panel on Climate Change.* Cambrigde, United Kingdom & New York, NY, USA: IPCC.

SMA SOLAR TECHNOLOGY AG 2013. Sunny Boy, Sunny Tripower, Sunny Mini Central; Technical Information.

SOLARBUZZ. 2012. *Inverter Prices* [Online]. Available: http://www.solarbuzz.com/facts-and-figures/retail-price-environment/inverter-prices [Accessed 5 May 2014].

STION CORPORATION 2012. Stion STN 135-150 Solar Modules Datasheet.

STION CORPORATION 2013. Stion STO 135-150 Solar Modules Datasheet.

STRYDOM, J. 2012. Optimizing FET On-Resistance. *Power Electronics* [Online]. Available: http://powerelectronics.com/discrete-power-semis/egan-fet-silicon-power-shoot-out-volume-11-optimizing-fet-resistance [Accessed 15 May 2014].

STRZELECKI, R. & BENYSEK, G. 2008. *Power Electronics in Smart Electrical Energy Networks,* London, Springer-Verlag London Limited.

SU, W. & WANG, J. 2012. Energy Management Systems in Microgrid Operations. *The Electricity Journal,* 25**,** 45-60.

SULLIVAN, J. E., CANNON JR, G. D., BURTON, D., JOHNSON, S. D. & WHITE, J. M. 2014. Why End Users Are Investing (Big) in Distributed Generation. *The Electricity Journal,* 27**,** 23-32.

SVENSK KRAFTMÄKLING. 2014. *El-certifikat Price Info* [Online]. Available: http://www.skm.se/priceinfo/ [Accessed July 13th 2014 2014].

TYAGI, V. V., RAHIM, N. A. A., RAHIM, N. A. & SELVARAJ, J. A. L. 2013. Progress in solar PV technology: Research and achievement. *Renewable and Sustainable Energy Reviews,* 20**,** 443-461.

U.S DEPARTMENT OF ENERGY 2010. $1/W Photovoltaic Systems - White Paper to Explore A Grand Challenge for Electricity from Solar. Washington.

U.S ENVIRONMENTAL PROTECTION AGENCY. 2013. *Global Emissions* [Online]. Available: http://www.epa.gov/climatechange/ghgemissions/global.html [Accessed 11 2013].

U.S. ENERGY INFORMATION ADMINISTRATION 2013. International Energy Outlook 2013. Washington: U.S. Energy Information Administration.

UNITED NATIONS 1987. Our Common Future: Report of the World Commission on Environment and Development. United Nations.

WALKER, G. 2001. Evaluating MPPT converter topologies using a MATLAB PV model. *Journal of Electrical & Electronics Engineering, Australia,* 21**,** 49.

WARD, D. J. 2001. Power quality and the security of electricity supply. *Proceedings of the IEEE,* 89**,** 1830-1836.

VARUN, BHAT, I. K. & PRAKASH, R. 2009. LCA of renewable energy for electricity generation systems—A review. *Renewable and Sustainable Energy Reviews,* 13**,** 1067-1073.

VATTENFALL AB 2014. Elnät: Säkringstariffer.

WELFORD, R. 2000. *Corporate Environmental Management: Towards Sustainable Development,* London, Earthscan Publications.

WENHAM, S. R. 2007. *Applied Photovoltaics,* UK, Earthscan.

WHOLESALE SOLAR. 2014. *Wholesale Solar* [Online]. Available: http://www.wholesalesolar.com/ [Accessed 8 May 2014].

YADAV, A. P. K., THIRUMALIAH, S. & HARITHA, G. Comparison of mppt algorithms for dc-dc converters based pv systems.

YUNAZ, I. A., KASASHIMA, S., INTHISANG, S., KRAJANGSANG, T., MIYAJIMA, S., YAMADA, A. & KONAGAI, M. Effect of light intensity on performance of silicon-based thin film solar cells. Photovoltaic Specialists Conference (PVSC), 2009 34th IEEE, 7-12 June 2009 2009. 000153-000157.

Appendix 1: Component Data

In appendix 1 the technical data of the rectifier, inverter, battery, solar panels and solar charge controller is presented in tables.

Rectifier

Mean Well S-1200-60	
DC Voltage	60V
Rated Current	20A
Rated Power	1200W
Max. Ripple and Noise	600mV at peak power
Voltage Adjustable Range	54-66V
Frequency Range	47-63Hz
Conversion Efficiency	87%

Inverter

Mean Well TS-1000-248	
Rated Power	1000W
THD	<3% at rated input
AC Regulation	+-3%
Frequency	50Hz +-0,1Hz
Nominal DC voltage	48V
Input Voltage Range	42-60V
DC current	25A
Conversion Efficiency	92%
No Load Dissipation	6W

Battery

Nilar Blåpack NiMH 48V Energy Module	
Battery Type	Bi-polar NiMH
Rated Voltage	48V
Voltage at 100% SOC	56.8V
Rated capacity (@ C/5)	11Ah
Energy	552Wh
Peak Power (10s @ 5C)	2976W
Maximum Continuous Discharge Current	33A
Standard Charge	0.1C for 12 hours
Fast Charge Current	0.5C

Solar panels

Stion STN135 Solar Modules	
Semi-conductor Type	CIGS
Nominal Power	135W
Module Efficiency at STC	12.4%
Vmpp	44.3V
Voc	58.7V
Impp	3.05A
Isc	3.45A
Area	1.09 m^2
Maximum Operating Temperature	80°C
Temperature Coefficient Isc	0.003%/°C
Temperature Coefficient Voc	-0.28%/°C
Temperature Coefficient Pmpp	-0.34%/°C
Limited Power	90% after 10 years 80% after 25 years
Frame	Black Anodized Aluminum

Solar Charge Controller

EP Solar e-Tracer 3415 MPPT Solar Charge Controller	
Nominal System Voltage	12/24/36/48V Auto-detect
Rated Output Current	30A
Nominal Power (48V)	1440W
Max. PV Voc	150V
Voltage Range	8-72V
Max. PV Input Power	1600W @48V
Grounding	Negative
Maximum Efficiency	98.3%

Appendix 2: Experiment Set-up

In this appendix a detailed description of each individual experiment conducted with the prototype system is presented in order to enable interested readers to evaluate and if wanted to replicate the experiments conducted.

Measurements collected and assorted channels in the DAU

- CH101 – Voltage measurement on the DC-side of the inverter (DC-line voltage)
- CH102 + Oscilloscope – Current measurement over the current shunt (converts current to DC voltage drop)
- CH105 – Current measurement using current probe (converts current to DC voltage)
    - The first measurement is the current into or out of the battery
    - The second measurement is the solar current between the solar charge controller and the positive terminal
    - The third measurement is after the current from the rectifier before the diode
- CH107 – Voltage measurement of the AC voltage after the inverter (measure AC voltage)
- Power meter 1: Upstream from the main power switch on incoming AC from the grid
- Power meter 2: On the AC-side of the inverter
- THD measurement: On the AC-line after the inverter

The incoming power from the solar panels is recorded for each run with solar power connected.

Experiment 1: The effect of load on system parameters
Components in use:

- AC–DC
- DC–AC
- Load: Electric stove on level 3(300W) (second half of the experiment)

Measurements:

1. CH101. 4 ms. 100VDC. 2000 Samples (The power meters are also checked during this run)
2. CH102. 4 ms. 1 VDC. 2000 Samples
3. CH107. 1 s. 300 VAC. 30 Samples

Description:
The experiment is conducted during steady state operations with only the rectifier and inverter connected to the system.

The experiment is conducted twice, first with no load (but with the inverter powered on) and then with nominal load. No parameters are changed during the experiments.

Experiment 2: Steady State
Components in use:

- DC–DC and solar panels (second half of the experiment)
- Battery including control unit and 12V external DC-source
- AC–DC
- DC–AC
- Load: Electric stove on level 3(300W)

Measurements:

1. CH101, 4 ms, 100 VDC, 2000 samples (Power meters are also checked during this run)
2. CH102, 4 ms, 100 mVDC, 2000 samples
3. CH105 (Battery current), 4 ms, 1 VDC, 2000 samples. Fluke, 10 mV/A
4. CH105 (Solar current), 4ms 1VDC, 2000 samples. Fluke, 10mV/A (second half only)
5. CH105 (Rectifier current), 4ms, 1VDC, 2000 samples. Fluke, 10mV/A (second half only)
6. CH107, 1 s, 300 VAC, 30 samples.

Description:
The system is in steady state through all the experiment. No parameters are changed during the experiment.

The experiment is conducted twice – first without and then with the solar charge controller and solar panels connected to the system. The aim of the experiment is to evaluate the effect of the solar power on noise and ripple both on the DC- and AC-line.

Experiment 3: Steady State Islanding Mode
Components in use:

- DC–DC and solar panels (second half of the experiment)
- Battery including control unit and 12V external DC-source
- DC–AC
- Load: Electric stove on level 3(300W)

Measurements:

1. CH101, 4 ms, 100 VDC, 2000 samples (Power meters are also checked during this run)
2. CH102, 4 ms, 100 mVDC, 2000 samples
3. CH105 (Battery current), 4 ms, 1 VDC, 2000 samples. Fluke, 10 mV/A
4. CH105 (Solar current), 4ms 1VDC, 2000 samples. Fluke, 10mV/A (second half only)
5. CH107, 1 s, 300 VAC, 30 samples.

Description:
The system is in steady state through all the experiment. No parameters are changed during the experiment.

The experiment is conducted twice – first without and then with the solar charge controller and solar panels connected to the system. Without the solar power the battery is the only power source, with solar power the two sources share the load. The aim of the experiment is to evaluate the effect of the solar power on noise and ripple both on the DC- and AC-line.

Experiment 4: Starting the inverter
Components in use:

- AC–DC
- DC–AC
- Load: Electric stove on level 3(300W)

Measurements:

1. CH101. 4 ms. 100VDC. 2000 Samples (The power meters are also checked during this run)
2. CH102. 4 ms. 1 VDC. 2000 Samples
3. CH107. 1 s. 300 VAC. 30 Samples

Description:
The system is initially unpowered, with the main power switch open. The inverter and load is turned on – but without any power source.

1 second after the start of the measurements the power switch is closed and the rectifier thus supply power to the inverter which is then turned on. The inverter is the entering start-up phase and draws current from the rectifier. The aim of the experiment is to analyze how the inverter affects the system during start up.

Experiment 5: Stabilizing battery current after connecting the battery
Components in use:

- Battery, including control unit and 12V external DC-source, (after start of the experiment)
- AC–DC
- DC–AC
- Load: Electric stove on level 3(300W)

Measurements:

1. CH101 100 VDC
   CH102 1 VDC
   CH105 1 VDC (Battery current)
   CH107 300 VAC
   All channels are measured simultaneously, 1 second interval, 600 samples

Description:
The experiment aims to evaluate how the battery current stabilizes after the battery is connected. Initially the system is in steady state, 10 seconds after the measurement starts the battery is connected into the DC-circuit and is kept connected throughout the experiment.

The power meters are read at the start and at the end of the experiment to compare the power drawn by the battery.

Experiment 6: Entering Islanding mode
Components in use:

- DC–DC and solar panels (second half of the experiment)
- Battery, including control unit and 12V external DC-source
- AC–DC (turned off at the start of experiment)
- DC–AC
- Load: Electric stove on level 3(300W)

Measurements:

1. CH101, 4 ms, 100 VDC, 2000 samples (Power meters are also checked during this run)
2. CH102, 4 ms, 100 mVDC, 2000 samples
3. CH105 (Battery current), 4 ms, 1 VDC, 2000 samples. Fluke, 10 mV/A
4. CH105 (Solar current), 4ms 1VDC, 2000 samples. Fluke, 10mV/A (second half only)
5. CH105 (Rectifier current), 4ms, 1VDC, 2000 samples. Fluke, 10mV/A (second half only)
6. CH107, 1 s, 300 VAC, 30 samples

Description:
The system has reached steady state at the start of the experiment and all components are in use (solar charge controller and panels in the second half only). The power required by the load surpasses what the solar panels can deliver.

The main power switch is turned off 1 second after measurements being started. The rectifier thus cannot supply any power to the load and the battery current switches from charging to discharging the battery.

Experiment 7: Reconnecting to the power grid
Components in use:

- DC–DC and solar panels (second half of the experiment)
- Battery, including control unit and 12V external DC-source
- AC–DC (turned on at the start of experiment)
- DC–AC
- Load: Electric stove on level 3(300W)

Measurements:

1. CH101, 4 ms, 100 VDC, 2000 samples (Power meters are also checked during this run)
2. CH102, 4 ms, 100 mVDC, 2000 samples
3. CH105 (Battery current), 4 ms, 1 VDC, 2000 samples. Fluke, 10 mV/A
4. CH105 (Solar current), 4ms 1VDC, 2000 samples. Fluke, 10mV/A (second half only)
5. CH105 (Rectifier current), 4ms, 1VDC, 2000 samples. Fluke, 10mV/A (second half only)
6. CH107, 1 s, 300 VAC, 30 samples

Description:
The system has reached steady state in islanding mode at the start of the experiment and all components are in use except the rectifier (solar charge controller and panels in the second half only). The power required by the load surpasses what the solar panels can deliver. The main power switch is turned on 1 second after measurements being started. The rectifier can thus again supply power to the load and charge the battery.

Experiment 8: Switching off the load
Components in use:

- DC–DC and solar panels (second half of the experiment)
- Battery, including control unit and 12V external DC-source
- AC–DC
- DC–AC
- Load: Electric stove on level 3(300W) (turned off at the start of experiment)

Measurements:

1. CH101, 4 ms, 100 VDC, 2000 samples (Power meters are also checked during this run)
2. CH102, 4 ms, 100 mVDC, 2000 samples
3. CH105 (Battery current), 4 ms, 1 VDC, 2000 samples. Fluke, 10 mV/A
4. CH105 (Solar current), 4ms 1VDC, 2000 samples. Fluke, 10mV/A (second half only)
5. CH105 (Rectifier current), 4ms, 1VDC, 2000 samples. Fluke, 10mV/A (second half only)
6. CH107, 1 s, 300 VAC, 30 samples

Description:
The system has reached steady state at the start of the experiment and all components are in use (solar charge controller and panels in the second half only). The power required by the load surpasses what the solar panels can deliver.

The load is turned off 1 second after the start of the measurements. The rectifier and if connected the solar panels thus supply all load to the battery.

Experiment 9: Switching on the load
Components in use:

- DC–DC and solar panels (second half of the experiment)
- Battery, including control unit and 12V external DC-source
- AC–DC
- DC–AC
- Load: Electric stove on level 3(300W) (turned on at the start of experiment)

Measurements:

1. CH101, 4 ms, 100 VDC, 2000 samples (Power meters are also checked during this run)
2. CH102, 4 ms, 100 mVDC, 2000 samples
3. CH105 (Battery current), 4 ms, 1 VDC, 2000 samples. Fluke, 10 mV/A
4. CH105 (Solar current), 4ms 1VDC, 2000 samples. Fluke, 10mV/A (second half only)
5. CH105 (Rectifier current), 4ms, 1VDC, 2000 samples. Fluke, 10mV/A (second half only)
6. CH107, 1 s, 300 VAC, 30 samples

Description:
The system has reached steady state at the start of the experiment and both rectifier and solar charge controller supplies current to the battery, with the inverter on but no load (solar charge controller and panels in the second half only). The power required by the nominal load surpasses what the solar panels can deliver. The load is turned on 1 second after the start of the measurements. The rectifier and if connected the solar panels thus supply all load to the battery.

Experiment 10: Total harmonic distortion in steady state
Components in use (shifting based on runs)

- DC–DC and solar panels (second half of the experiment)
- Battery, including control unit and 12V external DC-source
- AC–DC
- DC–AC
- Load: Electric stove on level 3 (300W) (level 1, 130W in half of the experiments)

Measurements:

- THD measurement: On the AC-line after the inverter

Description:
This experiment is conducted with the components used for each run being in steady state at the point of measurement. The current probe used for the measurements are connected to the outgoing AC-line between the inverter and the load.

The data from the measurement is shown instantly on the screen of the instrument and is thus subjected to some oscillations. The experiment is conducted in several consecutive runs where the components in use and the level of the load are adjusted between the runs. The different component configurations are shown in Table 14. All configurations are run twice – first with and then without the addition of the solar charge controller and solar panels.

Table 14: Component configuration in the THD measurement

Component Configuration
Battery; Load 130W
Battery; Load 300W
AC–DC; Load 130W
AC–DC; Load 300W
AC–DC + Battery; Load 130W
AC–DC + Battery; Load 300W
Battery; More sun than load (130W)